Enhancing Attachment of Non-Adherent Cells on Inert Surfaces

Sailakshmi Velamoor

A thesis submitted to Auckland University of Technology in partial fulfilment of the requirements for the degree of Master of Philosophy (MPhil)

September 2017

Table of Contents

Attestation of Authorship

I hereby declare that this submission is my own work and that, to the best of my knowledge and belief, it contains no material previously published or written by another person (except where explicitly defined by acknowledgement), nor material which to a substantial extent has been submitted for the award of any other degree or diploma of a university or other institution of higher learning.

Sailakshmi Velamoor

Auckland

September 2017

Acknowledgements

Firstly, I wish to thank my supervisor Steve Henry for his guidance and support. Also, I wish to take this opportunity to thank Kode Biotech for supporting me with a scholarship and making this project possible.

I would like to thank my other supervisor Eleanor Williams and colleagues at Kode Biotech–Stephanie, Ankita, Chris, Holly, Radhika and Pavithra–who made this journey a wonderful one. I also wish to thank AUT and post-graduate coordinator, Josephine Prasad, for helping me successfully complete this program.

Lastly, I wish to thank my family, especially my children, Shreenidhi and Shrinivas, for their patience and support they have given me throughout this program.

List of Figures

List of Tables

Abstract

In recent years, culturing cells on synthetic surfaces has a growing importance in many fields ranging from simple two-dimensional cell culture to biomedical applications such as tissue engineering, regenerative medicine, medical devices and biosensor chips. The extent of cell adhesion to these synthetic surfaces or biomaterials plays a decisive role in regulating the cells' subsequent proliferation and differentiation. While a wide range of surface modification technologies are available to modify surfaces and promote cell adhesion, many are either complicated or expensive. Kode™ Technology FSL constructs have the ability to modify both cells and surfaces, and thus have the potential to be adapted to cellular adhesion.

The aim of this study was to adhere proliferating non-adherent Jurkat cells to inert surfaces using Kode™ Technology. This was investigated using a biotin-streptavidin model. Findings reveal ability of FSL constructs to modify both cells and surfaces and facilitate direct adhesion in a dose dependent manner. Some cytotoxicity was observed under high insertion concentration. Although, presence of serum severely inhibits FSL insertion and retention, and cell adhesion to FSL modified surfaces, Kode™ has the potential to facilitate cellular adhesion to plastic and metal surfaces.

Chapter 1 Introduction

All complex life is built of cells that link together physically and biochemically to form tissues. The organization of cells into tissue is sophisticated with various cell types forming unique shapes and patterns. While the formation of native tissues is under the control of various biological processes, there are few ways to create tissue-like material in the laboratory. In recent years, culturing cells on artificial surfaces has a growing importance in many fields ranging from simple two-dimensional cell culture to biomedical applications such as tissue engineering, regenerative medicine, medical devices and biosensor chips. Biomaterials serve as a substrate for these cell populations to attach and expand, be implanted with cells as cell delivery vehicle, and/ or be used as a drug carrier to activate specific cellular responses in targeted regions. Limitations in these methods is the ability of cells to adhere to some biomaterials [1].

1.1 Significance of cell adhesion

In most applications, cells in contact with biomaterials require attachment to these surfaces for viability, growth, expansion and differentiation. Cells in native tissues adhere to the surrounding extracellular matrix (ECM) via cell membrane receptors, such as, integrins [2-4]. As synthetic biomaterials lack ECM, specialized receptors secreted by cells indirectly interact with the substrate through adhesive factors, such as fibronectin, are absorbed on to the surface from serum (see Figure 1). These interactions are merely mediated by weak non-specific interactions such as ionic attraction, van der Waal's forces, hydrogen bonding and hydrophobic interaction. Thus, cells adhere rather poorly to synthetic biomaterials, subsequently hampering the effectiveness of a cell-inert surface adhesion [5]. This could be overcome by coating the synthetic surfaces with natural or synthetic ECM derivatives.

Wide variety of natural and synthetic surfaces or biomaterials are available to use in biomedical and clinical applications. Natural biomaterials have excellent biocompatibility to enable cell adhesion and proliferation. Natural biomaterials could be either native ECM from allografts and xenografts or smaller building blocks, which include but are not limited to inorganic ceramics such as calcium phosphates and organic polymers like proteins, polysaccharides, lipids and polynucleotides. However, with limited mechanical and physical strength, natural materials may not be suitable for load shear applications. Also, owing to the complexity of composition and ultrastructure of native materials, synthesis of a mimetic with any degree of

fidelity is not yet feasible [6]. Another issue is the potential immunogenicity as natural biomaterials from allogenic or xenogenic sources may be antigenic to the hosts. In addition to relatively high costs associated with purification or *de novo* synthesis, their poor mechanical properties make them unsuitable for high strength applications [7,8].

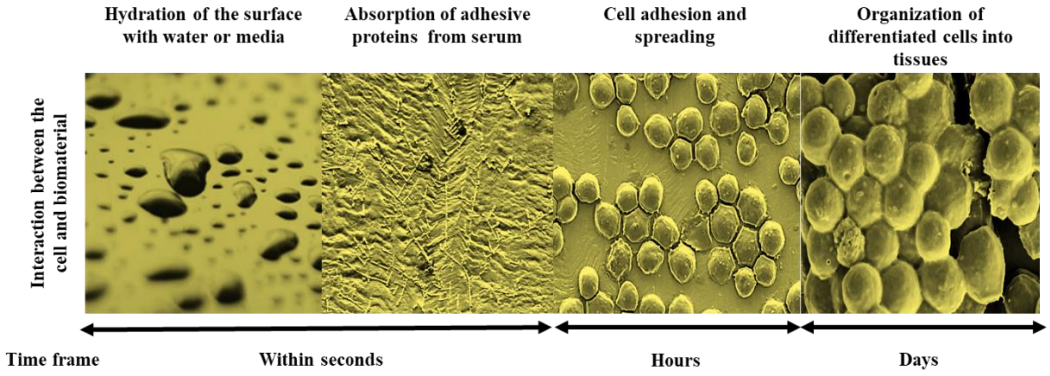

Figure 1 Cell adhesion to synthetic surfaces via absorption

Synthetic biomaterials, on the other hand, have better controllable physical and mechanical properties and could be manufactured reproducibly. Although a wide variety of materials are available, the choice of materials to be used is defined by their application. For example, metals are generally used in orthopaedic implants as the material needs to have good mechanical properties and can take high loads. However, this material is poorly capable of inducing any biological activity due to surface hardness, high friction coefficient, and wear resistance and bio-inertness [9]. Some of these issues could be overcome with the use of ceramics. The similarity in the chemistry of ceramics and that of native bone makes ceramics more usable as part of orthopaedic implants or as dental materials. Nevertheless, ceramics are quite brittle [10]. In recent years, the use of polymers in tissue engineering applications has increased tremendously. This is due to ease of fabricating them into various complex shapes and the range of physical and chemical properties possible with these materials. However, polymers are not as mechanically strong as metals and can undergo mechanical wear and breakdown. Also, changes in surface chemistry following absorption of water and biomolecules from surrounding environment and sterilization procedures may influence the chemical and mechanical properties of the polymer [10].

In summary, surface properties, such as surface chemistry, hydrophilicity or surface tension and topography are known to influence cell-substrate interaction [8]. Several studies have

shown that altering the surface properties ranging from simple changes to hydrophilicity of the material (by physicochemical modifications), to functionalization with charged groups, peptides, or proteins (by biofunctionalization) can improve cell-surface affinities [9,11-13]. For instance, the surface topography, chemistry and biocompatibility of polished titanium surfaces treated with different acids (HCl, HF and H_3PO_4) have higher roughness, lower cytotoxicity level and better biocompatibility than controls [14]. Similarly, biodegradable and biocompatible Poly lactic-co-glycolic acid (PLGA) which are popularly used for manufacturing tissue engineering scaffolds, still required incorporation of hydroxyapatite (HAp) and β-tricalcium phosphate through oxygen plasma treatment for enhanced cell adhesion, proliferation and differentiation of MC3T3-E1 cells [15]. Table 1 lists the nature of different biomaterials used in biotechnology applications along with the most common methods employed for modifying their surface.

1.1.1 Functionalizing synthetic surfaces

A variety of physicochemical surface modification strategies have emerged to create materials with improved biocontact properties [9,16,17]. This is achieved either by adding or removing material from the surface or by altering the material already present. For example, excess material from the surface are removed through mechanical modifications such as machining, polishing and grit blasting, to provide the surface with specific roughness, the structure or amplitude of which can optimize cell proliferation and cell adhesion [18]. Similarly, chemical strategies are employed for removing contaminants and cleaning the surfaces through alkali, alkaline or plasma etching [9,11,13,17,19]. Modification of surfaces with proteins, peptides, growth factors or any other bioactive molecules such as hydroxyapatite is emerging as a powerful tool to improve the biocompatibility of the synthetic material. Recently, Gabriel et al. (2012) have illustrated increased initial cell attachment and spreading following covalent immobilization of RGD-peptides on hydrophobic polymer polycaprolactone (PCL) surfaces [20]. Likewise, incorporation of the growth factor, bone morphogenetic protein-2 (BMP-2), on TiO_2/glass composites has shown to promote bone ingrowth in an *in-vivo* study [21].

Table 1 List of natural and synthetic materials used in cell culture with their advantages and disadvantages.

Materials	Examples	Advantages	Disadvantages	Major application	Modification methods
Natural [8,22]	Collagen, chitosan, hyaluronic acid, silk, chitin, fibrinogen, gelatine	Mimic native ECM	Poor mechanical properties, batch to batch variation, immunogenic problems	Enable cell adhesion on synthetic materials	Immobilizing on synthetic materials
Synthetic polymers [8,23-28]	Poly-ethylene glycol (PEG), hydrogels, PLGA, Polycaprolactone (PCL), Polyuxrethane (PU)	Controllable porosity, pore size and pore interconnectivity, structural shape	Hydrophobic surface, poor cell adhesion, proliferation and differentiation	Carriers for growth factors, drug delivery, gene transfection, cell therapy with hydrogels	Chemical grating, oxygen or amino plasma modification, biomimetic deposition, self-assembled monolayers
Metals [9,19,29-33]	Magnesium and its alloys, Ti and its alloys, Nitinol (nickel and titanium alloys)	High strength, ductility, fracture toughness and hardness	Lack of biological activity on the surface materials	Dental and orthopaedic implants	Acid and alkali etching, sol-gel dip coating, anodic oxidation, electrophoretic deposition
Ceramics [8,34-40]	Tri-Calcium phosphate, n-HAp Calcium phosphate glass	Promote osteointegration, functionalize inorganic materials	Low fracture toughness	Bone scaffolding	Silanization, covalent immobilization of biomolecules

A plethora of coating techniques are available to deposit the biomolecule of interest to attain desired biological response at the interface between the synthetic material and the surrounding living tissue. Examples include but not limited to plasma spraying [41], sputter deposition [42], sol–gel coating [33], electrophoretic deposition [43], biomimetic precipitation and the dipping method [11,17,44,45]. The advantages and disadvantages of some of these methods discussed by John et al. (2015) are presented in Table 2 [11].

In recent years, the designing of biomimetic biomaterials is gaining more interest as they elicit specific cellular responses and new tissue formation is mediated by biomolecular recognition [46]. Surface modification is simple and involves covalently [20,47] or non-covalently [11,48] coupling biomolecules such as adhesive proteins like collagen, RGD-peptide and fibronectin to biomaterial surface. Covalent coating ensures a strong linkage between the biomolecules and the surface. However, the surface is chemically modified to accommodate the bioactive molecules thereby changing the native surface property of the material. Moreover, it does not guarantee the right orientation and may damage complex molecules like proteins. Irrespective of the nature of the material (metals, natural or synthetic polymers, ceramics), non-specific protein absorption through non-covalent interactions such as hydrogen bonding and van der Waals forces is the first process observed at the cell-surface interface. Although, they employ a simple strategy, such interactions are weak and uncontrollable often resulting in protein unfolding and thereby resulting in decrease in biological activity [49]. The coatings and adherent cells are also easily lost during some processing, such as washing. These issues are shown to be circumvented by modifying surfaces by self-assembling monolayers (SAM) [50].

Self-assembly is the spontaneous interaction between the substrate and adsorbate molecules at the solid–liquid interface resulting in spontaneous thin film formation. Various studies of self-assembled proteins, RGD-like peptides [51], lipids [52] and nucleic acids [53] have provided chemists and material scientists with a rich lexicon of self-assembly motifs and rules. This allowed the construction of complex, adaptable and highly tuneable materials with potential biological activity. Most monolayers are formed through multiple non-covalent interactions, such as hydrogen bonding, electrostatic association and van der Waals forces [50,52,54-57]. Although non- covalent interactions are weak and random, studies have shown introducing desirable chemical functionalities onto surface by specific ligand/receptor interaction, such as antibody/antigen or biotin/(strept)avidin, provides a strong bonding with high affinity [58].

Table 2 List of advantages and disadvantages of surface coating technology (adapted from John et al. (2015) [59]).

Coating Technique	Thickness of layer (µm)	Advantages	Disadvantages
Plasma Spraying [25,32,41,60-70]	0-250	• Coat complex materials • high deposition rates	• Extremely high temperature • Coats only visible area • Coating decomposition due to high temperature • Amorphous coating
Sputter / pulsed-laser deposition [11,42,71]	0.2- 1.0	• Uniform coating on flat surfaces	• Expensive • Time consuming • Inability to coat complex or porous surfaces
Sol- gel coating [9,29,33]	< 1	• Coat complex shapes and porous substrates • Low processing temperatures • Relatively cheap • Very thin coatings	• Controlled atmosphere processing
Electrophoretic deposition [19,29]	100- 2000	• Uniform coating thickness • Rapid deposition rates • Coat complex materials	• Crack in coatings • High sintering temperatures
Biomimetic deposition [21,46,48,72]	<30	• Coating complex geometries • Co-deposition bio-molecules	• Time consuming • Controlled pH
Dipping method [11,19,33]	50- 500	• Inexpensive • Rapid coating • Coat complex substrates	• High sintering temperatures • Amorphous coating • Fragile due to thickness

1.2 Cell adhesion to synthetic surface

The cell adhesion to biomaterials is very important as it initiates intracellular signals ranging from cytoskeletal organization to cell polarity, proliferation or apoptosis. Given the crucial role of cell/material association, synthetic materials are modified using several strategies as discussed in the above section. Most of the widely used strategies are discussed in the sections below.

1.2.1 RGD and related peptides

Utilizing adhesive peptides that engage and activate integrin adhesion receptors on cell surface is the most widely used method for rendering materials biocompatible and promoting cell adhesion. Tri-amino acid sequence, arginine-glycine-aspartate, or RGD are the most extensively studied adhesive peptide in biomaterials field. RGD is the principal integrin-binding domain present within ECM proteins such as fibronectin, vitronectin, fibrinogen,

osteopontin, and bone sialoprotein. Immobilizing surfaces with RGD peptides has shown to mediate cell adhesion on any biomaterial surface [20,47,73,74]. RGD peptides attached to gold surfaces using self- assembled monolayers are shown to immobilize Chinese hamster ovary (CHO) cells which otherwise is not possible [75]. Likewise, strong adhesion of epithelial cells are detected through fluorescence microscopy in RGD functionalized porous silicon surface [76]. Covalent immobilization of RGD sequences to hydrophobic polymer polycaprolactone (PCL) demonstrated considerably higher initial attachment in osteoblasts, fibroblasts and endothelial cells [20].

RGD peptides have been combined with other types of adhesive peptides, such as the laminin receptors YIGSR sequence, or collagen the triple-helical GFOGER peptide to activate more subtypes of adhesive receptors and facilitate better adhesion [77]. In fact, adhesion of cardiac cells to silicone surfaces modified with synthetic RGD (fibronectin) and YIGSR (laminin) peptides demonstrated the same degree of cellular adhesion as their native proteins [78]. Despite all these advantages incorporation of RGD peptides on synthetic surfaces are applicable to only those cells that support integrin-based adhesion.

1.2.2 DNA based adhesion

DNA-programmed adhesions are also another strong platform for immobilizing cells to biomaterial surfaces. In addition to cell adhesion, extensive studies have shown that DNA self-assembled on gold surfaces through thiol linkage can have precise control of density and orientation of cell-specific ligands. The attachment is fast and to specific areas [79].

In addition to surfaces, the cells are also efficiently observed to be modified and immobilized on surfaces. For instance, using NHS-DNA (N-hydroxysuccimide- DNA), covalent attachment of DNA to amines of the cell membrane is achieved [80,81]. A study carried out by Selden et al. (2012) have demonstrated adhesion of Jurkat cells to a passivated glass surface by simply programming the adhesive properties of mammalian cells using single-stranded DNA oligonucleotides. The resulting chemically adherent cells are shown to maintain high viability and proliferative capacity. When observed under a light microscope, the modified cells are observed to behave identical to unmodified cells [81]. Although DNA strategies offer an effective means of programming adhesion, they may also inadvertently engage the adhesion machinery, perturb the cytoskeleton, or activate cell surface receptors due to the somewhat indiscriminate nature of the modification process [79].

1.2.3 Biotin-avidin affinity based adhesion

In recent years, biotin-avidin based cell adhesion has attracted increasing attention. The bond formation between the biotin and avidin is one of the strongest non-covalent bonds ($10^{15}M^{-1}$) and is unaffected by extremes of pH, temperature, organic solvents and most denaturing agents. In fact, the non-covalent interaction between the biotin and avidin is much higher than biospecific cell attachment reactions such as integrin-fibronectin (10^6 M^{-1}) or integrin-laminin (10^9 M^{-1}) [82].

In tissue engineering applications, biotin is conjugated to the cell membranes as almost all kinds of cells have abundant amine groups on their membranes that can be biotinylated with N-hydroxysuccinimide-D-biotin (NHS-D-biotin) [83-87]. For instance, sulfonated biotinyl-NHS was covalently linked to amine group on chondrocytes cell surface. The cells are then linked to polystyrene surfaces pre-absorbed with avidin [84,88]. Insertion of cells with biotin is also biologically acceptable as those reactions are recognized to be part of natural processes. Self- assembling of biotinylated lipids into cells membranes is an alternative strategy to biotinylate cell membranes which are then attached to different surfaces via a streptavidin linker [52,89]. Controlled adhesion of cells using biotin-avidin system was shown to be used in cell-based microarrays. For instance, Jurkat cells biotinylated with lectin, immobilized on streptavidin printed slides were used to construct microarray spots that was used to probe an array of cells for target protein abundance, activation state and subcellular localization[90].

1.3 Kode™ Technology and FSL constructs

Kode™ Technology is a surface engineering technology that can add functionality to both the cells and surfaces without causing any undesirable effect. Modification achieved through the function-spacer-lipid (FSL) constructs from Kode™ has an unparalleled flexibility to precisely control, manipulate and mimic biological surfaces. As the name implies, FSL constructs comprises of a function head (F), spacer (S) and the lipid tail (L) (see Figure 2) [91].

The function head (F) is the bioactive component of the construct which equips the cell and synthetic surfaces with novel function(s). The head group is interchangeable and designed to present almost any antigen, fluorophore [92], peptide, carbohydrate [91,93] or any other biological molecule [91]. For example, the biotin function head can be used in a cell membrane for adhering cells to wide range of synthetic surfaces [91]. A range of FSL head groups are available for modifying both the biological and non-biological surfaces along with their

established use in quality control, antibody mapping, diagnostic assay and *in-vivo* animal modelling as reviewed in Korchagina et al. (2015) [94].

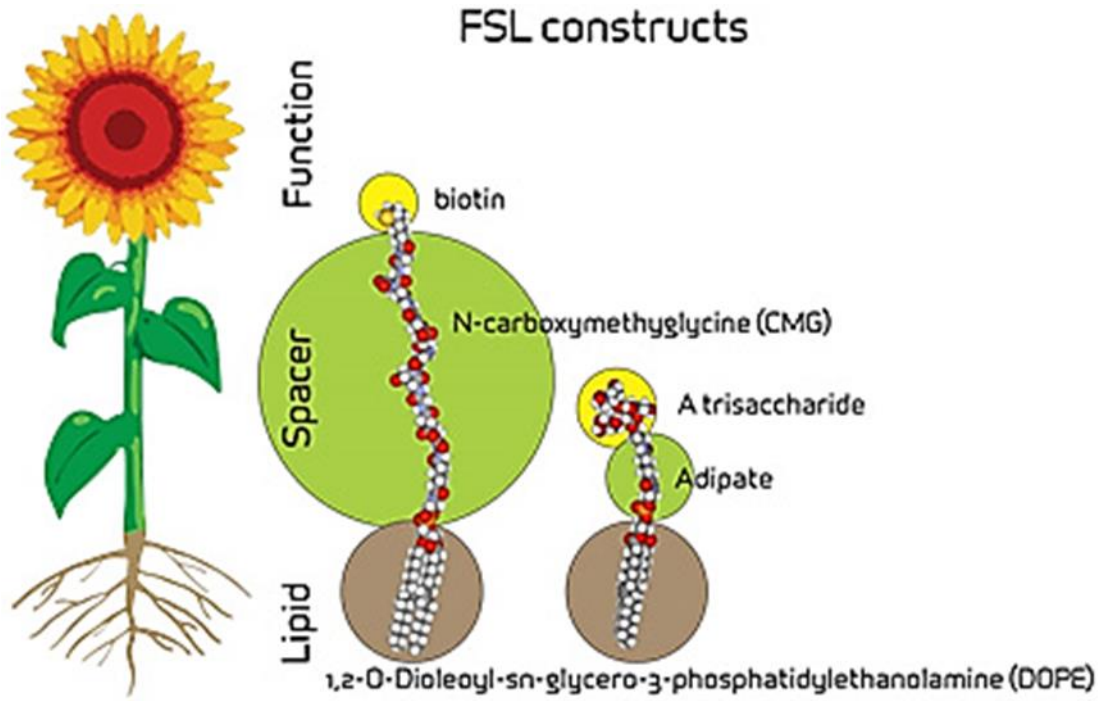

Figure 2 Schematic representation of FSL construct (Adapted from Barr (2013) [91]).

The spacer (S) is normally a long chain of amino acid that facilitates the chemistry to conjugate the lipid tail to the functional head. It also plays a key role in imparting solubility thereby allowing the construct to disperse in water, saline or biological media [91]. FSL spacers are either simple, short adipate linker or longer carboxymethylglycine (CMG). While an adipate linker (1.9 nm) was commonly used for conjugating the FSL blood antigens with the lipid tail, longer CMG (7.2 nm) spacer are now used for all applications including linking biotin to its lipid tail [91,94].

The primary function of the lipid is to make the FSL construct amphipathic which allows the FSL construct to be dispersed in water and spontaneously self-assemble onto surfaces or into membranes. A variety of lipids have been used to create FSL constructs, including 1,2-dioleoyl-sn-glycerol-3-phosphoethanolamine (DOPE), cholesterol, and natural and synthetic ceramides. DOPE is the most common lipid chosen for FSL constructs. It is a membrane phospholipid compatible with biological assays with its diacyl structure capable of being retained in the cell membrane [91,94].

1.3.1 Kodecytes

Studies from the AUT Centre for Kode™ Technology Innovation have established that FSL constructs can modify cells without any undesirable effect [93-97]. The process of modifying cells using Kode™ Technology is simple and generic. Modification involves incubation of cells with a solution of FSL constructs for 1-2 hours at 37°C. During this period, the lipid tail in the FSL, spontaneously and stably incorporates into the lipid bilayer of the plasma membrane. The resulting modified cells are termed as kodecytes.

Other than red cells, FSL constructs have been shown to modify the surface of bacteria, embryos, spermatozoa, zebrafish, epithelial/endometrial cells and even viruses [95]. While inactive (red cells) or fixed kodecytes were shown to stably retain FSL constructs indefinitely in lipid free media, retention of FSL constructs in live proliferating cells were observed to reduce to negligible levels after 24 hours, with/without serum presence [91,94,98,99].

1.3.2 Koding synthetic surfaces

Variations in the type of the biomaterial used depends on its application and there is no universal technique for modifying them all [9]. However, Kode™ Technology is potentially an alternative quick and easy platform for modifying any non-biological surface including paper, polystyrene, metals and glass. Modification is simple and involves incubation of these surfaces with FSL constructs in solution [97,100].

FSL construct are amphipathic in nature. When in solution, FSLs may form micellar structures. These micelles then coat the synthetic surfaces by two different mechanisms and depends on the surface type. If the surface is hydrophobic, the lipid tail of the construct interacts with the surface to directly anchor FSL constructs. In contrast, the construct adheres by exclusion of water processes when in contact with a hydrophilic surface (as shown in Figure 3). Once formed, the FSL coating is relatively resistant to removal by water, mild detergents, serum lipids, or solvents such as methanol. The attachment is relatively quick and the enzyme immunoassay and antibody based immunostaining carried out shows that there is no difference in the staining between 5 to 600 seconds of contact of FSL with the surface. [91,97,101].

Currently, the methods used for coating the FSL molecules include painting, soaking and inkjet printing. Controllable, flexible and precise patterning of biological molecules without any degradation has excellent use in biotechnology settings. This could be achieved by printing FSL constructs on surfaces such as metals, polymers and other surfaces. Soaking was useful to

modify microbeads that are directly taken for assays without any drying. Painting is useful for materials that could not be printed. Comparison of surfaces koded by drying (FSL constructs prior to washing and further processing) to non-drying surfaces demonstrated no significant difference in level of modification [91,94,97].

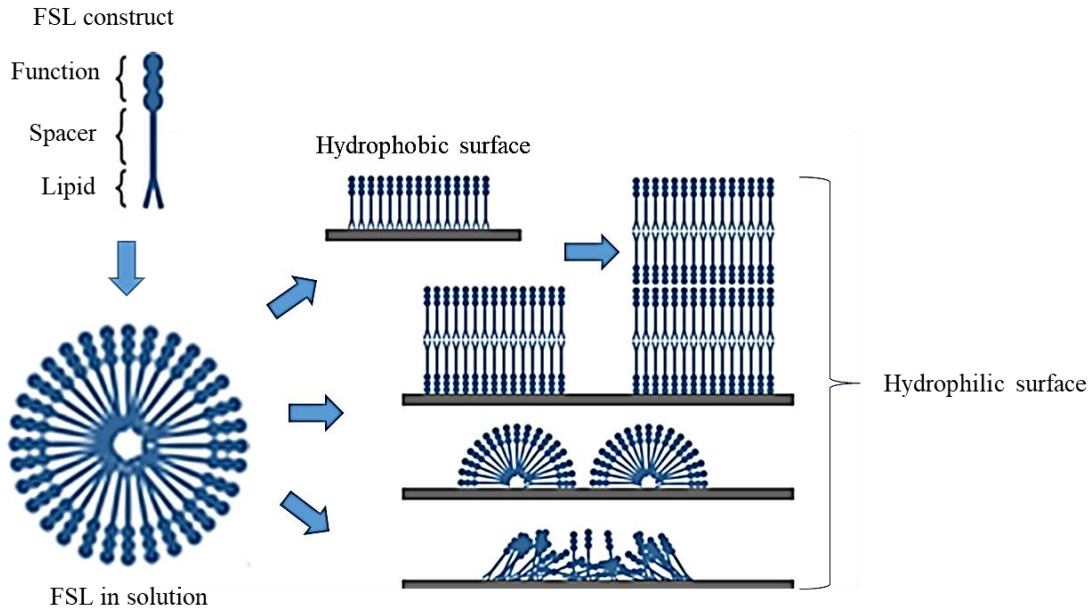

Figure 3 Mechanism of attachment to non-biological surfaces. Modified from Williams et al. (2016) [97].

A wide range of non-biological surfaces modified with FSL constructs have been shown to immobilize red cell kodecytes [91,94,97]. Based on these findings, it could be hypothesized that the FSL constructs could potentially be used for developing new platform to render therapeutic functions using synthetic materials and non- adherent cell lines. This thesis will attempt to assess the feasibility of using Kode™ FSL- biotin technology as a universal platform for adhering proliferating suspension cells to synthetic surfaces. This will be a cornerstone for developing new diagnostic and therapeutic application using non-adherent cells which includes some stem cells.

1.3.3 Adhering cells through Kode™ Technology

FSL constructs with a biotin via streptavidin and blood group A & B-tri via adhesion with antibodies have shown to facilitate adhesion of different types of cells to various synthetic surfaces [91]. Modification requires simple incubation of cells and surfaces with FSL and a secondary attachment with either an avidin or antibody. While the lipid tail of the FSL anchors

into the plasma membrane to introduce a biotin residue, surfaces are biotinylated through self-assembly of the construct on the surface (see Figure 3). Although, Dou et al. (2015) utilized a similar approach for adhering MC3T3 cells to hydrogels, biotinylation of cells and surfaces were mediated through chemical covalent interactions [87]. This has a possibility to modify the native properties of the cell or material surface which leads to disruption in cell and surface morphology and function. Another advantage of utilizing FSL constructs is its interchangeable function head. Thus, the potential of replacing the function head with RGD peptides, any antigen or ssDNA could potentially be developed to cause cell- surface adherence.

1.4 Methodological background

The literature is replete with various publications for adhering live cells to synthetic surfaces. Most of these are extensively investigated using adherent mammalian cells. Studies on adhering proliferating suspension cells is very limited [75,81,102,103]. Although Barr (2013) has established the adhesion of red cell to different surfaces, they are non-proliferating cells [91]. Thus, adhesion of proliferating non- adherent cells to synthetic surfaces would be investigated in this study.

1.4.1 Cell lines

Studies have established that FSL constructs are successful in modifying embryos, spermatozoa, zebrafish, epithelial/endometrial cells and red blood cells. As the aim of this project is focussed on attaching non-adhering cells, the most widely investigated Jurkat T-leukemic suspension cells were chosen for this investigation. Jurkat cells are commonly used for investigating the interaction mechanism between immune cells and target tumour cells for improving therapeutic efficacy. In fact, Jurkat cells have previously been modified with non-biotin FSL constructs as a novel therapeutic approach for the systemic treatment of HIV/AIDS [96].

1.4.2 FSL constructs

Affinity based biotin-avidin system has provided a universal matrix for adhering cells to synthetic surfaces [52,82-87,90,104]. Thus, FSL with a functional biotin head, CMG spacer and DOPE tail, commercially available from Kode Biotech, which are well established for insertion and membrane retention, would be used for modifying the cell and material surface. Other variants of FSL-biotin with ceramide or cholesterol as lipid tails are available (see Figure 4) and also would be investigated [94].

Biotin- CMG(2)- DOPE (FSL- Biotin with DOPE)
Molecular weight= 2079.32
Molecular formula= $C_{91}H_{149}N_{17}NaO_{32}PS$

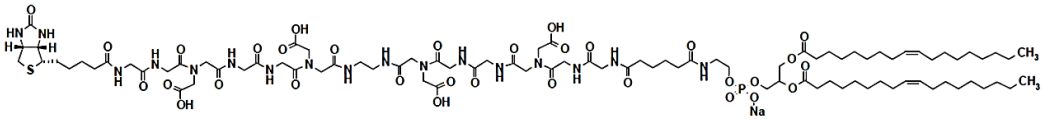

Biotin- CMG(2)- Av- Cholesterol (FSL- Biotin with Cholesterol)
Molecular weight= 1802.90
Molecular formula= $C_{77}H_{115}N_{17}Na_4O_{25}S$

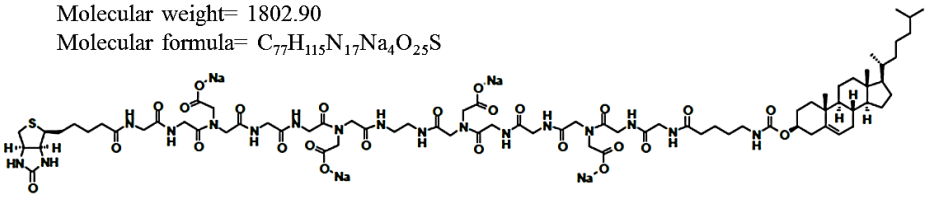

Biotin- CMG(2)- βAla-Mimetic(FSL- Biotin with synthetic ceramide)
Molecular weight= 1827.0
Molecular formula= $C_{78}H_{127}N_{17}Na_4O_{25}S$

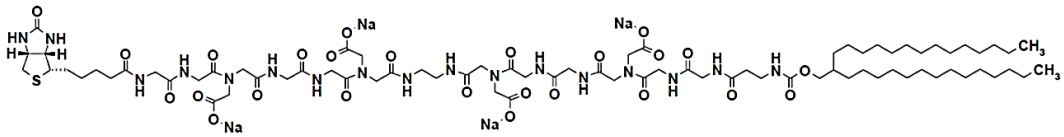

Figure 4 Structure of FSL-biotin variants with a DOPE, cholesterol or ceramide as lipid tail.

1.4.3 Immunofluorescence studies

Immunofluorescence detection has previously been established as very efficient to investigate the insertion and retention conditions of FSLs on cell membranes [91,98,99]. In this study, the insertion and retention of FSL-biotin into cell membrane would be elucidated by labelling the modified cells (kodecytes) with a streptavidin fluorophore (mostly streptavidin Alexa Fluor® 488). Either ImageJ or standard grading system would be used to semi- quantitively measure the strength of the fluorescence exhibited by the kodecytes.

1.4.4 Analysing kodecytes characteristics

Nearly all cells are sensitive to any changes to their size and shape. Insertion of any exogenous molecules into the surface of the cell has shown to bring about important cellular changes in shape, motility and cytoskeletal remodelling [105,106]. Therefore, the influence of FSL-biotin insertion on kodecyte's shape, size and viability would also be investigated. The presence of serum has shown to affect insertion and retention of FSL constructs [98,99] or any other

exogenous molecule insertions [107]. Thus, in this study, the presence of serum affecting the FSL-biotin insertion and retention on Jurkat cells would be investigated.

1.4.5 Synthetic surfaces for adhesion

The ability to culture cells *in vitro* is a fundamental aspect of modern science. Today, polystyrene plates are widely used as a platform for evaluating clinical and therapeutic complex biological systems. However, to enable cell adhesion, they are subjected to a range of different chemical functionalities like carboxyl, amine, hydroxyl or ketone groups to the surface using physicochemical treatments such as plasma modification. Despite all these strategies, adhesion of suspension cells such T-cells and stem cells still require pre-treatment strategies [108,109]. Therefore, the ability of FSL constructs to adhere to cell culture surfaces will also be investigated. In addition to polymers, the ability of FSL constructs to adhere biotin kodecytes to non-traditional surfaces like stainless-steel would be investigated.

1.5 Objective

The aim of this research is to:

1. Investigate the ability of FSL-biotin to modify laboratory cultured cells (Jurkat).
2. Determine the optimal concentration and culture conditions for effective insertion of FSL-biotin into Jurkat cells.
3. Determine the effect of FSL-biotin on cell size and cell viability and their persistence on Jurkat cells.
4. Investigate adhesion of suspension Jurkat cells to inert cell culture and metal surfaces using FSL-biotin-streptavidin model.

Chapter 2 Methods and Results

Previous studies have shown that insertion of FSL constructs can be used to safely and efficiently modify blood cells, endometrial cells and embryos [91,95,97-99,101]. In this study, two different types of standard tumour cell lines, MCF-7 and Jurkat cells, were used to establish the parameters and consequences of FSL-biotin insertion. MCF-7 cells are breast cancer cells and are adherent in nature and were used as controls to see if FSLs would prevent or impair normal adherence. As the focus of this study is to modify and adhere non- adherent cells to inert surfaces, optimization and characterization studies were widely carried out using non-adherent lymphoblastic T-Jurkat cells. Due to the developmental nature of these assays, parameters were slightly varied between assays to allow for continual optimisation of insertion conditions and detection using immuno-fluorescent staining. The ability and strength of modified Jurkat cells adherence to solid surfaces were investigated on both planar (microplates) and non- planar (microsphere) surfaces. Time dependent effect of FSL-biotin on cell viability was also evaluated using trypan blue assay.

2.1 FSL-biotin insertion in adherent cells

2.1.1 Culturing MCF-7 cells

MCF-7 cell lines were maintained in a complete media (CM) composed of Roswell Park Memorial Institute-1640 (RPMI 1640) medium (Life Technologies, cat# 11875) supplemented with 10% fetal bovine serum (FBS), 1% GlutaMax (Life Technologies, cat# 35050061) and 1% penicillin/streptomycin (Life Technologies, cat# 5140122). The cells were incubated in a 37°C incubator with an atmosphere of 5% CO_2 in air. The cells were passaged every 3-4 days before reaching confluence. The growth medium was aspirated and cells were washed thrice with 1× PBS, trypsinized and were dispersed by pipetting with fresh medium before cells were transferred to a new flask at 1: 3 ratio of old to new media. For optimization studies, MCF-7 breast cancer cells were seeded into Terasaki plates with a cell density of 1 x 10^5 cell/cm^2. Plates were incubated for approximately 24 hours at 37°C to prepare monolayers of approximately 70% confluence.

2.1.2 Preparing FSL constructs

A variety of lipids have been used to create FSL constructs, including 1,2-dioleoyl-sn- glycerol-3-phosphoethanolamine (DOPE), cholesterol, and natural and synthetic ceramides. FSLs with

ceramide and DOPE lipid tails were suggested to be best for insertion and membrane retention, however, there are no published data [94]. Therefore, investigations were carried out to determine the optimal lipid tail for FSL-biotin insertion into MCF-7 cells.

The FSL-biotin with DOPE tail (FSdL, Cat# 1887786-1) is available from Kode Biotech and widely used in most studies. However, the other variants of FSL-biotin, with ceramide (FScL; in R&D) and sterol (FSsL; 416661-1 R&D) as lipid tail, are still under development. MCF-7 cells were inserted with these three types of FSL-biotin and assessed for effective insertion. Figure 4 presents the molecular weight of FSL-biotin variants and 50µM concentrations from 5 $mgmL^{-1}$stock was prepared by dispersing 2µl of FSdL-biotin and 1.8µl of each FScL and FSsL in 998µl of insertion media. RPMI 1640 (without any serum components or antibodies or growth factors) was used as insertion media.

2.1.3 Koding MCF-7 cells with FSL-biotin variants

Each of the FSL-biotin variants listed in Figure 4 were incubated with MCF-7 breast cancer cells seeded into Terasaki plates with monolayers of MCF-7 cells with approximately 70% confluence. Cells were incubated with insertion media (RPMI) for 2 hours at 37°C. Cells in Terasaki plates, were then gently washed using PBS and plates blotted gently with paper towels.

Detection of FSL-biotin insertion into MCF-7 cells are assayed using biotin- streptavidin model. To analyse whether the biotin-streptavidin model worked under these conditions, a two-step experiment was devised whereby MCF-7 were incubated with or without FSL-biotin as per standard protocols (i.e., for 2 hours at 37°C). Immediately after washing, the cells/ kodecytes were further incubated with a secondary label streptavidin Alexa Fluor® 488 (0.1 $mgmL^{-1}$; Life Technologies; S11223) for 30 minutes in a humidified dark chamber at 37°C and 5% CO_2 concentration. Plates were washed thrice to remove any excess secondary antibody and PBS was added to each well to aid viewing under the fluorescence microscope. The sample was excited at 488 nm and emission recorded at 1.9s exposure using WIB filter (which is a low pass filter which transmits everything above 550nm) of the fluorescence microscope (Olympus BX-51 microscope and Optronics camera). To avoid prejudice of visual based analysis, the strength of the fluorescent signal exhibited by kodecytes were quantified using a graphical software- ImageJ. For this, all the images were converted to an 8- bit grey scale image and regions of cells with fluorescence were selected. The "Analyse" function in ImageJ, assigns a numerical grey value to each level of brightness between 0 to 255, with zero

representing lowest degree of brightness. From this, the mean grey value is automatically generated by the ImageJ software by dividing grey value of all the pixels in the selected region by the number of pixels within the area. Areas next to the cells with no fluorescence were selected to calculate the mean grey value of the background. The mean grey value of fluorescent samples is then divided by the mean grey value of their corresponding background to normalize uneven illumination and avoid any bias.

2.1.3.1 Results and interpretation

Indirect immunofluorescence visualized using streptavidin conjugated Alexa Fluor® 488 and their respective Direct interference contrast (DIC) images are presented in Figure 5. The results illustrate that all three different types of FSL-biotin, FSdL, FScL and FSsL, can transform MCF-7 cells into biotin kodecytes. The expression of FSL-biotin appears to be localized to cell membrane. While the presence of the cells was evident under DIC, absence of fluorescent staining in unmodified MCF-7 cells (in culture media) implies that the streptavidin Alexa Fluor® 488 binding to biotin kodecytes are very specific. Both modified and unmodified MCF-7 cells are observed to have a round morphology when observed under the DIC microscopy.

The fluorescent signal exhibited by biotin kodecytes inserted with FSdL-biotin appears to be stronger in comparison to FScL and FSsL. The results of normalized mean grey of biotinylated MCF-7 kodecytes graphically presented in Figure 6, as expected, agree with the above findings. One-way ANOVA was calculated using SPSS statistical software. Threshold of p is set to 0.01 and $p<0.01$ would be considered statistically significant. The calculations presented in Table 3 illustrate the increase in staining intensity in FSdL is statistically significant when compared to control and FSsL-biotin modified cells. Although, the intensity of FSdL modified cells are higher, the difference in fluorescent intensity between FScL, and FSdL is statistically insignificant. This would be expected as the structural difference between FScL and FSdL is minimal. Based on these findings and construct availability, FSdL-biotin was the construct of choice. FSL modification did not impact on cellular adhesion to cell culture surface.

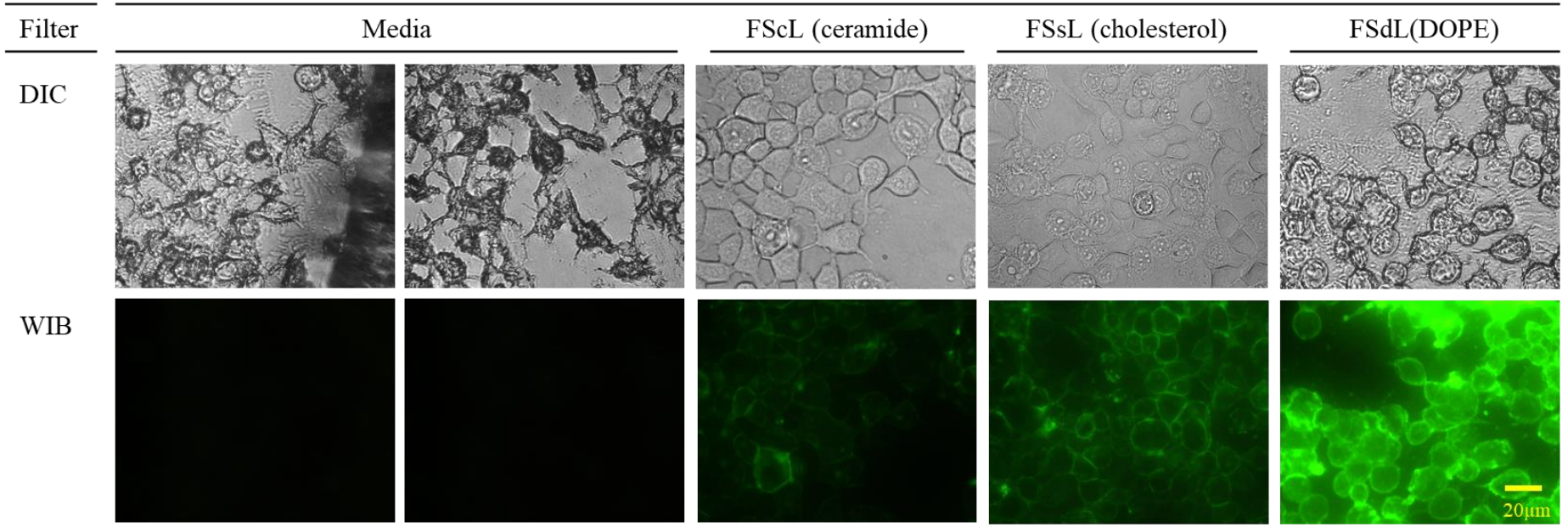

Figure 5 MCF-7 cells biotinylated using FSL-biotin with ceramide(FScL), cholesterol (FSsL) and DOPE (FSdL) tail. Each well was seeded with equal number of cells and cultured for 24 hours to get ~70% confluence before modifying them with FSL-biotin. Fluorescent images captured under the WIB filter, post FSL treatment, are presented with their respective DIC images. Untreated MCF-7 cells with/without (first column) secondary streptavidin Alexa Fluor® 488 were used as controls.

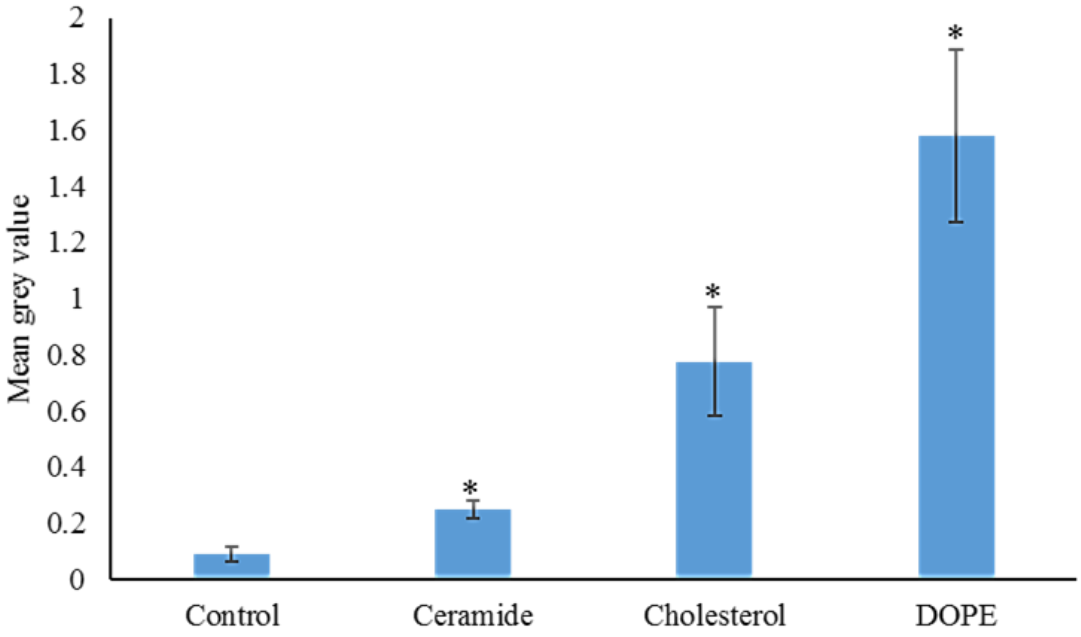

Figure 6 Normalized mean grey value measurements of FSL-biotin inserted into MCF-7 cells. The increase in fluorescent signal in cells inserted with FSL-biotin is statistically significant compared to the control cells ($p < 0.01$).

Table 3 One-way ANOVA calculations to determine the statistical significance of increase in fluorescent signal.

Untreated	vs	Treated	Mean Difference	Std. Error	*p* value	95% confidence interval	
						Lower bound	Upper bound
Control		Ceramide	0.52	0.13	0.009	-0.90	-0.15
		Cholesterol	0.88	0.13	0.000	-1.26	-0.51
		DOPE	1.49	0.13	0.000	-1.86	-1.12

2.1.4 Optimizing the FSdL-biotin insertion conditions

To determine the optimal insertion concentration and incubation period, monolayers of MCF-7 cells grown on Teraski plates were incubated with varying concentrations of FSdL-biotin. A stock solution of 5 mgmL $^{-1}$ was prepared by dispersing 1mg FSdL-biotin in 200µl of sterile PBS (1×). From the stock, FSL-biotin at concentrations 0.5, 10, 25 and 50µM were prepared. RPMI (without serum lipids) is used as insertion media. Cells were incubated at 37°C and 5% CO_2. Incubation period was varied between 30 to 120 minutes. After washing and blotting the excess PBS from the plates, kodecytes were incubated with streptavidin Alexa Fluor® 488 (0.1 mgmL^{-1}) for 30 minutes in culture conditions. After thorough washing, stained cells were viewed under the WIB filter of fluorescence Olympus BX-51 microscope. Corresponding DIC images were also recorded for every fluorescent image. Fluorescence intensity was quantified as mean grey value and normalized using ImageJ analysis as described in section 2.1.3.

2.1.4.1 Results and interpretation

Transformation of MCF-7 cells to biotin kodecytes were detected by using fluorophore tagged Streptavidin molecule. The intensity of the fluorescent signal was observed to increase with increasing incubation time and concentration (Figure 7 & Figure 8). Fluorescence is exhibited uniformly around the periphery of the kodecytes. However, the staining pattern varies between different conditions. At least 120 minutes of incubation is required to observe mild fluorescence in kodecytes modified with 0.5µM FSdL-biotin. At 5µM concentration, FSL molecules removed after an hour produced a mild staining while kodecytes incubated for 2 hours with FSL-biotin exhibited moderate staining (see Figure 7). Moderate to high intense patches of fluorescence are observed in 50µM kodecytes incubated between 30 to 120 minutes, respectively.

The mean grey value was analysed using ImageJ tool to obtain more quantitative data. The graphical plot presented in Figure 8 is normalized against the background to avoid any bias. The results illustrate the intensities observed under the fluorescence WIB filter, increases with FSdL-biotin insertion concentration and incubation time. ANOVA analysis with *post hoc* Dunnett T test (see Table 4) showed, after two hours of removal, the fluorescent intensity exhibited by all the kodecytes (inserted with 0.5, 5 and 50µM FSdL-biotin) is highly significant compared to the control (0µM) cells ($p<0.01$). However, when the incubation was reduced to an hour, only those cells inserted with 5 and 50µM FSL were observed with significant signals ($p<0.01$). With a 30-minute incubation period, only the kodecytes inserted with 50µM FSL-biotin are statistically significant relative to control cells.

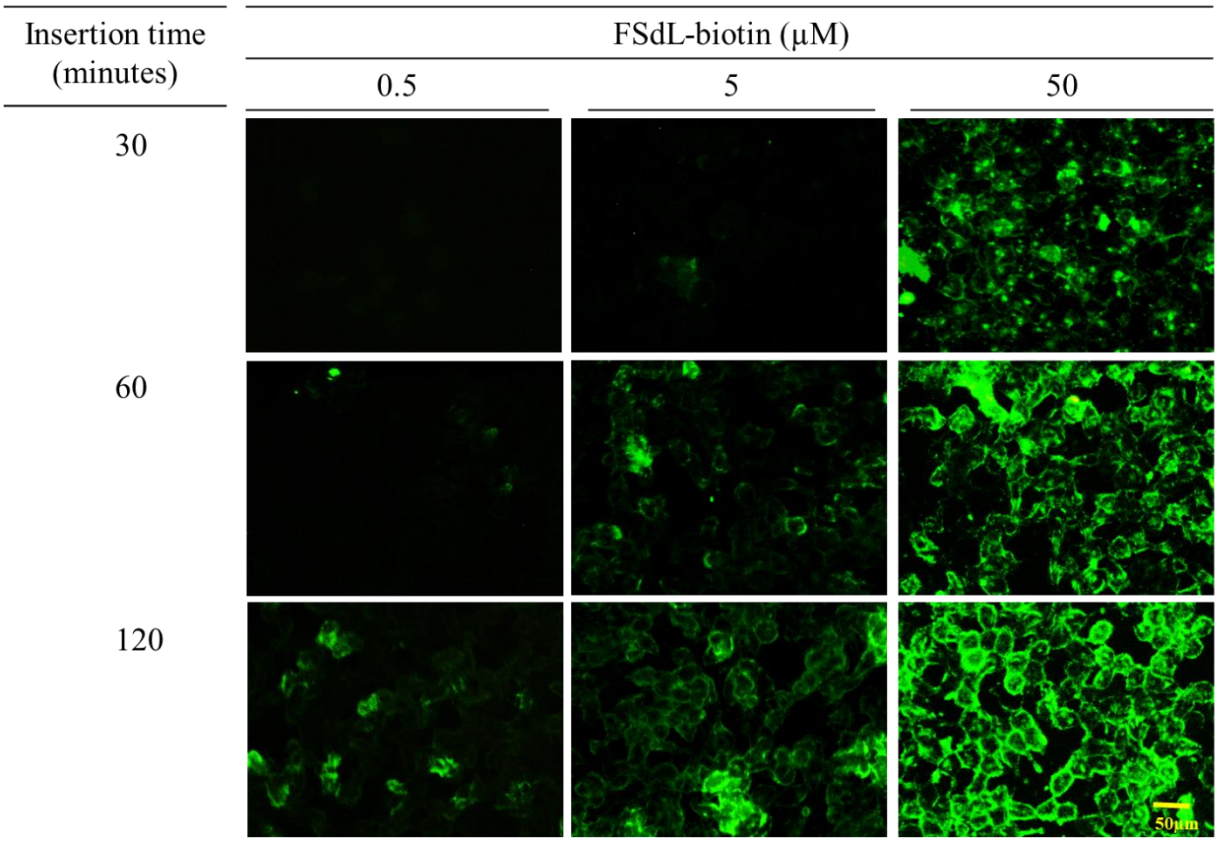

Figure 7 Comparison of FSdL-biotin insertion into MCF-7 cells at different concentration and time points. Cells treated with varying concentrations of FSdL-biotin were incubated at 3 different time points. Cells magnified at ×200 with 1.9s exposure.

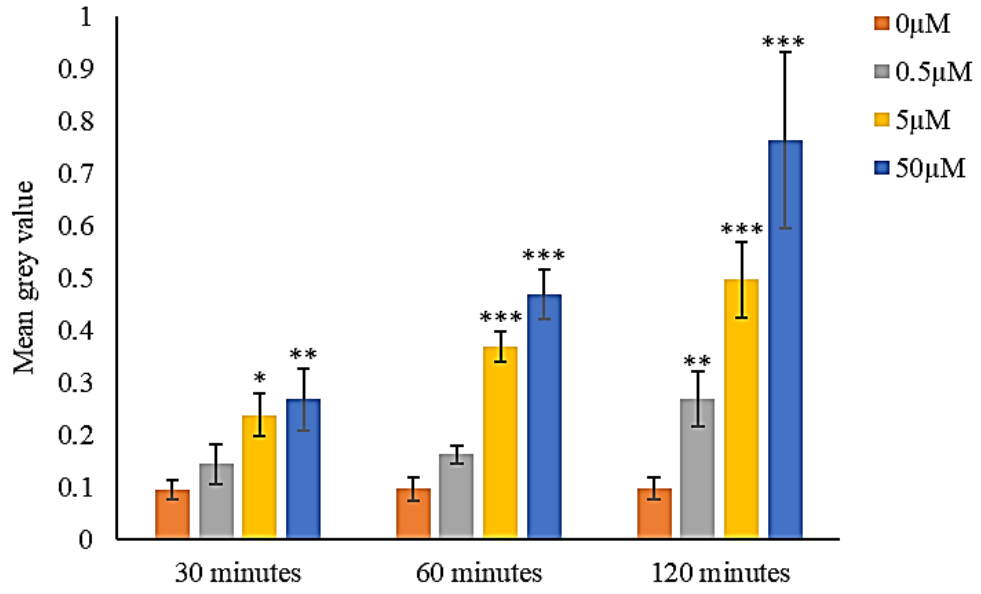

Figure 8 Fluorescence exhibited by MCF-7 kodecytes inserted at different concentrations and timepoints. Increase in fluorescent signal is semi-quantitively measured as mean grey value. One-way ANOVA with *post hoc* Dunnett carried out to test the statistical significance shows the increase in fluorescent intensity is statistically significant. $p<0.05$ (*), $p<0.01$(**) and $p<0.001$ (***).

Table 4 Statistical significance of fluorescent intensity increase, relative to concentration and incubation time. One-way ANOVA with *post-hoc* Dunnett was carried out for correcting for multiple comparisons and avoiding inflating α.

Untreated (µM)	vs	Treated (µM)	Time (minutes)	Mean Difference	*p* value	95% Confidence Interval	
						Lower Bound	Upper Bound
0		0.5	30	0.07	0.797	-0.09	0.22
		0.5	60	0.08	0.542	-0.07	0.24
		0.5	120	0.19	0.009	0.04	0.34
		5.0	30	0.16	0.036	0.01	0.31
		5.0	60	0.29	0.000	0.14	0.44
		5.0	120	0.42	0.000	0.27	0.57
		50.0	30	0.19	0.009	0.04	0.34
		50.0	60	0.39	0.000	0.24	0.54
		50.0	120	0.69	0.000	0.53	0.84

2.1.5 Koding MCF-7 cells in suspension

To assess the effect of FSdL-biotin insertion in suspension culture, 1×10^6 MCF-7 cells trypsinized and washed from the culture flask were incubated with an equivolume of FSdL-biotin in solution. A concentration of 50µM with an incubation period of 2 hours were used based on the results obtained from section 2.1.4 above. To detect the success of MCF-7 cells transformation to kodecytes, the cells were further incubated with streptavidin Alexa Fluor® 488 for 30 minutes at 37ºC in a 5% CO_2. The fluorescence exhibited by transformed kodecytes was captured under the WIB filter of Olympus BX-51 microscope with an exposure of 1.9s. Images captured under the DIC filter was used to confirm the presence of cells.

2.1.5.1 Results and interpretation

The results presented in Figure 9A illustrates the capability of FSL constructs to modify MCF-7 cells in suspension. The fluorescent signals exhibited by cells in suspension visually appear to be equivalent to the signal from monolayer culture. However, at higher magnification (×1000), the FSL insertion was observed to cover the entire cell surface area and had a punctate (marked with points and dots) pattern. This pattern was previously observed with RBCs and was believed to be an artefact related to clustering of the constructs in the membrane post reaction with streptavidin (Image courtesy Dr Eleanor Williams from AUT Centre for Kode™ Technology Innovation) (Figure 9B). The morphology of both modified and unmodified cells under the DIC filter are round in shape.

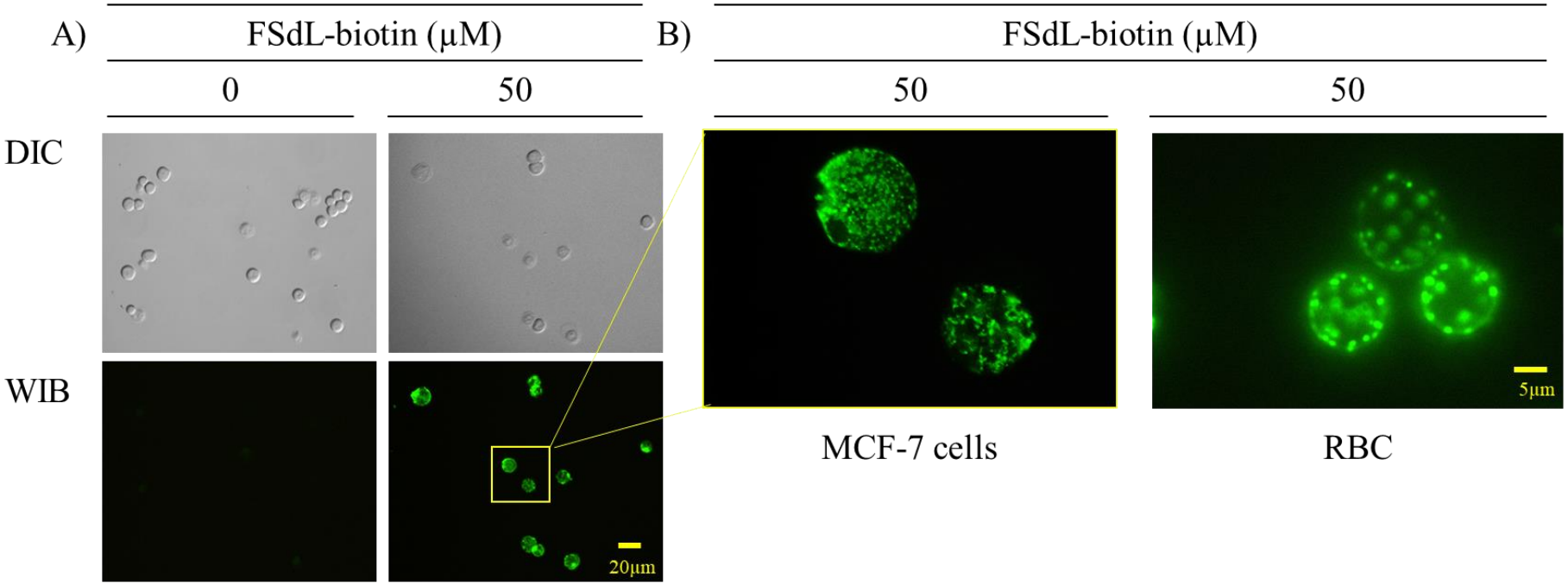

Figure 9 Fluorescent staining exhibited by MCF-7 cells modified by FSdL-biotin and streptavidin 488. A) Fluorescence is exhibited in only biotin kodecytes (bottom images). Binding of streptavidin fluorophore is specific to FSL-biotin inserted MCF-7 cells. DIC images on the top shows cells present in both the FSL unmodified and modified reactions. B) High magnification (×1000) of the FSL modified MCF-7 cells is presented as inset (from yellow box). Punctate (speckling) pattern observed at a similar magnification in red blood cells (RBC) is presented on the right. (RBC image courtesy Dr. Eleanor Williams).

2.2 FSdL-biotin insertion in non-adherent cells

2.2.1 Culturing Jurkat cells

The primary aim of this study was to modify and adhere non-adherent cells. Jurkat cells (a generous gift from Dr Hilary Sheppard Lab, University of Auckland) were routinely cultured in tissue culture flasks (Nunc; cat# 156367) using complete media (CM) constituting RPMI 1640 medium (Life Technologies, cat# 11875) supplemented with 10% (v/v) new born calf serum (Life Technologies, cat# 16016-159), 1× GlutaMax (Life Technologies, cat# 35050061) and 1% penicillin/streptomycin (Life Technologies, cat# 5140122). Actively growing cells were maintained between 2×10^6 to 3×10^6 cells/ ml and passaged every 3 days. The cell cultures were maintained at 37ºC in a 5% CO_2/95% air-humidified atmosphere. Medium was changed when the cell solution has adopted a yellow colour due to pH changes. This was carried out by spinning down the cultures at ×120g for 5 min (Megafuge; Thermofisher, cat# 50138896-b) in 15 ml centrifuge tubes to pellet live cells. After removing most of the debris in the supernatant, the pellets were resuspended in a fresh media. PBS was used for washing the cells. For subcultures, cells are spilt in a 1:3 ratio of old: new media. For optimization studies, Jurkat cells with a cell density of 1×10^6 cells/ml were mixed with an equal volume of FSdL-biotin in insertion media (RPMI without serum lipids).

2.2.2 Preparing FSdL-biotin

A stock solution of 5 mgmL $^{-1}$ was prepared by dispersing 1mg of FSdL-biotin in 200µl of sterile PBS. From the stock, FSdL-biotin at concentrations, 5, 10, 25 and 50µM, were prepared. Serum (lipid) free RPMI was used as insertion media.

2.2.3 Optimizing FSdL-biotin insertion conditions

For inserting FSdL-biotin, Jurkat cells with a cell density of 1×10^6 cells were harvested and washed thrice with sterile PBS. The media was replaced with an equivolume of freshly prepared FSdL-biotin. The cells were cultured at 37°C, 5% CO_2 concentration for 2 hours. After 2 hours, the FSL modified cells, also referred to as biotin kodecytes, were collected by centrifugation at 3000 rpm for 5 min (Sorvall; Cat# MC12V). After washing thrice with sterile PBS, the kodecyte pellets were resuspended in RPMI media.

Immunofluorescence was used to detect the successful transformation of Jurkat cells into biotin kodecytes. This was achieved by labelling the cells with streptavidin Alexa Fluor® 488 (0.1 mgmL $^{-1}$) for 30 minutes at 37°C and 5% CO_2 concentration. Cells were then washed and

analysed immediately using fluorescence microscopy (Olympus BX-51 microscope) for binding. The sample was excited at 488 nm and emission was analysed at >550 nm using WIB filter of the fluorescence microscope for 1.9s. Fluorescence exhibited by kodecytes was quantified as mean grey value and normalized using ImageJ analysis as described in section 2.1.3.

2.2.3.1 Results and interpretation

The presence of fluorescent staining on kodecytes, shown in Figure 10, verifies the insertion of FSL molecule into the Jurkat cell surface. All the images were captured using an exposure time of 1.9s. As observed from the fluorescent images, it is evident that all the cells could be modified by FSL-biotin. Also, the strength of the fluorescent signal appears to increase in a dose dependent manner. The fluorescent intensity exhibited by the kodecytes, quantified as mean grey value (see Figure 11), confirms this. One-way ANOVA with *post-hoc* Dunnett was used to test the statistical significance in comparison to unmodified cells. While the increase is marginally significant with 5µM insertion ($p<0.05$), it becomes highly significant ($p< 0.001$) as the concentration of FSL inserted is increased (Table 5). No fluorescence is observed in unmodified (0µM FSL-biotin) or control cells (images not shown). This shows that the streptavidin Alexa Fluor® 488 binding to biotin kodecytes are specific. At higher magnifications, (bottom row of Figure 10), the fluorescent staining was observed to have the punctate pattern as observed in Figure 9. As the concentration was increased, round patches of brightly fluorescent discrete domains were revealed. The diameter of the cell also appears to have increased with increasing FSL concentration that is investigated in the next section.

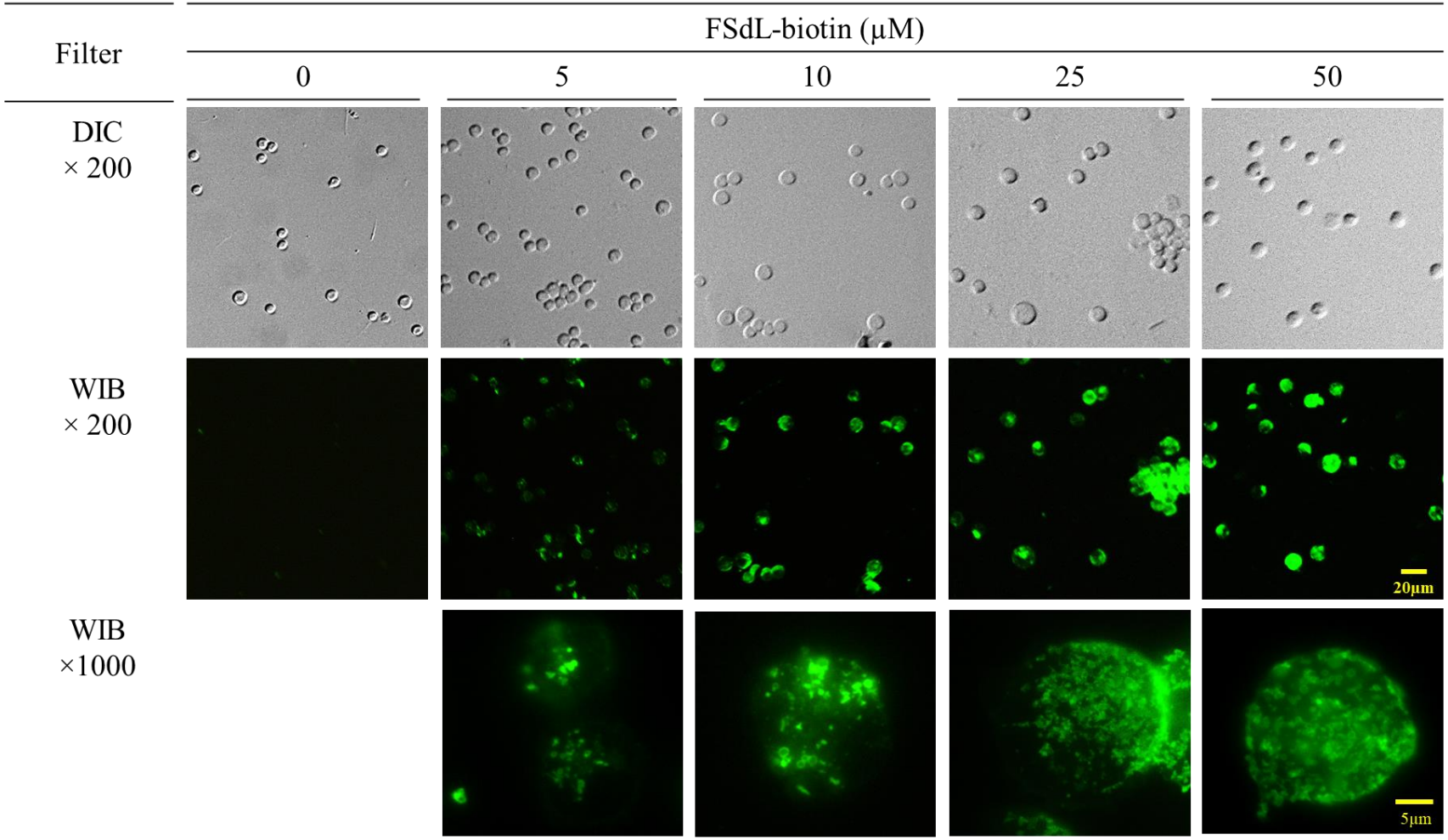

Figure 10 Immunofluorescence detection of FSdL-biotin modified Jurkat cells (kodecytes). Jurkat cells were modified with varying concentrations of FSdL-biotin and conjugated with streptavidin Alexa Fluor® 488. Images captured under the DIC and the fluorescent signals exhibited by kodecytes captured using the WIB fluorescence filter are presented in first two rows. Higher magnification images in the bottom row show typical variation in staining pattern.

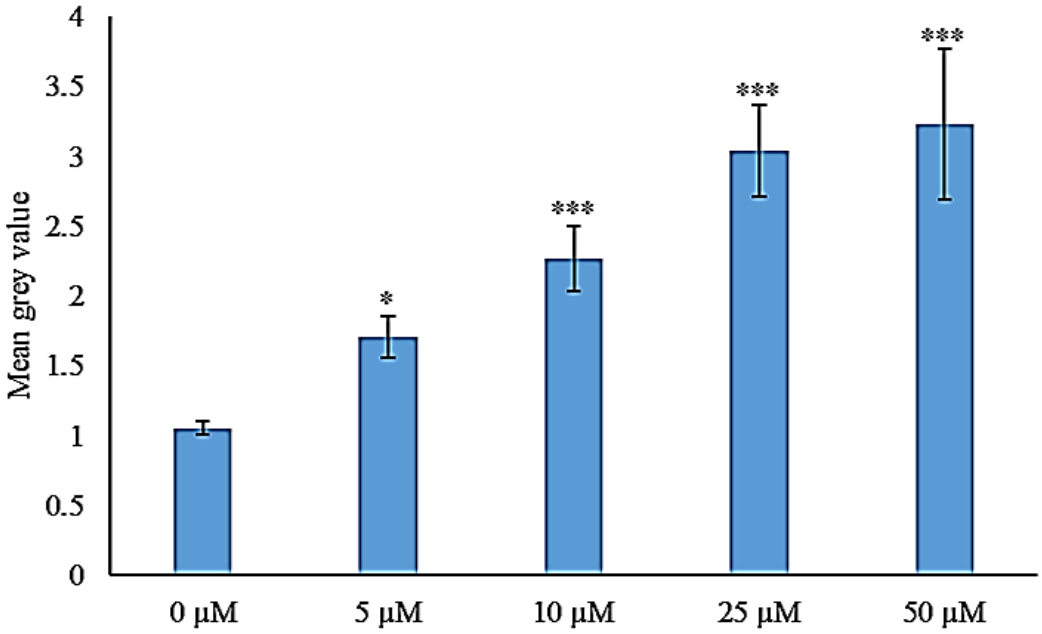

Figure 11 Fluorescent strength exhibited by biotin kodecytes quantified as normalized mean grey value. ANOVA analysis with *post hoc* Dunnett implies that the increase is statistically significant.

Table 5 Increase in fluorescence intensity statistically analyzed with one-way ANOVA and *post-hoc* Dunnett.

Untreated (µM)	Treated (µM)	Mean Difference	Std. Error	*p* value	95% Confidence Interval	
					Lower Bound	Upper Bound
0	5	0.65	0.20	0.011	0.14	1.17
	10	1.22	0.20	0.000	0.70	1.74
	25	1.99	0.20	0.000	1.47	2.50
	50	2.18	0.20	0.000	1.66	2.70

2.3 Retention studies for non-adherent Jurkat cells

Retention studies were carried out to investigate the stability of FSdL binding to Jurkat cells. This was accomplished by harvesting kodecytes from culture at regular intervals following FSL-biotin treatment and labelling them with streptavidin Alexa Fluor® 488. The stability of FSL-biotin binding to kodecytes were visually detected under the WIB filter of fluorescence microscope. Serum provides essential growth factors and nutrients for healthier cell growth. Therefore, the effect of FSL-biotin insertion and retention in complete media (CM) was also simultaneously investigated. CM contains RPMI added with 10% new born calf serum, 1× GlutaMax and 1% pencillin-streptomycin.

2.3.1 Optimizing the retention concentration and conditions

Jurkat cells with a cell density of 1×10^6 cells were harvested and washed thrice with sterile PBS. The cells were incubated with an equivolume of freshly prepared FSdL-biotin. For studying the effect of serum, RPMI was replaced with CM used for culturing Jurkat cells (see section 2.2.1) as insertion media. Cells were cultured at 37°C, 5% CO_2 concentration for 2 hours. After 2 hours, the FSL biotin kodecytes, were collected by centrifugation at 3000 rpm for 5 min (Sorvall; Cat# MC12V). After washing thrice with sterile PBS, the kodecyte pellets were resuspended in RPMI/ CM and returned to culture conditions. To test the persistence of FSL constructs, small aliquots of kodecytes were harvested from culture at regular intervals (0, 12 and 24 hours) and immediately tagged with streptavidin Alexa Fluor® 488 (0.1 mgmL $^{-1}$) for 30 minutes at 37°C and 5% CO_2 concentration. Kodecytes were then washed and analysed immediately for fluorescence under the WIB filter of the fluorescent microscope (Olympus BX-51 microscope). Retention studies involve comparison of fluorescence strength from multiple parameters, such as different insertional and retentional conditions and; different concentrations, from various experiments. In addition, there were variations in order cells were visualized and number of cells used for used for visualization over time. Thus, fluorescent intensity from retentional studies were semi- quantitatively quantified using the standard grading system.

2.3.1.1 Results and interpretation, at 0-hour

The results presented in Figure 12 compares the intensity of fluorescence produced by kodecytes inserted using serum free RPMI or CM (with 10% serum) as the insertion media. Intensities in kodecytes inserted with RPMI are comparable to previous results in Figure 10. Kodecytes inserted with the presence of serum (CM) also illustrates increase in fluorescence with increasing FSdL-biotin concentration. However, the fluorescent signal exhibited by kodecytes in CM is less compared to RPMI insertion optically. A semi-quantitative measurement of FSL expression achieved by using a standard grading system based on the emitted fluorescence is presented in Table 6. While the fluorescent intensity was graded at medium (++) to strong (+++) in kodecytes where the FSLs were inserted in RPMI (serum free media), intensity displayed by kodecytes inserted in the presence of serum (in CM), was mild (+) to medium (++).

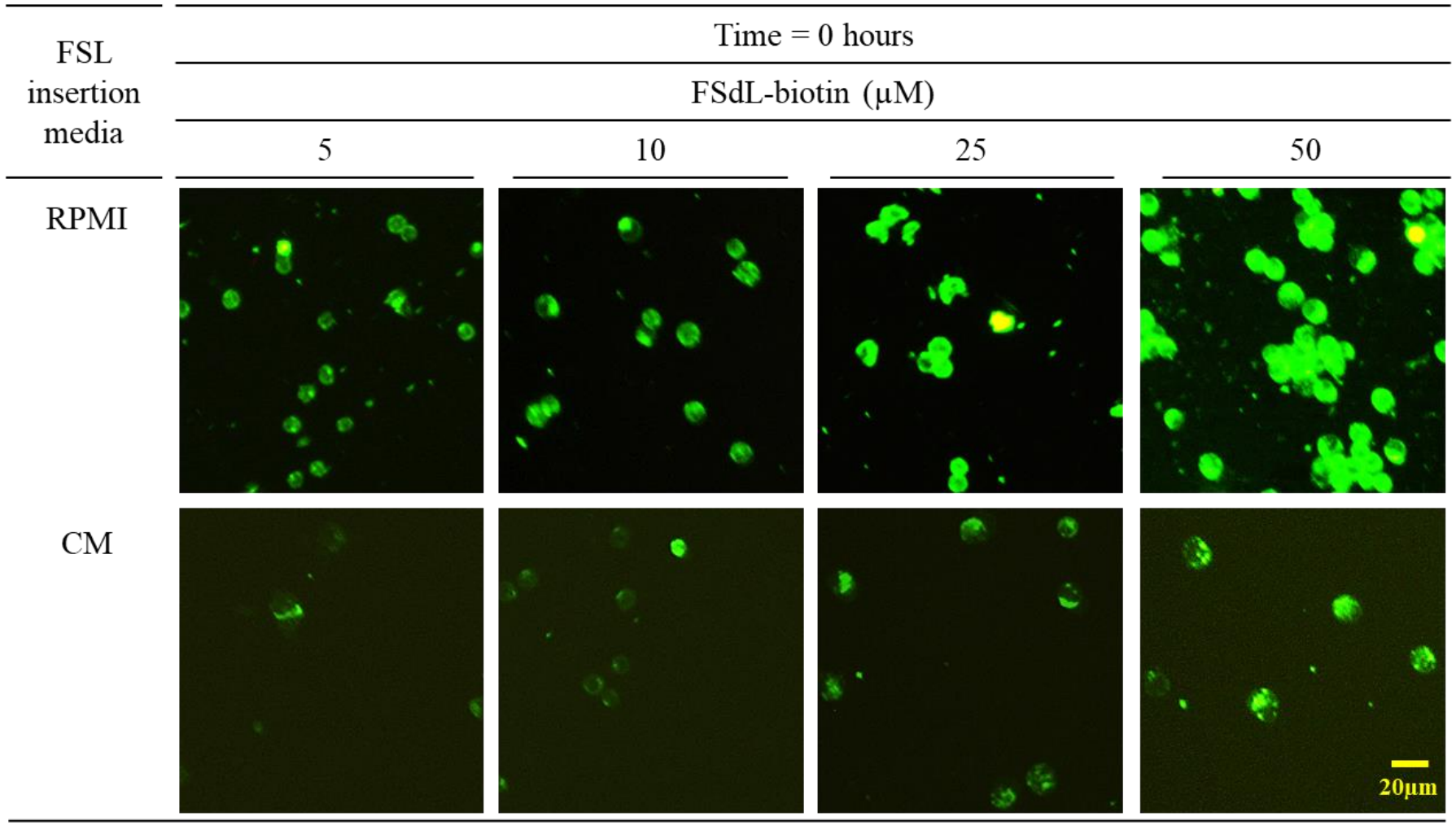

Figure 12 Insertion of FSdL-biotin into Jurkat cells in the presence (CM) or absence (RPMI) of serum. Fluorescence detection using streptavidin alexa flour® 488 (0.2 $mgmL^{-1}$) immediately after 2 hours of FSdL-biotin insertion (0-hour) showed that the insertion of FSL was inhibited in the presence of serum.

Table 6 Fluorescent intensity of biotin kodecytes at 0- hour, graded based on the fluorescence emission under WIB filter, with exposure of 1.9s

FSL insertion media	Time= 0 hour			
	FSL- biotin (µM)			
	5	10	25	50
RPMI	++	++	+++	+++
CM	+	+	++	++

2.3.1.2 Results and interpretation, at 12-hours

After 12 hours, 100µl aliquots of kodecytes inserted in RPMI/CM and cultured in the presence (CM) or absence of serum (RPMI), were tagged with streptavidin 488 and observed under the Olympus BX-51 to determine the persistence of FSL-biotin. Figure 13 shows the DIC and fluorescent images of RPMI inserted kodecytes cultured either in RPMI or CM. Compared to 0-hour, a typical decrease in fluorescence is observed across different treatments. Kodecytes cultured in RPMI have better efficacy in retaining the fluorescence than kodecytes cultured in serum enhanced media (CM). DIC and fluorescent images of kodecytes inserted in CM and cultured in RPMI or CM are presented in Figure 14. From the results, it is evident that >50% of CM inserted kodecytes did not fluoresce after 12 hours, presumably due to less insertion.

The strength of the fluorescent signal exhibited by biotin kodecytes is semi-quantitatively measured using standard grading system and presented in Table 7. The results show the fluorescence emitted by RPMI inserted kodecytes cultured in serum free RPMI exhibits moderate (++) to strong (+++) intensity at concentrations ≥10µM. However, when cultured in CM with 10% serum, the intensity is reduced showing a mild (+) to moderate (++) grading. At 12 hours, regardless of the culture media, biotin kodecytes inserted in the presence of serum (CM) express a mild (+) or negligible staining. Kodecytes observed with negligible fluorescent levels are presented with a negative (-) sign. Based on these findings, it could be implied that the presence of serum in the insertion media limits the persistence of FSL-biotin on biotin kodecytes to 12 hours and CM prevents or hinders FSL insertion.

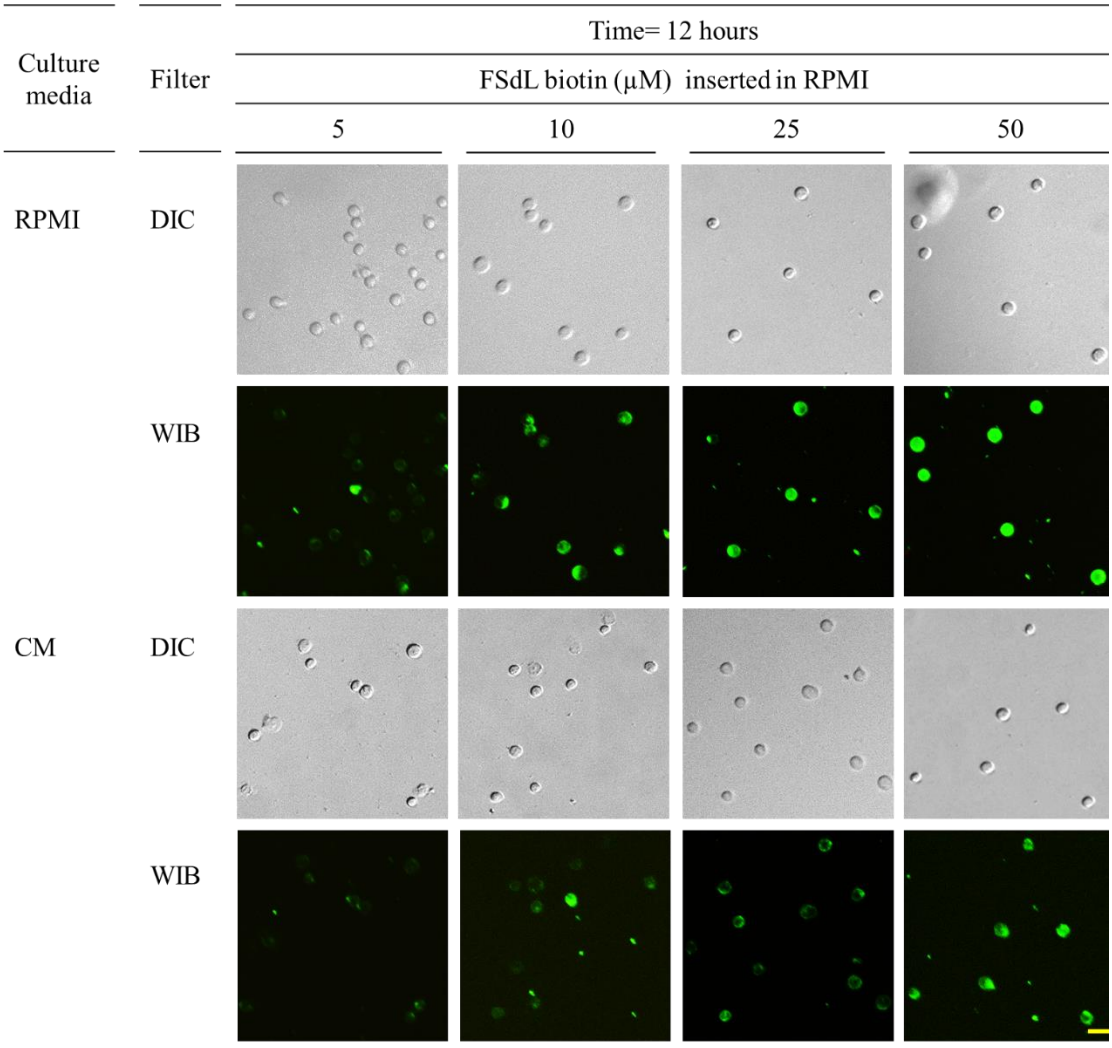

Figure 13 Fluorescent images of RPMI inserted biotin kodecytes after 12-hour culture. Varying concentration of biotin kodecytes, after FSL insertion, are suspended in either RPMI or CM for further culture. The first and second rows show the DIC and fluorescent images of biotin kodecytes inserted and cultured in RPMI media respectively. In the bottom two rows, DIC and fluorescent images of kodecytes cultured in CM (with 10% serum) are presented (scale bar = 50μm).

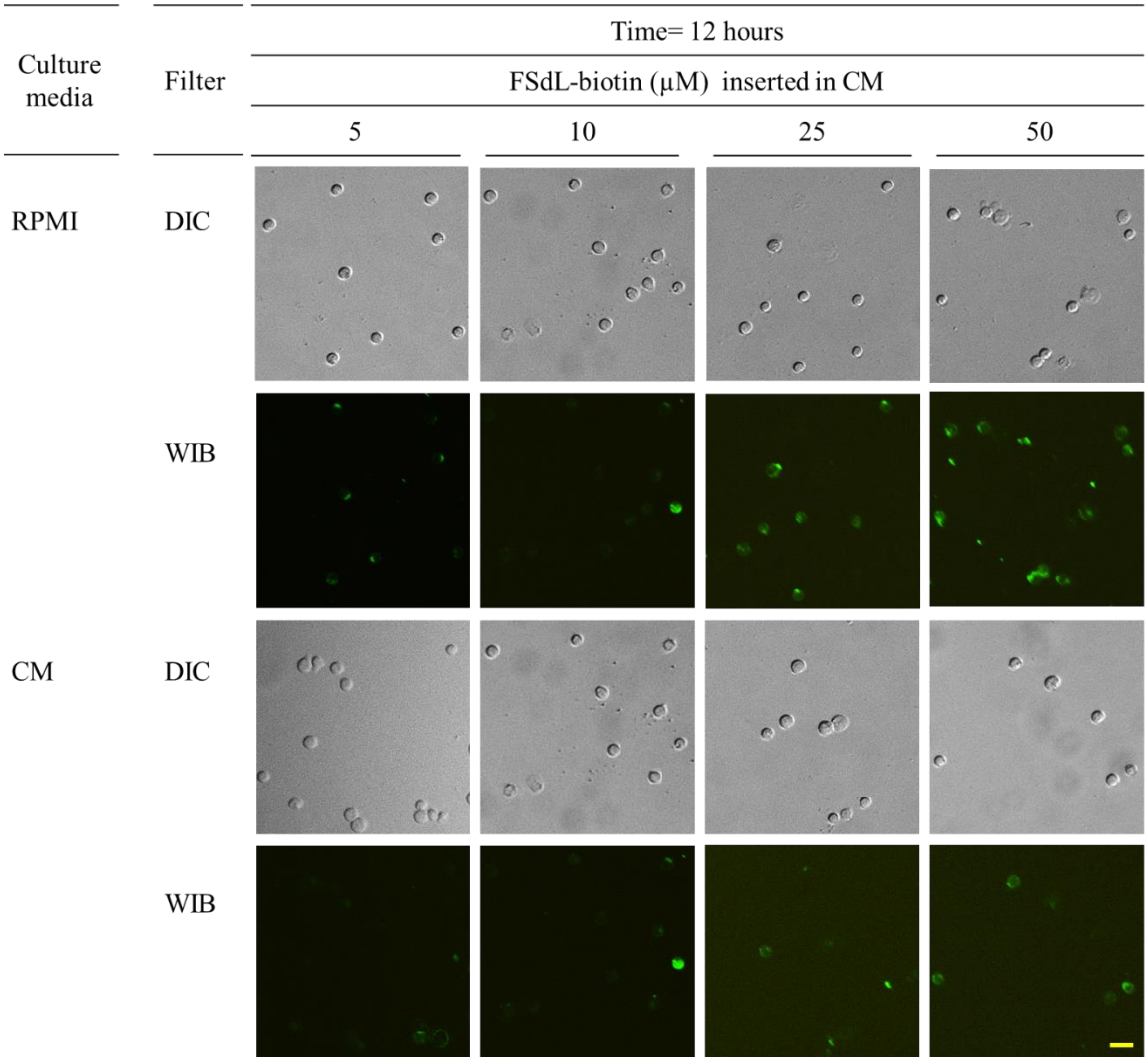

Figure 14 Fluorescent images of CM (with 10% serum) inserted biotin kodecytes after 12-hour culture. Varying concentration of FSL-biotin was inserted into Jurkat cells using CM (with 10% serum) as insertion media and further cultured in either RPMI or CM. The first two rows present images captured from the DIC and fluorescence filter for CM inserted kodecytes cultured in RPMI. Kodecytes inserted and cultured in CM are presented in the lower two rows (scale bar = 50μm).

Table 7 Fluorescent intensity of biotin kodecytes graded based on the fluorescence emission at 12-hour

FSL insertion media	**Retention media**	**Time= 12 hour**			
		FSL- biotin (μM)			
		5	**10**	**25**	**50**
RPMI (serum free)	RPMI	+	++	+++	+++
	CM	-	+	+	++
CM (10% serum)	RPMI	-	-	+	+
	CM	-	-	+	+

2.3.1.3 Results and interpretation, at 24-hours

The ability of RPMI inserted kodecytes to retain FSL molecules was investigated 24-hours after insertion. The DIC images and fluorescent images captured using the WIB filter of Olympus BX-51 microscope are presented in Figure 15. The intensity of fluorescence is greatly reduced across different treatments compared to their respective treatments at hours 0 and 12. While kodecytes inserted with ≥10µM FSdL-biotin and retained in RPMI media were observed to exhibit mild to moderate fluorescent staining, loss of fluorescent signal in CM cultured kodecytes is evident from their respective DIC images. Regardless of the culture medium, fluorescent staining was completely lost in 5µM kodecytes. Fluorescence intensity grading is consistent with the observations made from images captured under the WIB filter at exposure 1.9s. As the intensity of fluorescence exhibited by kodecytes inserted in CM (with 10% serum) were negligible or very mild at 12 hours, immunofluorescence studies on them were not investigated at 24-hours.

2.3.1.3.1 Optimal conditions for FSL retention

Jurkat cells, at concentration 10µM or more, inserted and cultured in RPMI have retained FSdL-biotin beyond 24 hours. Although kodecytes cultured in presence of serum (CM) express fluorescence, the intensity is weaker in comparison to RPMI cultured kodecytes. In fact, the fluorescence was observed to completely disappear at lower concentration, within 12 hours. Based on these findings, it is evident that maximum retention of FSdL-biotin is achieved when cells are inserted and retained in serum free RPMI media. A minimum of 10µM FSdL-biotin inserted has shown to persist for at least 24 hours at the cell surface.

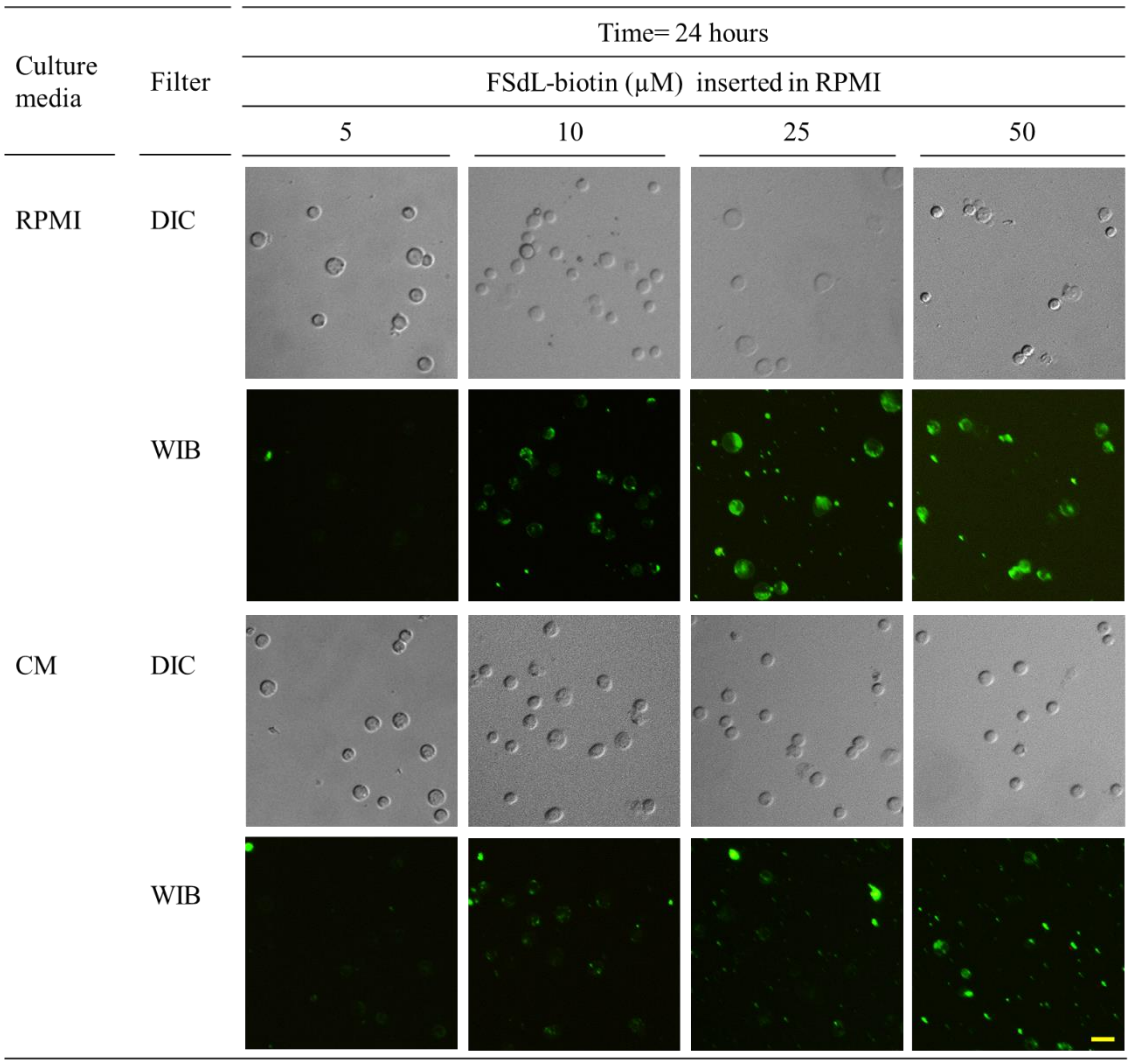

Figure 15 Persistence of FSdL-biotin on RPMI inserted kodecytes after 24 hours. DIC and fluorescence images in the first two rows represent RPMI inserted kodecytes cultured in RPMI. Bottom two rows show FSL persistence in CM cultured kodecytes (scale bar = 50µm).

Table 8 Fluorescent intensity of biotin kodecytes graded based on the fluorescence emission at 24-hours

FSL insertion media	**Retention media**	**Time= 24-hour**			
		FSL- biotin (µM)			
		5	**10**	**25**	**50**
RPMI (serum free)	RPMI	-	+	++	+++
	CM	-	+	+	+

2.4 Characterizing Jurkat biotin kodecytes

2.4.1 Structure of kodecytes

Light microscopy images have limited resolution (as the maximum magnification is generally ×1000). In contrast, Scanning Electron Microscopy (SEM; Hitachi SU-70) is widely used for studying the ultrastructure of biological samples. For viewing the samples under SEM, kodecytes were fixed overnight at 4°C with 2.5% glutaraldehyde. Fixed cells were then washed and dehydrated with graded ethanol series, starting with 25%, 50%, 75%, and 95% ethanol and three exchanges of anhydrous 100% ethanol. Although, it is appreciated that this procedure will probably remove the FSL constructs, the prior fixation with glutaraldehyde should be adequate to maintain the size and structure. However, studies have shown ethanol, used in dehydration step, can fuse with the lipids on the cell surface via hydrogen bonding. This has shown to result in overall changes to cell size and shape [110,111]. In the present study, ethanol is used to dehydrate the cells for SEM analysis as it easier and less hazardous compared to alternative methods [112]. Although it could be argued that the same treatments are used for the tests and controls and the relative effect is expected to be proportional, insertion of FSL into cells increases the lipid content on the cell surface and therefore, the treatment with ethanol could potentially have more impact on kodecytes than the control cells.

Prior to viewing with SEM, the dehydrated samples were mounted using a double-sided carbon tape and sputter coated with platinum at 25mV for 60s (Hitachi; E-1045). Sputter coating was carried out to increase the surface conductivity and reduce the accumulation of surface charge. Images were captured in SEM using the standard voltage of 5KV. The results presented in Figure 16 shows that cells display a round morphology in both unmodified and modified Jurkat cells and agrees with previous observation as in Figure 10. While the unmodified Jurkat cell surfaces appear irregular, surface appeared to become regular with increasing FSL-biotin insertion.

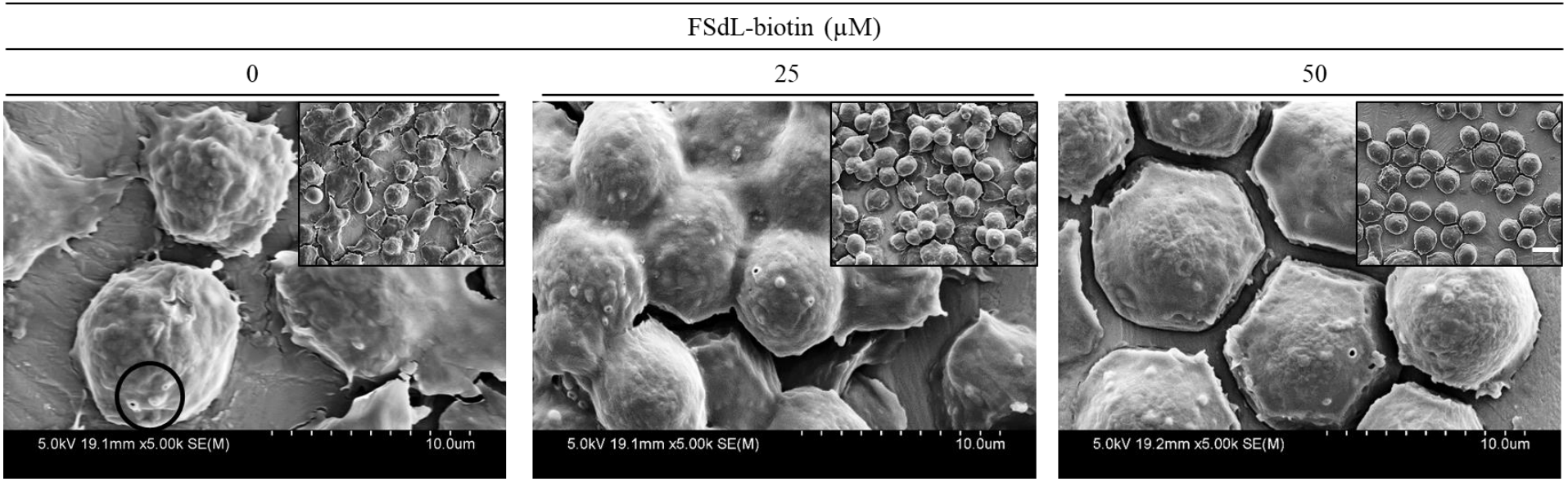

Figure 16 SEM images of unmodified and modified Jurkat cells. Images captured at lower magnifications are presented in the inset (scale bar- 10μm). Pores indicated in circles are shown more in detail in Figure 17.

At higher magnification (×5000), pores were observed on the surface of both the control and FSL modified cells and were not of any significance in number of occurrences. Some of these pores were observed to have an opening on the cell surface. The diameter of these structures was in order of ~500nm magnitude (Figure 17).

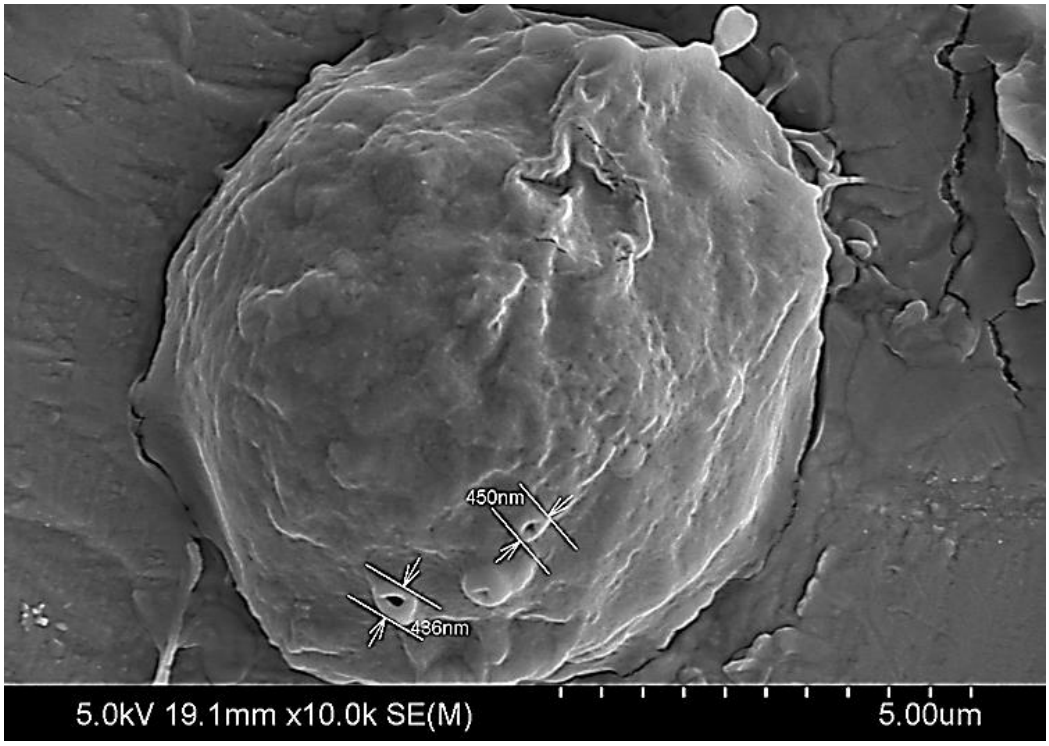

Figure 17 SEM image of Jurkat cell showing the membrane pores. The pores were present on both normal cells and kodecytes as shown in Figure 16.

2.4.2 Size of the kodecytes

The size of the kodecytes was previously observed to potentially be enlarged as the concentration of FSdL-biotin increased. Therefore, the diameter of both biotin kodecytes and control cells were measured immediately after 2 hours of insertion. A straight line (in multiple directions) drawn across the longest axis of the cell (approximately dividing it into two halves) was chosen as the diameter and was measured using the automated measure function in SEM. Diameter of at least random 10 cells per image were measured and mean diameter of kodecytes treated with different concentrations of FSL-biotin are plotted in Figure 18. The diameter of the kodecytes at concentrations ≥25µM, appear to be approximately 20% larger than control cells. Subsequent culturing of kodecytes in RPMI for 24 hours did not show any changes to cell diameter. One- way ANOVA statistical analysis carried out with *post hoc* Dunnett test shows that increase in cell diameter at both 0 and 24 hours at concentrations ≥25µM is statistically significant compared to their respective control.

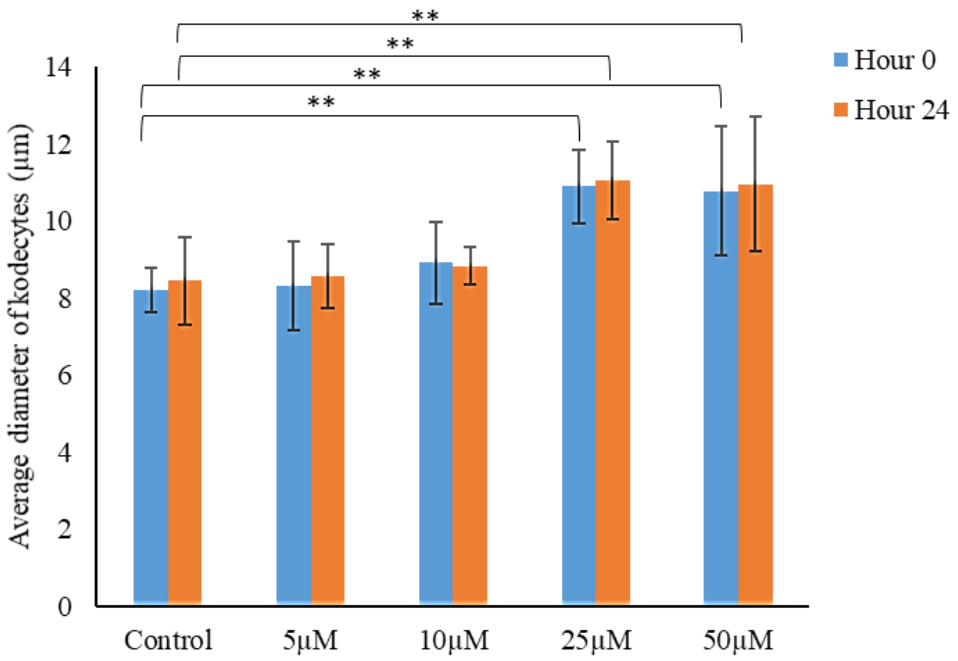

Figure 18 Average diameter of kodecytes at 0 and 24-hour post FSdL-biotin insertion.

Table 9 One- way ANOVA with *post hoc* Dunnett test carried out to test the significance of cell diameter increase following FSL-biotin insertion.

Time (hour)	Untreated	vs	Treated (µM)	Mean Difference	Std. Error	*p* value	95% Confidence Interval	
							Lower Bound	Upper Bound
0	Control		5	0.16	0.67	1.000	-2.02	2.34
0	Control		10	-1.35	0.67	0.536	-3.53	0.83
0	Control		25	-2.99	0.67	0.002	-5.17	-0.81
0	Control		50	-3.09	0.67	0.001	-5.27	-0.92
24	Control		5	-0.49	0.67	0.998	-2.67	1.68
24	Control		10	-0.36	0.67	1.000	-2.54	1.81
24	Control		25	-3.19	0.67	0.001	-5.37	-1.01
24	Control		50	-3.09	0.67	0.001	-5.27	-0.92

2.4.2.1 Trypan Blue cell counting and viability

Cells were collected by centrifugation and resuspended in RPMI media. The cell suspension was mixed with an equal volume of trypan blue solution (0.4% in PBS) and live and dead cells were counted using a haemocytometer. Trypan Blue Solution (0.4%) is a cell stain routinely used to assess the cell viability [104,113,114]. For this assay, the haemocytometer (improved Neubauer® chamber) was used. After gently suspending the cells evenly into medium by repeated pipetting, 10µl of suspension was loaded into haemocytometer from the edge of the coverslip. Every count was duplicated by analysing two ruled counting areas. Using the 10× objective of a microscope, the cells in each grid were counted using a counter. Both viable

(unstained) cells, which do not uptake trypan blue, and non-viable (blue stained) cells were counted. For calculating the cell number, following conventions were used.

$$\text{Number of cells} = \text{number of cells} \times \text{dilution factor} \times 10^4 \text{ cells/ ml}$$

At least 200 cells were counted for each measurement.

FSL toxicity and kodecytes growth rate

Cellular growth (total number of cells) and cytotoxic effects of various concentrations of FSL-biotin were measured by manually counting the live and dead modified or unmodified kodecytes using the trypan blue assay immediately after insertion. Figure 19 shows the effect of FSL-biotin insertion on cell viability, at 0- hour, under different insertion condition. As the concentration of FSL-biotin inserted is increased there is an apparent slight decrease in number of live cells. Statistical analysis carried out with one-way ANOVA with default *post hoc* Tukey shows that the decrease in kodecytes viability, at concentrations ≤25µM, is not significant. However, at 50µM insertions, the decrease in number of live cells was statistically significant, compared to control cells ($p< 0.001$). Regardless of the concentration used for insertion, the viability of cells inserted in the presence of serum (CM) was unaffected and comparable to that of control cells. Even with a maximal of 50µM insertion, the percentage of live cells was >90%. This is probably because the insertion was less inefficient in the presence of serum and this supports the concept that the inserted material was responsible for the loss and not the presence of the material.

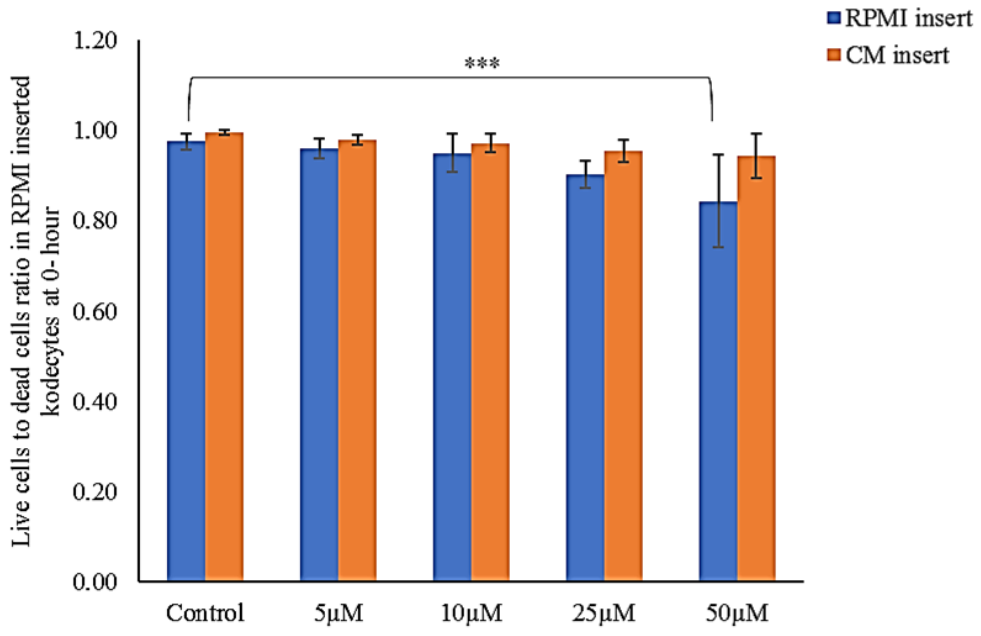

Figure 19 Schematic plot showing kodecytes live cell to dead cell ratio, at 0 hour, under different insertion conditions.

Table 10 One way-ANOVA with *post hoc* Tukey testing significance of FSL insertion on cell viability

Untreated	vs	Treated (µM)	Insert	Mean Diff.	Std. Error	*p* value	95% Confidence Interval	
							Lower Bound	Upper Bound
Control		5	RPMI	0.01	0.03	1.000	-0.06	0.09
			CM	0.02	0.03	1.000	-0.06	0.10
Control		10	RPMI	0.03	0.03	0.985	-0.05	0.01
			CM	0.02	0.03	1.000	-0.06	0.10
Control		25	RPMI	0.07	0.03	0.087	-0.01	0.15
			CM	0.04	0.03	0.794	-0.04	0.12
Control		50	RPMI	0.13	0.03	0.000	0.05	0.21
			CM	0.05	0.03	0.467	-0.03	0.13

To determine the growth rate, kodecytes inserted in RPMI or CM were then resuspended either in serum free RPMI or CM with 10% serum for further culturing and counted after 24 hours. Retention studies illustrate that the FSL-biotin inserted in the presence of serum (CM) does not insert well or persist in kodecytes beyond 12 hours, hence only viability of kodecyte inserted with serum free RPMI were analysed for 24 hours. The results presented in Figure 20 show a consistent increase in kodecytes number at concentrations ≤25µM. However, one- way statistical ANOVA analysis with *post hoc* Tukey shows that the growth rate of kodecytes, cultured either in RPMI or CM, is significant for insertions up to 10µM (Table 11). At 25µM, the growth rate is only marginally significant. The growth rate is observed to be severely inhibited at 50µM insertion. Number of kodecytes cultured in CM was greater than their respective RPMI insertions at any given concentration, however, one-way ANOVA analysis shows that the increase was not statistically significant (Table 12).

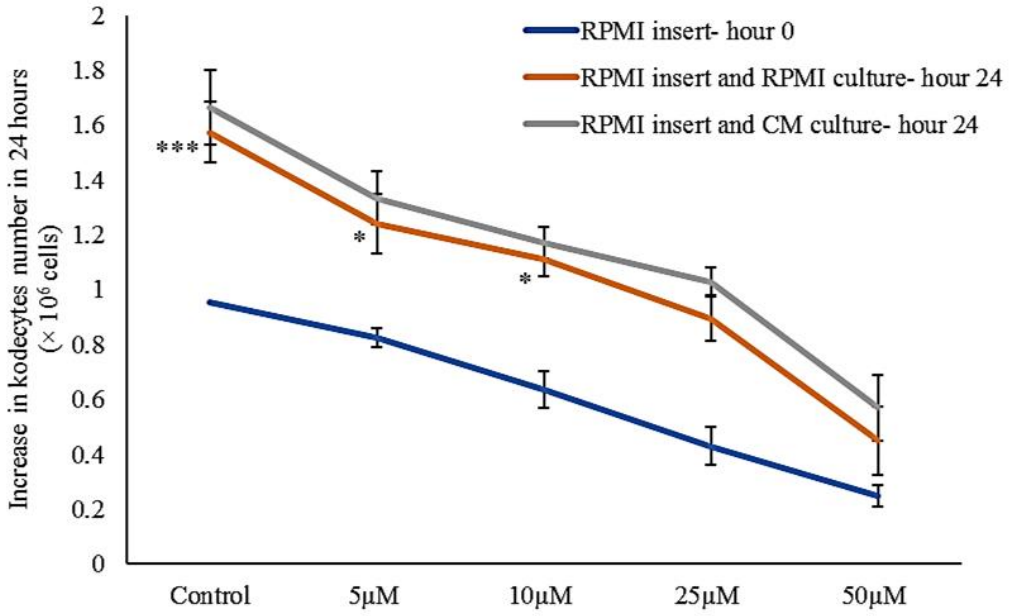

Figure 20 Schematic plot showing increase in kodecyte's number after 24 hours FSdL-biotin insertion. The rate of cell growth concentrations ≥25µM, is significant low compared to control cells (p<0.01 at 25 µM and p<0.001 at 50µM).

Table 11 Growth rate of biotin kodecytes compared to control cells statistically analysed with one- way ANOVA and *post hoc* Tukey, over a 24- hour period.

Conc. (µM) (0 hr vs 24 hr)	**Mean Difference**	**Std. Error**	***p* value**	**95% Confidence Interval**	
				Lower Bound	**Upper Bound**
Control	-0.62	0.09	0.000	-1.14	-0.10
5	-0.41	0.04	0.026	-0.60	-0.22
10	-0.47	0.05	0.013	-0.70	-0.25
25	-0.46	0.08	0.070	-0.97	0.04
50	-0.20	0.04	0.055	-0.38	-0.02

Table 12 Growth rate statistically analysed with one- way ANOVA and *post- hoc* Dunnett between RPMI and CM cultured kodecytes.

Conc. (µM) (RPMI vs CM)	**Mean Difference**	**Std. Error**	***p* value**	**95% Confidence Interval**	
				Lower Bound	**Upper Bound**
Control	0.09	0.07	1.000	-0.36	0.18
5	0.24	0.07	0.145	-0.02	0.51
10	0.06	0.07	1.000	-0.33	0.21
25	0.14	0.07	0.964	-0.40	0.13
50	0.12	0.07	0.991	-0.39	0.15

2.5 Surface modification and cell adhesion

The ability to attach cells to surfaces has huge applications in tissue engineering, regenerative medicine, medical devices industry, biosensors and wound healing. FSL molecules have already shown to adhere red cells to various surfaces using biotin- avidin model. Thus far, successful transformation of Jurkat cells and MCF-7 into biotin kodecytes has been established. The ability of FSL-biotin to attach non- adherent, proliferating Jurkat cells is investigated further. Initially, the adhesion of biotin kodecytes to tissue culture surfaces was determined. Following that, the adhesion ability of biotin kodecytes to FSL modified metal surfaces was investigated.

2.5.1 Cell adhesion to tissue culture surface

2.5.1.1 Kodecytes adhesion to tissue culture treated polystyrene

To investigate the ability of FSL constructs to enable cell adhesion, tissue culture treated polystyrene (TCP) plates were initially coated with FSL-biotin. Coating was carried out by placing a drop (10µl) of 0.1µM FSdL-biotin (unpublished data) to 96-well polystyrene plate (Falcon; cat # 353072) and was left to air dry (for at least 30 minutes). After rinsing the surfaces with 1×PBS, the surfaces were then flooded with 0.2 $mgmL^{-1}$streptavidin (Life Technologies; cat # 434301) and incubated for 30 minutes at room temperature (RT). Streptavidin coated (or koded) plates were ready for kodecyte adhesion after removing excess streptavidin by aspiration and thorough washing with sterile PBS. Surfaces, each time, were rinsed for at least 5× with sterile PBS to remove any unbound molecules.

Biotin kodecytes (10µM) were prepared by incubating Jurkat cells with FSdL biotin for 2 hours at 37°C and 5% CO_2 (as described in section 2.2.1). After thorough washing for at least thrice with sterile PBS, kodecytes (1×10^5 cells/ ml) were incubated in the 96-well streptavidin koded plates for an hour at 37°C. The cells were then rinsed (for 5× with PBS) to remove unbound kodecytes. Fixation was carried out by incubating the cells with 2.5% glutaraldehyde (Sigma; cat # 111-30-8), overnight at 4°C. The following day, surfaces were washed to remove any unbound molecules and observed under the DIC filter of the Olympus BX-51 microscope.

2.5.1.1.1 Results and interpretation

The results presented in Figure 21 compares the adhesion of control cells and biotin kodecytes in streptavidin koded TCP surfaces. From the results, it is evident that, even after repeated washing, biotin kodecytes firmly adhered to FSL-biotin-streptavidin modified surfaces.

Kodecytes did not adhere to surfaces modified with either FSL biotin or streptavidin alone. This might be due to the blocking of cell binding site by FSL-biotin or streptavidin molecule, respectively. More interesting to note was adhesion of biotin kodecytes to untreated TCP surfaces. This could either be due to the hydrophilicity induced by physical and/ chemical modification on the TCP surfaces or through charged interactions between the hydroxyl groups on TCP plates and biotin molecule on the kodecyte surface [115,116]. Adhesion of unmodified Jurkat cells (0µM) to untreated TCP surfaces clearly indicates the ability of the cells to attach to these surfaces in the absence of serum and are consistent to findings from Audiffred et al. (2010). Hence, as suggested by Audiffred et al. (2010), the adhesion observed might be mediated due to induced hydrophilicity and through charged interactions between the hydroxyl groups on TCP and cell-surface integrins [116].

Adhesion of biotin kodecytes on FSL-biotin-streptavidin modified TCP surfaces appeared to be in a monolayer. In contrast, adhesion of both modified (10µM) and unmodified (0µM) cells were random and scattered in untreated TCP surfaces. While the morphology of modified cells (10µM) on FSL- streptavidin surface and unmodified (0µM) Jurkat cells on untreated TCP surfaces was round, 10µM kodecytes adhered to untreated TCP surfaces were irregular.

2.5.1.2 Jurkat cell transient adhesion in tissue culture vs non-tissue culture treated surfaces

Further experiment was carried out to investigate the transient adhesion of Jurkat cells in non-tissue culture treated (nTCP) surfaces. Jurkat cells from culture were washed and resuspended into either RPMI or CM (containing 10% serum). Approximately, 1×10^5 cells in either RPMI or CM were suspended into 96-well nTCP plates and incubated for 2 hours at 37°C and 5% CO_2. Cells incubated in TCP plates were used as controls.

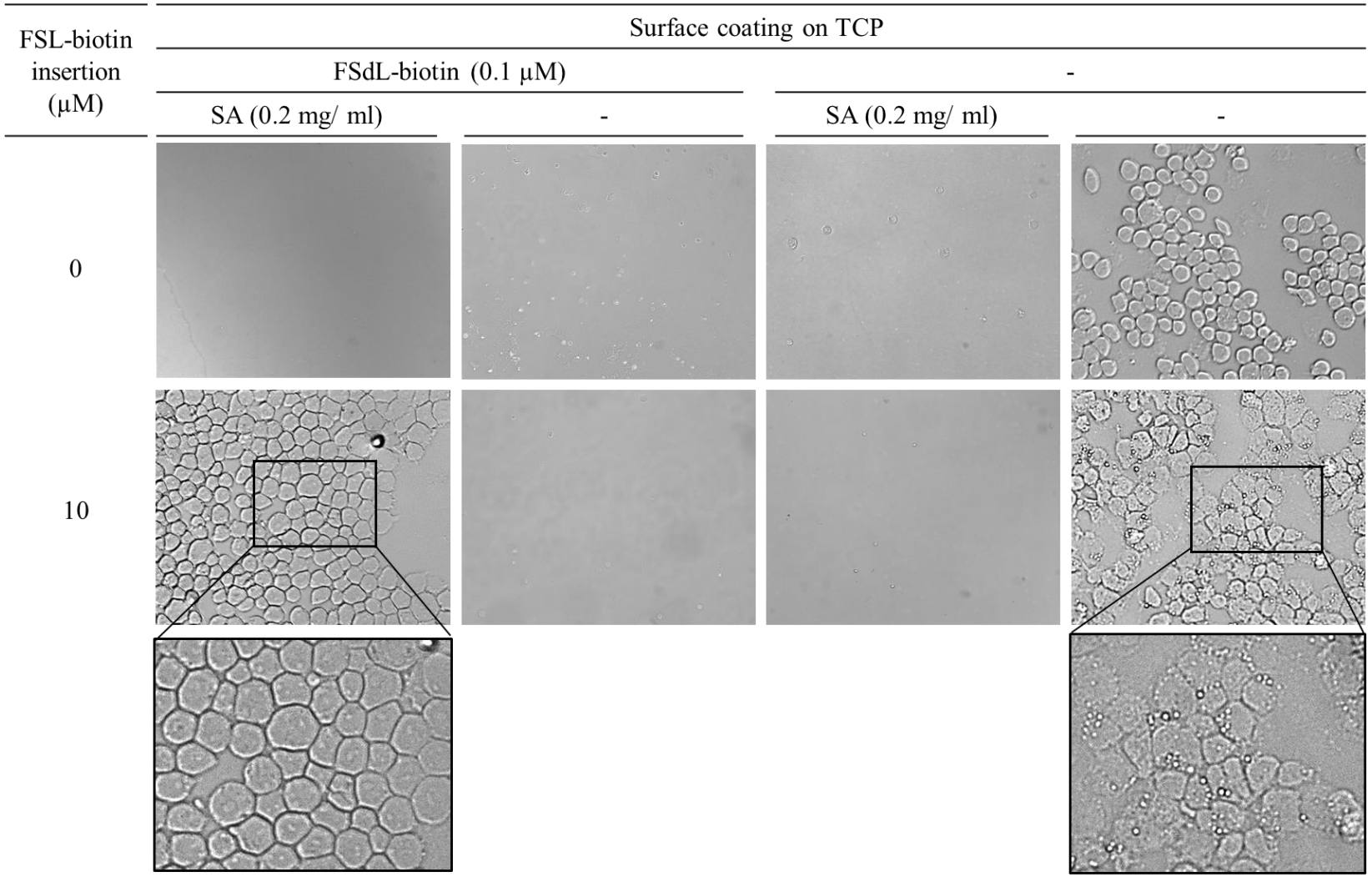

Figure 21 Adhesion of biotin kodecytes to FSL modified 96-well TCP plates. Biotin kodecytes adhered to both FSL modified and unmodified TCP plates. While Jurkat cells did not adhere to FSL modified TCP wells, they are observed to randomly adhere to unmodified TCP surfaces. No cell/ kodecyte adhesion is observed on surfaces treated with FSL-biotin (0.1μM) or SA (0.2 $mgmL^{-1}$) alone. Insets are (×200 magnification) images of kodecytes adhered to streptavidin modified and untreated surfaces.

2.5.1.2.1 Results and interpretation

The results presented in Figure 22 show that the Jurkat cells, either cultured in RPMI or CM, do not adhere to nTCP plates. This suggests surface treatments carried out in TCP surfaces to induce hydrophilicity and surface charge is the primary reason for cell adhesion to TCP plates. While Jurkat cells adhered to TCP surfaces, no adhesion was observed in the presence of serum. This was consistent with Audiffred et al. (2010) findings [116]. Based on these findings, adhesion of Jurkat cells to nTCP surfaces, using FSL constructs, were investigated.

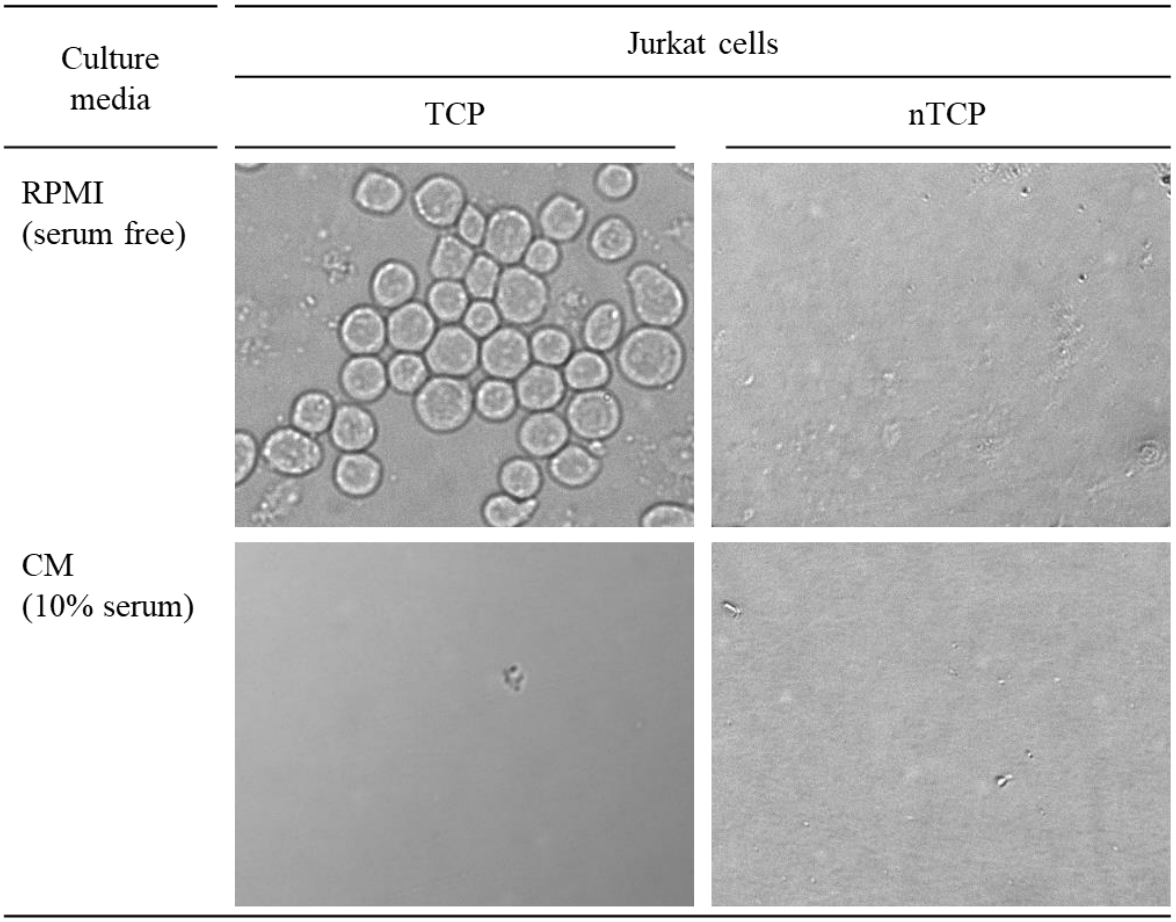

Figure 22 Determining transient adhesion of Jurkat cells on untreated nTCP surfaces in the presence and absence of serum.

2.5.1.3 Kodecytes adhesion to nTCP surfaces

To investigate the adhesion of kodecytes to nTCP plates (Falcon; cat # 351172) biotin kodecytes (10µM) were attached to nTCP surfaces koded with 0.1µM FSL-biotin as described in section 2.5.1.1 above. Kodecytes attached to surfaces were observed under the DIC filter of Olympus BX-51 microscope.

2.5.1.3.1 Results and interpretation

The results illustrate FSL mediated adhesion of Jurkat cells to inert nTCP surfaces via FSL-biotin-streptavidin model (Figure 23). Despite several wash steps, most of the 10µM kodecytes firmly adhered to FSL-streptavidin modified nTCP surfaces. However, they did not adhere to surfaces modified with FSL or streptavidin alone. As suggested earlier, this might be due the blocking of binding sites by these molecules. Opposed to the findings from TCP plates, unmodified Jurkat cells (0µM) did not adhere to untreated nTCP surfaces (Figure 23). While TCP plates are modified to generate charged groups, and alter the surface chemistry from hydrophobic to hydrophilic, nTCP surfaces lacks such treatments and are hydrophobic. However, adhesion of 10µM kodecytes to untreated nTCP surfaces was consistent to findings using TCP plates. This suggest that the adhesion might be mediated by surface charge on the biotin moiety present on the kodecyte surface. As observed on TCP plates, kodecytes on both the FSL modified and unmodified surfaces have a round morphology. While cell placement on modified surface appeared to be slightly regular, kodecytes adhered to unmodified surfaces are random and scattered.

2.5.1.3.2 SEM of kodecyte adhesion to surfaces

The biotin kodecytes adhered to FSL modified nTCP and control surfaces were further analyzed under the SEM. For preparing the samples for SEM analysis, the gluteraldehyde fixed kodecytes attached to the 96- well plates were dehydrated in graded ethanol series as decribed in section 2.4.1. Then, the 96-well plates were were carefully cut to edges using a Dremel® 200 and uniformally coated with platinum for 60s using a ion-sputter (Hitachi; E-1045). After mounting the samples, images were captured at different magnifications at 5kV using the Hitachi SU-70 SEM.

The kodecytes were observed to spread uniformly onto both the FSL-koded and unmodified nTCP surfaces (see Figure 24). While the adhesion of kodecytes to koded nTCP surfaces is mediated by biotin and streptavidin affinity, adhesion of biotin kodecytes to untreated nTCP surfaces might be mediated by surface charge on the FSL-biotin that is inserted into the Jurkat cell surface. Cytoplasmic projections protruding from the kodecytes were noticed on both the surfaces.

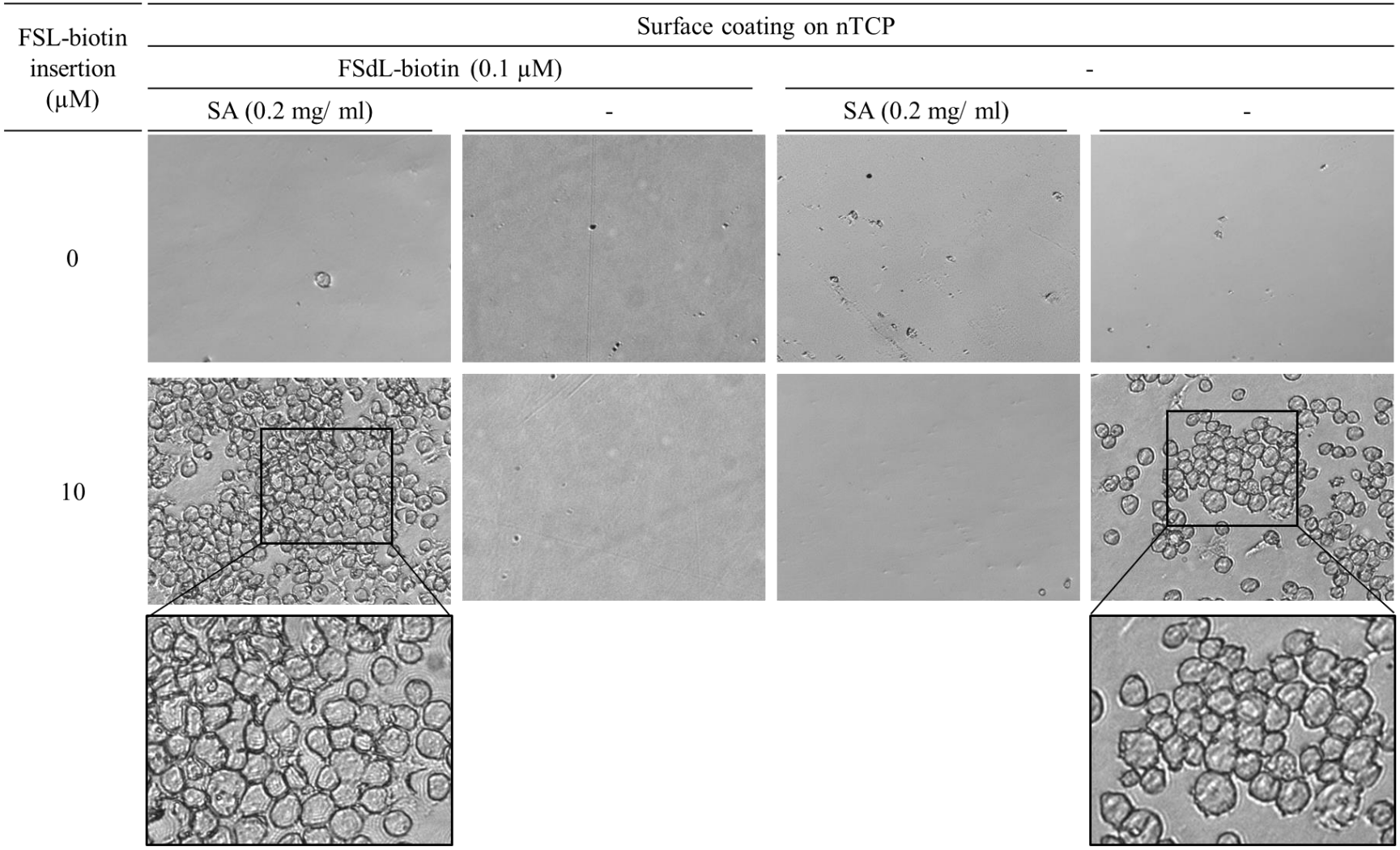

Figure 23 Adhesion of modified Jurkat cells to inert nTCP surface, mediated by streptavidin as a bridge. Biotin kodecytes adhered to both FSL modified and unmodified nTCP plates. Jurkat cells did adhere neither to FSL modified nor to unmodified surface. No cell/kodecyte adhesion was observed on surfaces treated with FSL-biotin (0.1μM) or SA (0.2 $mgmL^{-1}$) alone. Inset are ×200 magnification.

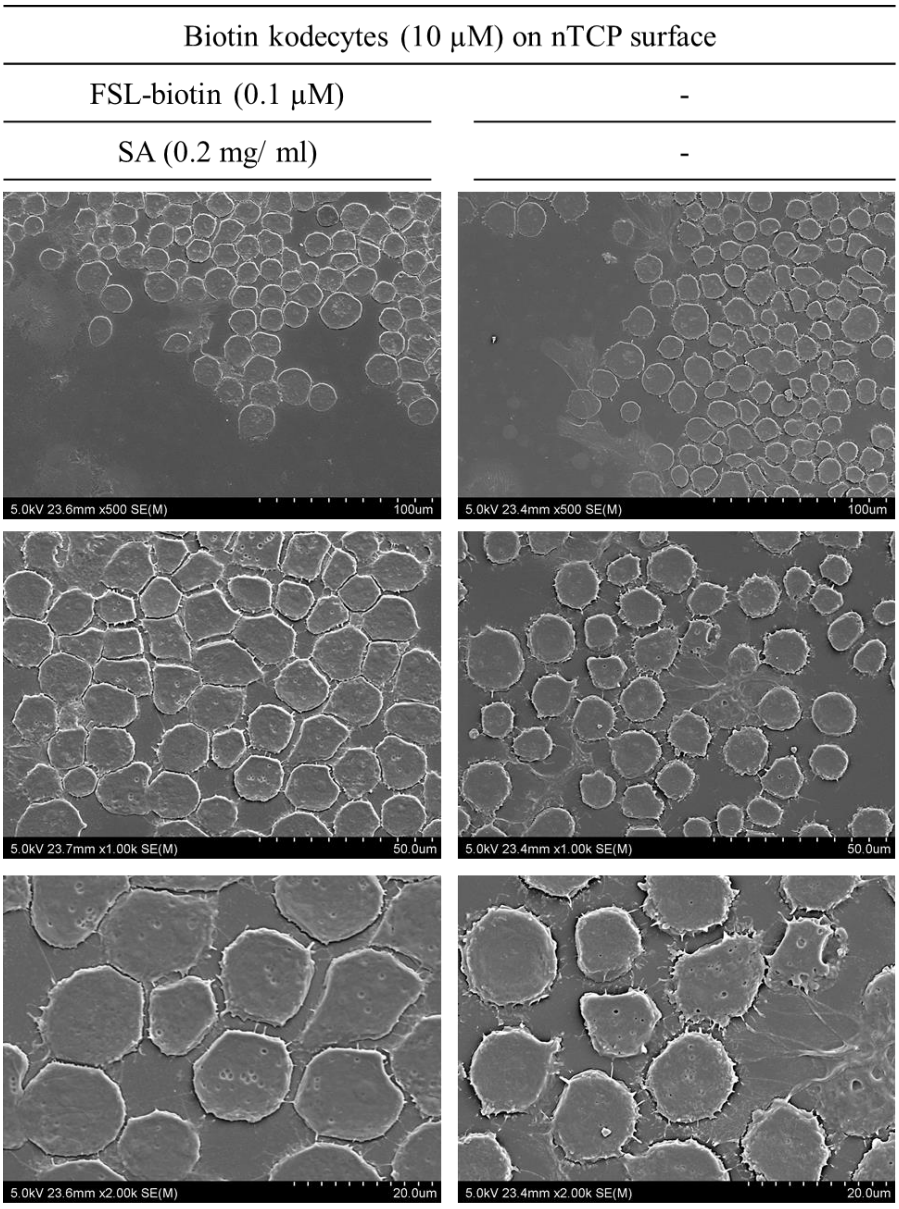

Figure 24 Adhesion of biotin kodecytes to modified and unmodified nTCP plates, observed under SEM.

2.5.1.4 Effect of serum in cell adhesion

Kodecytes, at concentrations ≥ 10µM, inserted in the presence (CM) and cultured in RPMI, retained FSL molecules for a maximum of 12 hours. In comparison to RPMI inserted kodecytes, the viability and cell growth was marginally higher in CM inserted cells. Thus, the ability of FSL constructs to adhere these kodecytes, inserted in CM, was further investigated. For this study, kodecytes at 10, 25 and 50µM concentrations were prepared using either RPMI or CM as insertion media. This was then incubated for an hour at 37°C in FSL modified nTCP plates, using either RPMI or CM as attachment media. The surfaces were washed and fixed as

described in section 2.5.1.1. The air-dried plates were observed under DIC filter of Olympus BX-51 microscope.

The results presented in Figure 25 show that the kodecytes, both inserted in the presence (CM) or absence (RPMI) of serum, adhere to FSL modified surfaces only when they were incubated with serum free RPMI. Adhesion of kodecytes to nTCP surfaces was observed to increase in a concentration dependent manner. This is expected as at higher concentrations, more FSL-biotin gets inserted into the cell surfaces resulting in more kodecyte adhesion. Since the presence of serum (CM) has shown to reduce FSL-biotin insertion into cells, adhesion of CM inserted kodecytes to nTCP surfaces was comparatively less compared to RPMI inserted kodecytes. These results illustrate that the adhesion of kodecytes to surfaces is hindered in the presence of serum. Hence, serum free RPMI media would be a better choice for insertion and adhesion.

2.5.2 Cell adhesion to metal surfaces

2.5.2.1 Cell adhesion to non-planar surfaces (microbeads)

Varying concentrations of FSdL-biotin (0.01, 0.1, 0.5, 1, 5, 10, 25 and 50µM) were prepared from 5 $mgmL^{-1}$ stock. Each 1×10^5 Jurkat cells were incubated with 100µl of varying FSdL-biotin solutions for 2 hours at 37°C and 5% CO_2. The cells were thoroughly washed by centrifugation and resuspended in PBS. Simultaneously, streptavidin beads (50µl from a stock concentration of 10 $mgmL^{-1}$) (Invitrogen; cat # 11206D) were washed thrice with PBS by centrifugation (for 1 min on high using Immufuge centrifuge). For a final concentration of 0.2 $mgmL^{-1}$, 50µl of streptavidin beads was diluted into 950µl of 1× PBS. An equal volume of biotin kodecytes (100µl) and streptavidin beads (0.2 $mgmL^{-1}$) were then mixed thoroughly and incubated for an hour at 37°C and 5% CO_2. Unbound kodecytes in the supernatant were removed and beads were washed 3× with PBS by centrifugation (for 15s on low using Immufuge centrifuge). The kodecytes adhered to streptavidin beads were fixed with 2.5% glutaraldehyde for an hour at RT. After washing (3× with PBS), the kodecytes bound to microbeads were observed under the DIC filter of Olympus BX-51 microscope.

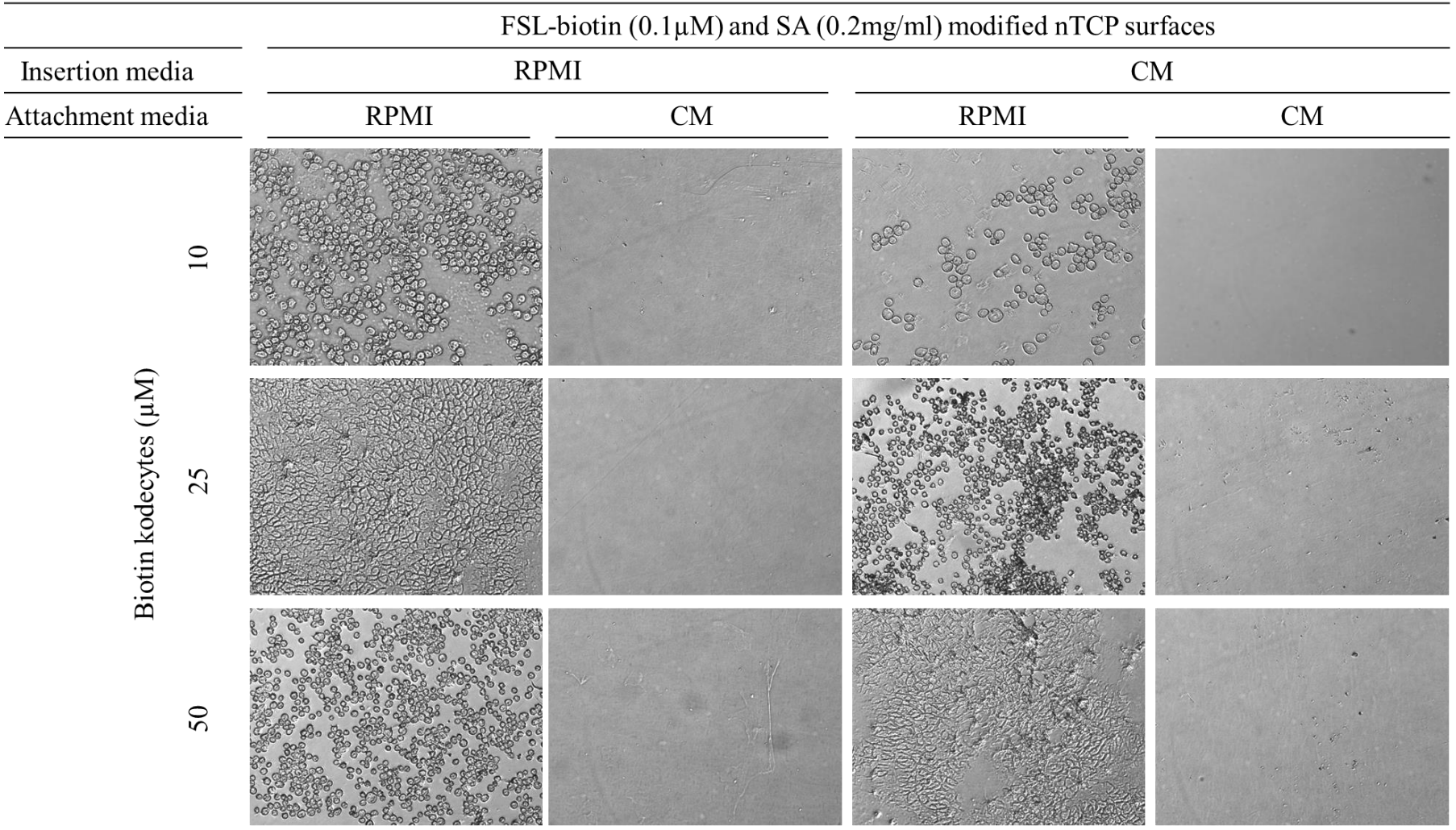

Figure 25 Effect of serum on kodecytes adhesion to FSL modified surface. Irrespective of the insertion media used, kodecytes adhered to FSL modified nTCP surfaces when cultured in RPMI during the adhesion process. Presence of serum prohibited cell adhesion.

2.5.2.1.1 Results and interpretation

Figure 26 shows biotin kodecytes attached to non-planar streptavidin microbeads. A minimum of 0.05µM FSL-biotin have shown to sufficiently enable cell surface attachment. As the concentration of FSL-biotin increases, the number of microbeads attached per cell also increases. The kodecytes were also observed to cluster with increasing FSL insertion concentration. This suggests that a monolayer attachment of cells to surfaces could be achieved at lower FSL-biotin concentration. There was no evident attachment of streptavidin beads to untreated Jurkat cells. Other than cell culture surfaces, this study has established that FSL constructs could successfully attach live-proliferating non-adherent cells to non-planar microbeads.

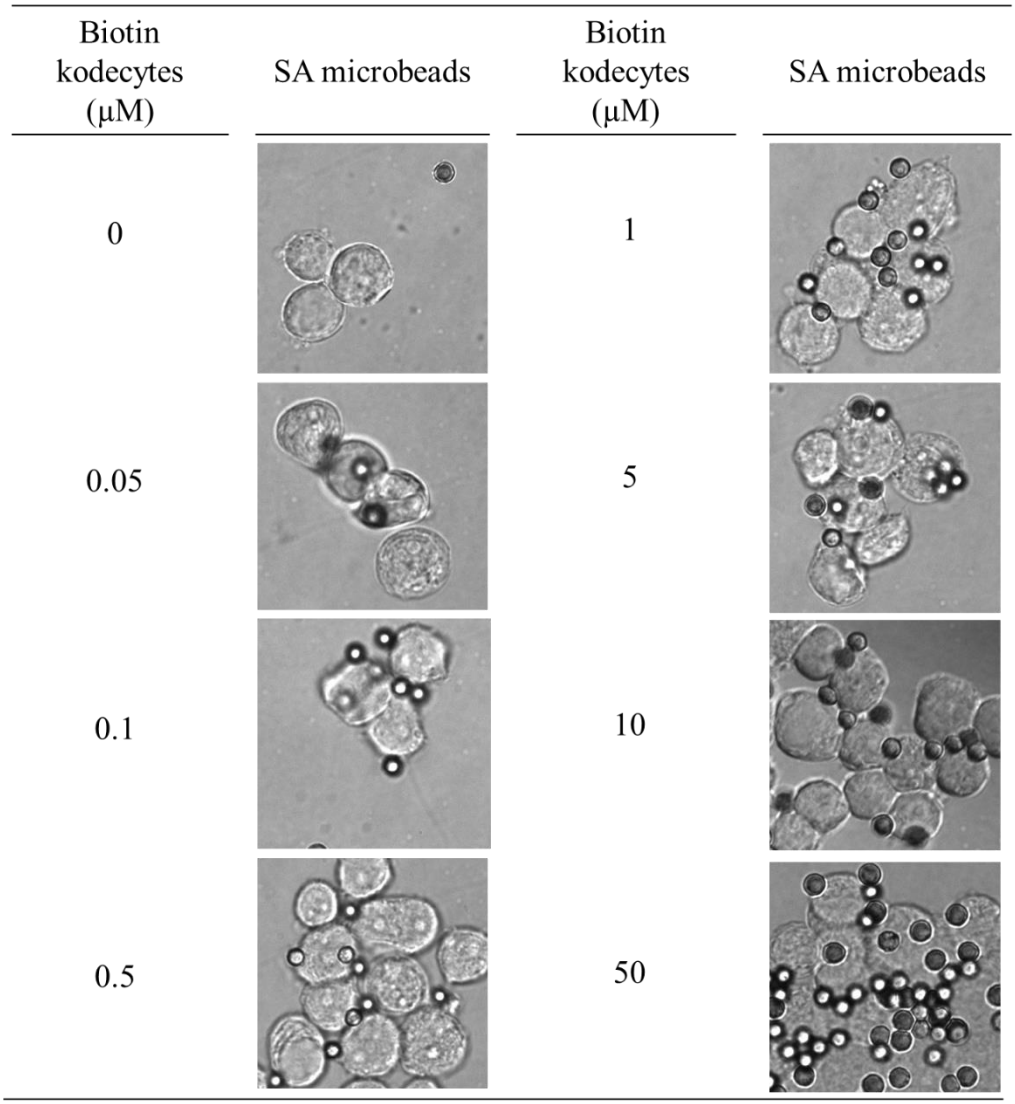

Figure 26 Attaching biotin kodecytes modified with varying concentration of FSL-biotin to streptavidin microbeads.

2.5.2.2 Kodecytes adhesion to planar stainless-steel surfaces

The study was further extended to investigate the adherence of modified Jurkat cells to planar stainless steel 316L (SS 316L) surfaces. For this, Jurkat cells at a cell density of 1×10^6 cells/ ml, were modified by incubating them with 10µM FSdL-biotin (in RPMI), for 2 hours at 37°C and 5% CO_2. Concurrently, pre-autoclaved SS 316L sheets were coated by placing 10µl of 0.1µM FSL-biotin and left to air dry for 30 minutes. After 30 minutes, the SS 316L surfaces were washed thoroughly for at least 5× with sterile PBS to remove any unbound FSL from the surface and flooded with streptavidin (0.2 $mgmL^{-1}$). Surfaces were incubated with streptavidin for 30 minutes at RT. After washing the surfaces thoroughly, biotin kodecytes were incubated on FSL modified surfaces for an hour at 37°C and 5% CO_2. Any unbound kodecytes were removed by repeated washing. The cells were then fixed by incubating them with 2.5% glutaraldehyde, overnight at 4°C. The following day, the fixative was aspirated and the surfaces washed. The degree of kodecytes attachment to stainless steel surfaces were analysed under the SEM. Therefore, surfaces were dehydrated in graded ethanol series and air dried as described in section 2.4.1. Surfaces were washed each time with sterile PBS and or distilled water for at least five times to ensure only bound cells were observed.

2.5.2.2.1 Results and interpretation

For imaging the surfaces under SEM, surfaces were mounted and sputter coated with platinum for 60s using the Hitachi Ion Sputter. All images with different magnifications were captured at 5kV. Biotin kodecytes adhered to FSL-biotin and streptavidin koded SS 316L, despite repeated washing of the surfaces for at least five times (Figure 27). There was no adhesion of kodecytes to untreated SS 316L surfaces (images not shown). Metals, in general, are less biocompatible and their surface properties is different to that of the cell culture plates. Therefore, their ability to interact with different zones of FSL constructs also varies [97]. Hence, non-adhesion of biotin kodecytes to these surfaces is not unexpected. In contrast to the observations on TCP and nTCP surfaces (Figure 21 & Figure 23), kodecytes adhered to stainless steel surface presented a spherical morphology. Although, few cytoplasmic projections anchored the cells to the stainless-steel surface, cells did not spread well across the surface. Therefore, optimal conditions for effective cell adherence need to be further investigated.

There was no adhesion of kodecytes to untreated SS 316L surfaces. This indicates that the adhesion of biotin kodecytes on stainless- steel surface is mediated by the FSL Biotin-streptavidin bonding. However, the uneven spreading of the cells on the surface indicates that the conditions for modifying and adhering the kodecytes to these surfaces requires further optimization.

Magnification	Biotin kodecytes (10 μM)
×100	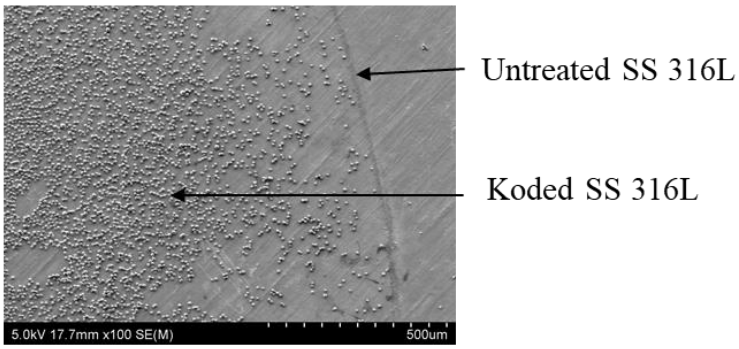
×1000	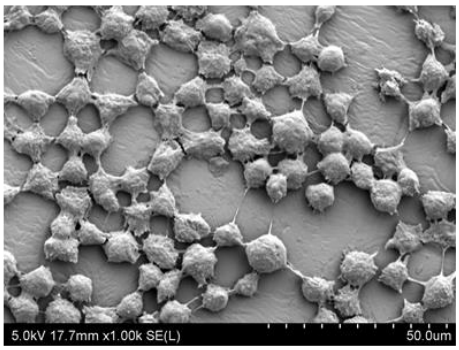
×2000	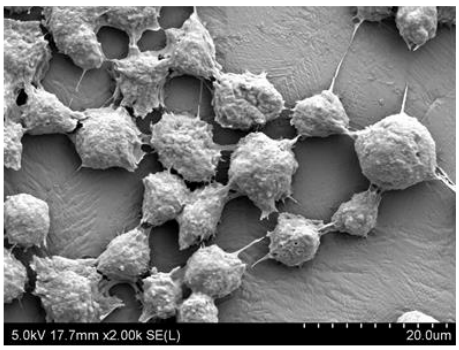

Figure 27 SEM images illustrating adhesion of biotin kodecytes to koded SS 316L surfaces.

2.6 Summary of results

Based on the findings from FSL-biotin insertion and retention studies, the results are summarised as;

- FSL-biotin does not prevent adherent cells from adhering
- FSL-biotin could be used to modify both adherent and non-adherent laboratory cultured tumour cells and cause them to adhere.
- FSL-biotin with DOPE tail (FSdL) has greater insertional efficacy in comparison to ceramide (FSsL) or cholesterol (FScL) lipid tail.
- The presence of serum during insertion or retention greatly reduces the FSL persistence on cell surface.
- Cell size and viability was affected when FSL-biotin was inserted at higher concentrations (50µM).
- FSL-biotin at 10µM was considered to be optimal for further studies due to the following reasons;
    - The FSL-biotin persist on kodecytes for at least 24 hours, irrespective of the insertion/ culture media
    - Cell viability was ≥95%
    - Changes to cell size was minimal (if any)

Adhesion studies investigated with non-adherent Jurkat cells using FSL-biotin and streptavidin model shows;

- FSL-biotin and streptavidin is able to adhere biotin kodecytes to plastic and metal surfaces.
- FSL-biotin alone can cause adhesion to some plastic surfaces
- Increased FSL insertion increased kodecytes attachment.
- The presence of serum severely hinders the adhesion of kodecytes to surfaces.
- Further optimization is required for adhering kodecytes to stainless steel surfaces

Chapter 3 Discussion

FSL constructs have been used to create novel modifications to many biological and non-biological surfaces and have established use in quality control, antibody mapping, antibody/toxin neutralization, diagnostic assays and immune modification [93,96-99,101,117]. The potential of FSL constructs to adhere red cells to a wide range of synthetic material was further explored for immobilizing proliferating suspension cells. This is the first study to report the adhesion of non- adherent Jurkat cells to cell culture plastics, microspheres and metal surfaces using FSL constructs. It was achieved by modifying the cells and material surfaces with FSL-biotin. Streptavidin was used as linker molecules to attach the biotin modified cells to the biotin modified material surface. Although, PBS have been previously used as an insertion media for dispersing molecules [52,84,118,119], RPMI was preferred and evaluated as insertion media (with and without added serum) to maintain optimal culture conditions.

3.1 Cell surface modification

Conventionally, biotin modified cells were prepared by chemically crosslinking N -hydroxyl-succinimide (NHS) biotin to amine groups present on the cell surface [84,87,120-123]. But these modifications are random and have been reported to change cell morphology and function [116,124]. Exogenous incorporation of lipid mediated insertion of biotin molecules on cell surfaces has also been reported and is to less likely to interact with components in the plasma membrane [52,89,107,118,125]. Kode™ uses a similar technology to these other technologies but is also different and has several potential advantages. For instance, unlike other lipidated molecules FSL constructs contain spacer of varying length. Apart from imparting solubility which allows FSL dispersion into water or any other biological media [91,94,101], they also distance the function head further from the cell surface. An increase in distance between the head and lipid tail potentially reduces the steric hindrance and increases both sensitivity and specificity of the inserted functional group. Apart from the spacer, FSL also have a variety of lipid tails. For instance, FSL-biotin with three different lipid tails including DOPE (FSdL), ceramide (FScL) and cholesterol (FSsL) are available from Kode™ [91,96]. Although, studies have shown both FSL-biotin with DOPE or ceramide as lipid tail to be best for insertion and retention on cell membrane [96], findings from this study show that the insertion of FSL-biotin with DOPE tail (FSdL) is a better choice than ceramide or cholesterol. Insertion of molecules using DOPE as a lipid tail was also found to be very effective in stable attachment of molecules

on cell membrane surface [107,125]. Additional advantages of using Kode™ Technology over other studies [52,89,107,118,125,126] is its universal ability to modify both biological or non-biological surfaces. Furthermore, FSL-biotin can simultaneously be added with other FSL's with functional groups such carbohydrates into the same cells without causing any undesirable effects [99,127-129].

3.1.1 FSL-biotin insertion and retention

Insertion of FSL-biotin into Jurkat cells was detected by fluorescence microscopy via streptavidin Alexa Fluor® 488. The presence of fluorescence was used as an indication of biotin accessible on the modified Jurkat cell (kodecyte) surface. Although speckling occurred, this was believed to be an artefact due to streptavidin labelling and not due to distribution of the FSL in the membrane. While most other studies using FSL-biotin used a minimum of 50µM of the construct for cell surface modification [91,98,99,129], this study shows that cells surfaces are modified with FSL-biotin at concentrations as low as 0.5µM. When the concentration of FSL-biotin increased, as expected, the number of biotin molecules accessible on the cell surface also increased. The strength of the fluorescence signal on kodecytes, although reduced persisted beyond 24 hours at FSL-biotin insertion concentrations ≥10µM (Table 13). This signifies that adhesion of Jurkat kodecytes to synthetic surfaces could potentially extend beyond 24 hours. This contrasts with the findings using endometrial cells where the fluorescence was observed to shift to interior of the cell within 24 hours post insertion [98]. However, in those experiments endometrial cells were adherent cells and modifications were carried out when cells were adhered to the surface. It is possible this difference is a consequence of adherence and limited exposure of the FSL to the cell surface. This remains to be established. On the other hand, Jurkat cells are non-adherent and almost the entire surface of the cell is accessible for FSL-biotin insertion and might be a reason for longer persistence. As suggested in other studies, the loss of FSL molecules overtime might probably be due to metabolic endocytosis and expulsion [93,94,130,131]. It is also worth noting that the FSL constructs directly involved in adhesion are unlikely or at least less likely to be recycled as rapidly as unbound constructs. This could therefore allow adhesion well beyond 24 hours. Additionally, after binding to the surfaces for a period of time, the FSL adhered cells probably also develop their own adhesion independent of FSL.

Persistence of FSL-biotin reduced and disappeared within 24 hours in the presence of serum. This is likely due to binding of FSL to serum lipids which reduces the efficiency of insertion

and is supported by other studies [94,98,99,107,125]. DIC images reveal that kodecytes survived normally even after losing FSL from the cell surface and this agrees with findings from Oliver et al. (2011) [128].

Table 13 Overview of FSL- biotin retention on kodecytes inserted and cultured in different media

FSL insertion media	**Inserted in RPMI***		**Inserted in CM****	
Growth media post insertion	**RPMI**	**CM**	**RPMI**	**CM**
0 hours	++++	+++	++	++
12 hours	+++	++	+	+
24 hours	++	+	-	-

* No serum; ** RPMI+10% serum

3.1.2 Morphological changes following FSL insertion

Insertion of high levels of FSL-biotin into Jurkat cells was observed to be accompanied by number of changes to the kodecytes surface including cell size variation, appearance and viability. It is possible that this could be due ethanol dehydration step used for SEM analysis. Cells were dehydrated with ethanol as it a simple technique for dehydrating the cells compared to alternative techniques such as critical point drying, osmium tetroxide or hexamethyldisilazane [112]. Interaction of ethanol with the lipids on the cell surface via hydrogen bonding has shown to cause overall changes to size and shape of the cell [110,111]. Initially, fixation of cells with 2.5% glutaraldehyde was considered to be sufficient to retain the structural integrity, however literature shows that aldehyde fixation might as well contribute to a small loss of lipids from the cell surface. In addition, it was also shown to create some membrane blebbing, few vacuoles and secondary structure changes to proteins [132]. Although, all these changes are reported to be relatively small and negligible, it might be a contributing factor for overall discrepancies observed in kodecytes morphology, which have more lipid in their membranes than do unmodified cells.

Although, previous studies show no undesirable effect following FSL insertion into cells [91,95,97-99], this is first study to report some cytotoxicity at higher concentrations. This is not uncommon for most of the exogenous molecules inserted into live cell surfaces [107,130,133]. However, most of the cells inserted with biotin moieties [52,84,120] have always shown to have a viability >95%.

3.2 Synthetic surface modification

Modification of synthetic surfaces generally requires complex physicochemical treatment or biological functionalization for adhering cells [8,9,19,45,134,135]. This study has demonstrated a simple method for modifying synthetic surfaces to enable cell adhesion (using FSL constructs). Modification occurs within seconds of contact of FSL-biotin with surface. Varying the incubation time and; drying and non-drying of FSL on surfaces appeared to have no effect on cell attachment [91,97]. While the lipid tail spontaneously inserts into the lipid bilayer of the cell, FSL constructs modify non-biological surfaces by spontaneous self-assembling of FSL as monolayers or bi/multilayers [97]. Once modified, the modification is stable for long periods and is relatively resistant to removal by water, mild detergents, serum lipids, or solvents such as methanol [91,97]. Although, FSL constructs can be inkjet printed on wide variety of surfaces to provide a reliable and controllable cell adhesion [91]. This is not suitable to this study, as surface needed to be kept sterile for cell culture. Streptavidin was used as linker molecule for adhering biotin kodecytes to FSL-biotin modified surfaces. Streptavidin was attached to material surface rather than the kodecytes as observed in most of the biotin-avidin adhesion studies [83,84,87,136]. The attachment of streptavidin to koded surfaces is mediated by the strong biotin-avidin bond. However, in other studies, strep(avidin) has been attached to surfaces by weak non-covalent interactions. For instance, Schmidt & Healy (2013) physiosorbed avidin derivatives to material surfaces to bind to cells via biotinylated RGD motifs [83]. Physiosorption is mediated by weak non- covalent interactions and has a limited life span at the interface for its bound molecule [137]. Likewise, Tsai and Wang (2004) used a simple absorption method for incorporating avidin into polymer surfaces [138]. Although, Dou et al. (2015) attached biotinylated MC3T3 cells to biotin modified surfaces, streptavidin was bound to biotinylated MC3T3. Both the cell and synthetic surfaces were modified using chemical covalent interactions and this has the potential to affect the properties of the native cell/ material surface [87].

3.2.1 Cell adhesion to planar tissue-culture and stainless surfaces

From this work and previous studies [91,94,97], we know that FSL constructs can be used for adhering suspension cells to wide range of synthetic surfaces using biotin-streptavidin model. In addition, biotin kodecytes in the absence of streptavidin also adhered to both TCP and nTCP plate without any modification. This offers an alternative mechanism for attachment and kodecytes could made with other heads which facilitate direct attachment. Adhesion of

kodecytes to TCP surfaces is expected as the surfaces are subjected to various physicochemical treatments to generate surface charge to enhance cell adhesion [116,139,140]. Interaction of surface charge on the biotin moiety with the unmodified nTCP surface might be the reason for kodecytes adhesion to nTCP surfaces. Consistent with Audiffred et al. (2010) findings, unmodified Jurkat cells were observed to attach to TCP plates in the absence of serum [116]. Studies show that the non-adherent cells which are generally spherical in shape transform to have elongated projections when firmly adhered to surface and then proceed to spread [103,141]. Thus, uniform spreading of biotin kodecytes on these polystyrene surfaces with/without FSL modification could indicate firm adhesion and potential for further expansion of kodecytes on these surfaces.

The presence of serum, unlike in other studies [83,103], prevented kodecytes or Jurkat cell attachment to any TCP/ nTCP surfaces. While non-adhesion of kodecytes might be due of interaction of serum lipids with FSL constructs, increased adhesion of non- adhesive globular proteins to unmodified polystyrene surfaces might be the cause for non- adhesion of Jurkat cells [103,142]. In recent years, tissue engineering applications prefer serum-free media or completely-defined media as there is a possibility of transmission of animal derived (xeno) antigens and infectious agents present in serum to the recipient of the cell therapy. Moreover, the precise composition of calf serum remains unclear and often there are significant variations between batches [143-145]. Since the adhesion of Jurkat cells or kodecytes are not dependent on serum- absorbed proteins, this would be an added advantage to expand the use of FSLs in tissue engineering applications.

Kodecytes adhered to only stainless-steel surfaces when modified with FSL-biotin and streptavidin. Although few cytoplasmic projections from the cells were observed on adhered kodecytes, the cells still presented a spherical morphology. Although this is in contrast to our observation with tissue culture surfaces, it is expected as the surface characteristics including surface charge and hydrophilicity of stainless steel is different to polystyrene and hence, their relative abilities to interact with different zones of FSL constructs also vary [97]. Further studies are still required to determine the optimal conditions for firm adhesion of Jurkat cells to stainless-steel surfaces.

3.2.2 Cell adhesion to non-planar microbead surfaces

In addition to cell culture and metal surfaces, findings from the current study demonstrate adhesion of live cells to non-planar microsphere surfaces. Although microbeads have

previously been attached to red cells and IgM antibodies [91,97,100], this is the first study to report adhesion of non- red cells to microbeads using this technology. In recent years, use of beads have been explored both in the lab and in the clinic for a wide range of applications ranging from treatment of diabetes to creating immunological tolerance [113,146,147]. For instance, selective modification of PEG-co-PLL microbeads with cell surface cadherin receptors and pancreatic tissue specific ECM components has been demonstrated to provide a native-like cell- cell and cell- ECM interaction. The resulting interaction between the β-cells and microbeads has shown improved survival and function of pancreatic β-cells, which has been a long-standing obstacle for diabetes therapy [148]. Likewise, polystyrene microbeads incorporated with immunomodulatory peptides derived from human CD47 via biotin-streptavidin binding supressed both the phagocytic uptake and tumour growth in a subcutaneous *in-vivo* model [146]. A range of different microspheres including paramagnetic beads have been modified with FSL constructs [91,97,100], and all these strategies could potentially be constructed using the Kode™ platform by simply replacing biotin with RGD or any other peptide/antibody of interest.

3.3 Conclusion

The results from this study demonstrates the potential of FSL constructs from Kode™ Technology to immobilize non- adherent Jurkat cells to different non-biological surfaces. These proof-of-concept experiments illustrates that potential use of this technology to adhere other non-adherent cells, such stem cells, that have important use in various biological and medical fields but are limited by their inability to adhere to synthetic surfaces [149-151]. In addition, direct attachment of biotin kodecytes to unmodified cell culture plates offers an alternative mechanism for facilitating direct cell adhesion by just replacing the biotin with other head groups such as RGD or other adhesion molecules. Since the characteristics of each cell and material surface varies, parameters such as optimal concentration for FSL insertion and retention and attachment conditions needs to be determined for each surface intended to be modified. Because of the ability of FSL constructs to be custom-designed according to requirements, there is an added potential to incorporate growth and differentiation factors and some antibacterial properties into FSL constructs for enhancing cell survival, proliferation and differentiation.

Chapter 4 References

1. Bacakova, L., Filova, E., Parizek, M., Ruml, T., & Svorcik, V. (2011). Modulation of cell adhesion, proliferation and differentiation on materials designed for body implants. *Biotechnology Advances, 29*(6), 739-767. doi:http://dx.doi.org/10.1016/j.biotechadv.2011.06.004

2. Di Cio, S., & Gautrot, J. E. (2016). Cell sensing of physical properties at the nanoscale: Mechanisms and control of cell adhesion and phenotype. *Acta Biomaterialia, 30*, 26-48. doi:http://dx.doi.org/10.1016/j.actbio.2015.11.027

3. Iwamoto, D. V., & Calderwood, D. A. (2015). Regulation of integrin-mediated adhesions. *Current Opinion in Cell Biology, 36*, 41-47. doi:http://dx.doi.org/10.1016/j.ceb.2015.06.009

4. Leijten, J., Chai, Y. C., Papantoniou, I., Geris, L., Schrooten, J., & Luyten, F. P. (2015). Cell based advanced therapeutic medicinal products for bone repair: Keep it simple? *Advanced Drug Delivery Reviews, 84*, 30-44. doi:http://dx.doi.org/10.1016/j.addr.2014.10.025

5. Mrksich, M. (1998). Tailored substrates for studies of attached cell culture [journal article]. *Cellular and Molecular Life Sciences CMLS, 54*(7), 653-662. doi:10.1007/s000180050193

6. Keane, T. J., & Badylak, S. F. (2014). Biomaterials for tissue engineering applications. *Seminars in Pediatric Surgery, 23*(3), 112-118. doi:http://dx.doi.org/10.1053/j.sempedsurg.2014.06.010

7. Murphy, C. M., O'Brien, F. J., Little, D. G., & Schindeler, A. (2013). Cell-scaffold interactions in the bone tissue engineering triad [Review]. *European Cells & Materials, 26*, 120-132.

8. Parchi PD, V. O., Andreani L, Piolanti N, Cirillo G, Iemma F, Hampel S and Lisanti M. (2013). How Nanotechnology can Really Improve the Future of Orthopedic Implants and Scaffolds for Bone and Cartilage Defects. *J Nanomedine Biotherapeutic Discov, 3*(114). doi:10.4172/2155-983X.1000114

9. Nouri, A., & Wen, C. (2015). Introduction to surface coating and modification for metallic biomaterials. In *Surface Coating and Modification of Metallic Biomaterials* (pp. 3-60): Woodhead Publishing. Retrieved from http://www.sciencedirect.com/science/article/pii/B9781782423034000016. doi:http://dx.doi.org/10.1016/B978-1-78242-303-4.00001-6

10. Bauer, S., Schmuki, P., von der Mark, K., & Park, J. (2013). Engineering biocompatible implant surfaces: Part I: Materials and surfaces. *Progress in Materials Science, 58*(3), 261-326. doi:http://dx.doi.org/10.1016/j.pmatsci.2012.09.001

11. John, A. A., Subramanian, A. P., Vellayappan, M. V., Balaji, A., Jaganathan, S. K., Mohandas, H., Yusof, M. (2015). Review: physico-chemical modification as a versatile strategy for the biocompatibility enhancement of biomaterials [10.1039/C5RA03018H]. *RSC Advances, 5*(49), 39232-39244. doi:10.1039/C5RA03018H

12. Carré, A., & Lacarrière, V. (2010). How Substrate Properties Control Cell Adhesion. A Physical–Chemical Approach. *Journal of Adhesion Science and Technology, 24*(5), 815-830. doi:10.1163/016942409X12598231567862

13. Mitra, J., Tripathi, G., Sharma, A., & Basu, B. (2013). Scaffolds for bone tissue engineering: role of surface patterning on osteoblast response [10.1039/C3RA23315D]. *RSC Advances, 3*(28), 11073-11094. doi:10.1039/C3RA23315D

14. Zareidoost, A., Yousefpour, M., Ghaseme, B., & Amanzadeh, A. (2012). The relationship of surface roughness and cell response of chemical surface modification of titanium. *Journal of Materials Science. Materials in Medicine, 23*(6), 1479-1488. doi:10.1007/s10856-012-4611-9

15. Roh, H.-S., Jung, S.-C., Kook, M.-S., & Kim, B.-H. (2015). In vitro study of 3D PLGA/n-HAp/β-TCP composite scaffolds with etched oxygen plasma surface modification in bone tissue engineering [Article]. *Applied Surface Science*. doi:10.1016/j.apsusc.2015.12.243

16. Ranella, A., Barberoglou, M., Bakogianni, S., Fotakis, C., & Stratakis, E. (2010). Tuning cell adhesion by controlling the roughness and wettability of 3D micro/nano silicon structures. *Acta Biomaterialia, 6*(7), 2711-2720. doi:http://dx.doi.org/10.1016/j.actbio.2010.01.016

17. Oliveira, S. M., Alves, N. M., & Mano, J. F. (2014). Cell interactions with superhydrophilic and superhydrophobic surfaces. *Journal of Adhesion Science and Technology, 28*(8-9), 843-863. doi:10.1080/01694243.2012.697776

18. Linez-Bataillon, P., Monchau, F., Bigerelle, M., & Hildebrand, H. F. (2002). In vitro MC3T3 osteoblast adhesion with respect to surface roughness of Ti6Al4V substrates. *Biomolecular Engineering, 19*(2–6), 133-141. doi:http://dx.doi.org/10.1016/S1389-0344(02)00024-2

19. Liu, X., Chu, P. K., & Ding, C. (2010). Surface nano-functionalization of biomaterials. *Materials Science and Engineering: R: Reports, 70*(3–6), 275-302. doi:http://dx.doi.org/10.1016/j.mser.2010.06.013

20. Gabriel, M., Nazmi, K., Dahm, M., Zentner, A., Vahl, C.-F., & Strand, D. (2012). Covalent RGD Modification of the Inner Pore Surface of Polycaprolactone Scaffolds. *Journal of Biomaterials Science, Polymer Edition, 23*(7), 941-953. doi:10.1163/092050611X566793

21. von Walter, M., Herren, C., Gensior, T. J., Steffens, G. C. M., Hermanns-Sachweh, B., Jahnen-Dechent, W., Erli, H. J. (2008). Biomimetic modification of the TiO2/glass composite Ecopore with heparinized collagen and the osteoinductive factor BMP-2. *Acta Biomaterialia, 4*(4), 997-1004. doi:http://doi.org/10.1016/j.actbio.2008.01.020

22. Langer, R., & Tirrell, D. A. (2004). Designing materials for biology and medicine [Article]. *Nature, 428*(6982), 487-492. doi:10.1038/nature02388

23. Brahatheeswaran Dhandayuthapani, Y. Y., Toru Maekawa, and D. Sakthi Kumar. (2011). Polymeric Scaffolds in Tissue Engineering Application: A Review. *International Journal of Polymer Science, 2011*. doi:10.1155/2011/290602

24. Ahn, J., Son, S. J., & Min, J. (2013). The control of cell adhesion on a PMMA polymer surface consisting of nanopillar arrays. *Journal of Biotechnology, 164*(4), 543-548. doi:http://dx.doi.org/10.1016/j.jbiotec.2012.12.017

25. Armentano, I., Ciapetti, G., Pennacchi, M., Dottori, M., Devescovi, V., Granchi, D., . . . Kenny, J. M. (2009). Role of PLLA plasma surface modification in the interaction with human marrow stromal cells. *Journal of Applied Polymer Science, 114*(6), 3602-3611. doi:10.1002/app.31008

26. Banerjee, I., Mishra, D., & Maiti, T. K. (2009). PLGA Microspheres Incorporated Gelatin Scaffold: Microspheres Modulate Scaffold Properties. *International Journal of Biomaterials, 2009*, 9. doi:10.1155/2009/143659

27. Fu, S., Ni, P., Wang, B., Chu, B., Zheng, L., Luo, F., Qian, Z. (2012). Injectable and thermo-sensitive PEG-PCL-PEG copolymer/collagen/n-HA hydrogel composite for guided bone regeneration. *Biomaterials, 33*(19), 4801-4809. doi:http://dx.doi.org/10.1016/j.biomaterials.2012.03.040

28. Yang, G.-H., Kim, M., & Kim, G. (2015). A hybrid PCL/collagen scaffold consisting of solid freeform-fabricated struts and EHD-direct-jet-processed fibrous threads for tissue regeneration. *Journal of Colloid and Interface Science, 450*, 159-167. doi:http://dx.doi.org/10.1016/j.jcis.2015.02.070

29. Mahapatro, A. (2015). Bio-functional nano-coatings on metallic biomaterials. *Materials Science and Engineering: C, 55*, 227-251. doi:http://dx.doi.org/10.1016/j.msec.2015.05.018

30. Popat, K. C., Leoni, L., Grimes, C. A., & Desai, T. A. (2007). Influence of engineered titania nanotubular surfaces on bone cells. *Biomaterials, 28*(21), 3188-3197.

31. Solař, P., Kylián, O., Marek, A., Vandrovcová, M., Bačáková, L., Hanuš, J., Biederman, H. (2015). Particles induced surface nanoroughness of titanium surface and its influence on adhesion of osteoblast-like MG-63 cells. *Applied Surface Science, 324*, 99-105. doi:http://dx.doi.org/10.1016/j.apsusc.2014.10.082

32. Hirano, M., Yamane, M., & Ohtsu, N. (2015). Surface characteristics and cell-adhesion performance of titanium treated with direct-current gas plasma comprising nitrogen and oxygen. *Applied Surface Science, 354, Part A*, 161-167. doi:http://dx.doi.org/10.1016/j.apsusc.2015.02.153

33. Liu, J.-X., Yang, D.-Z., Shi, F., & Cai, Y.-J. (2003). Sol–gel deposited TiO2 film on NiTi surgical alloy for biocompatibility improvement. *Thin Solid Films, 429*(1–2), 225-230. doi:http://dx.doi.org/10.1016/S0040-6090(03)00146-9

34. Al-Munajjed, A. A., Plunkett, N. A., Gleeson, J. P., Weber, T., Jungreuthmayer, C., Levingstone, T., . . . O'Brien, F. J. (2009). Development of a biomimetic collagen-hydroxyapatite scaffold for bone tissue engineering using a SBF immersion technique. *Journal of Biomedical Materials Research Part B: Applied Biomaterials, 90B*(2), 584-591. doi:10.1002/jbm.b.31320

35. Cunniffe, G. M., Dickson, G. R., Partap, S., Stanton, K. T., & O'Brien, F. J. (2009). Development and characterisation of a collagen nano-hydroxyapatite composite scaffold for bone tissue engineering [journal article]. *Journal of Materials Science: Materials in Medicine, 21*(8), 2293-2298. doi:10.1007/s10856-009-3964-1

36. Jones, G. L., Walton, R., Czernuszka, J., Griffiths, S. L., El Haj, A. J., & Cartmell, S. H. (2010). Primary human osteoblast culture on 3D porous collagen-hydroxyapatite scaffolds. *Journal of Biomedical Materials Research Part A, 94A*(4), 1244-1250. doi:10.1002/jbm.a.32805

37. Roh, H.-S., Jung, S.-C., Kook, M.-S., & Kim, B.-H. In vitro study of 3D PLGA/n-HAp/β-TCP composite scaffolds with etched oxygen plasma surface modification in bone tissue engineering. *Applied Surface Science.* doi:http://dx.doi.org/10.1016/j.apsusc.2015.12.243

38. Guo, C. Y., Matinlinna, J. P., Tsoi, J. K.-H., & Hong Tang, A. T. (2015). Residual Contaminations of Silicon-Based Glass, Alumina and Aluminum Grits on a Titanium Surface After Sandblasting [journal article]. *Silicon*, 1-8. doi:10.1007/s12633-015-9287-6

39. Lorrison, J. C., Dalgarno, K. W., & Wood, D. J. (2005). Processing of an apatite-mullite glass-ceramic and an hydroxyapatite/phosphate glass composite by selective laser sintering. *Journal of Materials Science: Materials in Medicine, 16*(8), 775-781. doi:10.1007/s10856-005-2616-3

40. Pi, F., Dillard, P., Limozin, L., Charrier, A., & Sengupta, K. (2013). Nanometric Protein-Patch Arrays on Glass and Polydimethylsiloxane for Cell Adhesion Studies. *Nano Letters, 13*(7), 3372-3378. doi:10.1021/nl401696m

41. Khorasani, M. T., Mirzadeh, H., & Irani, S. (2008). Plasma surface modification of poly (l-lactic acid) and poly (lactic-co-glycolic acid) films for improvement of nerve cells adhesion. *Radiation Physics and Chemistry, 77*(3), 280-287. doi:http://dx.doi.org/10.1016/j.radphyschem.2007.05.013

42. Saulou, C., Despax, B., Raynaud, P., Zanna, S., Seyeux, A., Marcus, P., Mercier-Bonin, M. (2012). Plasma-Mediated Nanosilver-Organosilicon Composite Films Deposited on Stainless Steel: Synthesis, Surface Characterization, and Evaluation of Anti-Adhesive and Anti-Microbial Properties on the Model Yeast Saccharomyces cerevisiae. *Plasma Processes and Polymers, 9*(3), 324-338. doi:10.1002/ppap.201100033

43. Lackner, J. M., & Waldhauser, W. (2010). Inorganic PVD and CVD Coatings in Medicine — A Review of Protein and Cell Adhesion on Coated Surfaces. *Journal of Adhesion Science and Technology, 24*(5), 925-961. doi:10.1163/016942409X12598231568023

44. Mohanty, S., Sanger, K., Heiskanen, A., Trifol, J., Szabo, P., Dufva, M., Wolff, A. (2016). Fabrication of scalable tissue engineering scaffolds with dual-pore microarchitecture by combining 3D printing and particle leaching. *Materials Science and Engineering: C, 61*, 180-189. doi:http://dx.doi.org/10.1016/j.msec.2015.12.032

45. Hildebrand, H. F., Blanchemain, N., Mayer, G., Chai, F., Lefebvre, M., & Boschin, F. (2006). Surface coatings for biological activation and functionalization of medical devices. *Surface and Coatings Technology, 200*(22–23), 6318-6324. doi:http://dx.doi.org/10.1016/j.surfcoat.2005.11.086

46. Shin, H., Jo, S., & Mikos, A. G. (2003). Biomimetic materials for tissue engineering. *Biomaterials, 24*(24), 4353-4364. doi:http://dx.doi.org/10.1016/S0142-9612(03)00339-9

47. Kämmerer, P., Heller, M., Brieger, J., Klein, M., Al-Nawas, B., & Gabriel, M. (2011). Immobilisation of linear and cyclic RGD-peptides on titanium surfaces and their impact on endothelial cell adhesion and proliferation. *Cells and materials, 21*, 364-372.

48. Rahmany, M. B., & Van Dyke, M. (2013). Biomimetic approaches to modulate cellular adhesion in biomaterials: A review. *Acta Biomaterialia, 9*(3), 5431-5437. doi:http://dx.doi.org/10.1016/j.actbio.2012.11.019

49. Chevalier, S., Cuestas-Ayllon, C., Grazu, V., Luna, M., Feracci, H., & de la Fuente, J. M. (2010). Creating Biomimetic Surfaces through Covalent and Oriented Binding of Proteins. *Langmuir, 26*(18), 14707-14715. doi:10.1021/la103086b

50. Hasan, A., & Pandey, L. M. (2015). Review: Polymers, Surface-Modified Polymers, and Self Assembled Monolayers as Surface-Modifying Agents for Biomaterials. *Polymer-Plastics Technology and Engineering, 54*(13), 1358-1378. doi:10.1080/03602559.2015.1021488

51. Sobers, C. J., Wood, S. E., & Mrksich, M. (2015). A gene expression-based comparison of cell adhesion to extracellular matrix and RGD-terminated monolayers. *Biomaterials, 52*, 385-394. doi:http://dx.doi.org/10.1016/j.biomaterials.2015.02.045

52. Sarkar, D., Vemula, P. K., Zhao, W., Gupta, A., Karnik, R., & Karp, J. M. (2010). Engineered mesenchymal stem cells with self-assembled vesicles for systemic cell targeting. *Biomaterials, 31*(19), 5266-5274. doi:http://dx.doi.org/10.1016/j.biomaterials.2010.03.006

53. Douglas, E. S., Chandra, R. A., Bertozzi, C. R., Mathies, R. A., & Francis, M. B. (2007). Self-assembled cellular microarrays patterned using DNA barcodes [10.1039/B708666K]. *Lab on a Chip, 7*(11), 1442-1448. doi:10.1039/B708666K

54. Stephanopoulos, N., Ortony, J. H., & Stupp, S. I. (2013). Self-assembly for the synthesis of functional biomaterials. *Acta Materialia, 61*(3), 912-930. doi:http://dx.doi.org/10.1016/j.actamat.2012.10.046

55. Love, J. C., Estroff, L. A., Kriebel, J. K., Nuzzo, R. G., & Whitesides, G. M. (2005). Self-Assembled Monolayers of Thiolates on Metals as a Form of Nanotechnology. *Chemical Reviews, 105*(4), 1103-1170. doi:10.1021/cr0300789

56. Kim, D. J., Lee, J. M., Park, J.-G., & Chung, B. G. (2011). A self-assembled monolayer-based micropatterned array for controlling cell adhesion and protein adsorption. *Biotechnology and Bioengineering, 108*(5), 1194-1202. doi:10.1002/bit.23029

57. Faucheux, N., Schweiss, R., Lützow, K., Werner, C., & Groth, T. (2004). Self-assembled monolayers with different terminating groups as model substrates for cell adhesion studies. *Biomaterials, 25*(14), 2721-2730. doi:http://dx.doi.org/10.1016/j.biomaterials.2003.09.069

58. Mahmudov, K. T., Kopylovich, M. N., Guedes da Silva, M. F. C., & Pombeiro, A. J. L. (2016). Non-covalent interactions in the synthesis of coordination compounds: Recent advances. *Coordination Chemistry Reviews*. doi:http://doi.org/10.1016/j.ccr.2016.09.002

59. Krutty, J. D., Schmitt, S. K., Gopalan, P., & Murphy, W. L. (2016). Surface functionalization and dynamics of polymeric cell culture substrates. *Current Opinion in Biotechnology, 40*, 164-169. doi:http://dx.doi.org/10.1016/j.copbio.2016.05.006

60. Hauser, J., Zietlow, J., Köller, M., Esenwein, S. A., Halfmann, H., Awakowicz, P., & Steinau, H. U. (2009). Enhanced cell adhesion to silicone implant material through plasma surface modification [journal article]. *Journal of Materials Science: Materials in Medicine, 20*(12), 2541-2548. doi:10.1007/s10856-009-3826-x

61. Khor, K. A., Gu, Y. W., Pan, D., & Cheang, P. (2004). Microstructure and mechanical properties of plasma sprayed HA/YSZ/Ti–6Al–4V composite coatings. *Biomaterials, 25*(18), 4009-4017. doi:http://dx.doi.org/10.1016/j.biomaterials.2003.10.089

62. Latifi, A., Imani, M., Khorasani, M. T., & Daliri Joupari, M. (2014). Plasma surface oxidation of 316L stainless steel for improving adhesion strength of silicone rubber coating to metal substrate. *Applied Surface Science, 320*, 471-481. doi:http://dx.doi.org/10.1016/j.apsusc.2014.09.084

63. Liu, W., Zhan, J., Su, Y., Wu, T., Wu, C., Ramakrishna, S., El-Newehy, M. (2014). Effects of plasma treatment to nanofibers on initial cell adhesion and cell morphology. *Colloids and Surfaces B: Biointerfaces, 113*, 101-106. doi:http://dx.doi.org/10.1016/j.colsurfb.2013.08.031

64. Qiu, Z.-Y., Chen, C., Wang, X.-M., & Lee, I.-S. (2014). Advances in the surface modification techniques of bone-related implants for last 10 years. *Regenerative Biomaterials, 1*(1), 67-79. doi:10.1093/rb/rbu007

65. Roy, M., Bandyopadhyay, A., & Bose, S. (2011). Induction plasma sprayed Sr and Mg doped nano hydroxyapatite coatings on Ti for bone implant. *Journal of Biomedical Materials Research Part B: Applied Biomaterials, 99B*(2), 258-265. doi:10.1002/jbm.b.31893

66. Schröder, K., Finke, B., Jesswein, H., Lüthen, F., Diener, A., Ihrke, R., Nebe, J. B. (2010). Similarities between Plasma Amino Functionalized PEEK and Titanium Surfaces Concerning Enhancement of Osteoblast Cell Adhesion. *Journal of Adhesion Science and Technology, 24*(5), 905-923. doi:10.1163/016942409X12598231567989

67. Wang, G., Liu, X., Gao, J., & Ding, C. (2009). In vitro bioactivity and phase stability of plasma-sprayed nanostructured 3Y-TZP coatings. *Acta Biomaterialia, 5*(6), 2270-2278. doi:http://dx.doi.org/10.1016/j.actbio.2009.01.023

68. Yang, C.-H., Wang, Y.-T., Tsai, W.-F., Ai, C.-F., Lin, M.-C., & Huang, H.-H. (2011). Effect of oxygen plasma immersion ion implantation treatment on corrosion resistance and cell adhesion of titanium surface. *Clinical Oral Implants Research, 22*(12), 1426-1432. doi:10.1111/j.1600-0501.2010.02132.x

69. Yuan, Y., Liu, C., Zhang, Y., Yin, M., & Shi, C.-o. (2007). Radio frequency plasma polymers of n-butyl methacrylate and their controlled drug release characteristics: I. Effect of the oxygen gas. *Surface and Coatings Technology, 201*(15), 6861-6864. doi:http://dx.doi.org/10.1016/j.surfcoat.2006.09.020

70. Zhang, W., Luo, Y., Wang, H., Jiang, J., Pu, S., & Chu, P. K. (2008). Ag and Ag/N2 plasma modification of polyethylene for the enhancement of antibacterial properties and cell growth/proliferation. *Acta Biomaterialia, 4*(6), 2028-2036. doi:http://dx.doi.org/10.1016/j.actbio.2008.05.012

71. Paital, S. R., He, W., & Dahotre, N. B. (2010). Laser pulse dependent micro textured calcium phosphate coatings for improved wettability and cell compatibility [journal article]. *Journal of Materials Science: Materials in Medicine, 21*(7), 2187-2200. doi:10.1007/s10856-010-4085-6

72. Park, C. H., Rios, H. F., Jin, Q., Bland, M. E., Flanagan, C. L., Hollister, S. J., & Giannobile, W. V. (2010). Biomimetic hybrid scaffolds for engineering human tooth-ligament interfaces. *Biomaterials, 31*(23), 5945-5952. doi:10.1016/j.biomaterials.2010.04.027

73. Zheng, Y., Xiong, C., Li, X., & Zhang, L. (2014). Covalent attachment of cell-adhesive peptide Gly-Arg-Gly-Asp (GRGD) to poly(etheretherketone) surface by tailored silanization layers technique. *Applied Surface Science, 320*, 93-101. doi:http://dx.doi.org/10.1016/j.apsusc.2014.09.091

74. Dou, X.-Q., Li, P., Zhang, D., & Feng, C.-L. (2013). RGD anchored C2-benzene based PEG-like hydrogels as scaffolds for two and three dimensional cell cultures [10.1039/C3TB20155D]. *Journal of Materials Chemistry B, 1*(29), 3562-3568. doi:10.1039/C3TB20155D

75. Sánchez-Cortés, J., & Mrksich, M. (2009). The Platelet Integrin αIIbβ3 Binds to the RGD and AGD Motifs in Fibrinogen. *Chemistry & biology, 16*(9), 990-1000. doi:10.1016/j.chembiol.2009.08.012

76. Flavel, B. S., Sweetman, M. J., Shearer, C. J., Shapter, J. G., & Voelcker, N. H. (2011). Micropatterned Arrays of Porous Silicon: Toward Sensory Biointerfaces. *ACS Applied Materials & Interfaces, 3*(7), 2463-2471. doi:10.1021/am2003526

77. Bellis, S. L. (2011). Advantages of RGD peptides for directing cell association with biomaterials. *Biomaterials, 32*(18), 4205-4210. doi:10.1016/j.biomaterials.2011.02.029

78. Boateng, S. Y., Lateef, S. S., Mosley, W., Hartman, T. J., Hanley, L., & Russell, B. (2005). RGD and YIGSR synthetic peptides facilitate cellular adhesion identical to that of laminin and fibronectin but alter the physiology of neonatal cardiac myocytes. *American Journal of Physiology - Cell Physiology, 288*(1), C30-C38. doi:10.1152/ajpcell.00199.2004

79. Wang, S., Cai, X., Wang, L., Li, J., Li, Q., Zuo, X., Fan, C. (2016). DNA orientation-specific adhesion and patterning of living mammalian cells on self-assembled DNA monolayers †Electronic supplementary information (ESI) available: Details in experimental section and supporting figures. See DOI: 10.1039/c5sc04102c Click here for additional data file. *Chemical Science, 7*(4), 2722-2727. doi:10.1039/c5sc04102c

80. Hsiao, S. C., Shum, B. J., Onoe, H., Douglas, E. S., Gartner, Z. J., Mathies, R. A., . . . Francis, M. B. (2009). Direct Cell Surface Modification with DNA for the Capture of Primary Cells and the Investigation of Myotube Formation on Defined Patterns. *Langmuir : the ACS journal of surfaces and colloids, 25*(12), 6985-6991. doi:10.1021/la900150n

81. Selden, N. S., Todhunter, M. E., Jee, N. Y., Liu, J. S., Broaders, K. E., & Gartner, Z. J. (2012). Chemically programmed cell adhesion with membrane-anchored oligonucleotides. *Journal of the American Chemical Society, 134*(2), 765-768. doi:10.1021/ja2080949

82. Pan, J.-f., Liu, N.-h., Shu, L.-y., & Sun, H. (2015). Application of avidin-biotin technology to improve cell adhesion on nanofibrous matrices [journal article]. *Journal of Nanobiotechnology, 13*(1), 37. doi:10.1186/s12951-015-0096-2

83. Schmidt, R. C., & Healy, K. E. (2013). Effect of avidin-like proteins and biotin modification on mesenchymal stem cell adhesion. *Biomaterials, 34*(15), 3758-3762. doi:10.1016/j.biomaterials.2013.01.081

84. Tsai, W.-B., & Wang, M.-C. (2005). Effect of an avidin–biotin binding system on chondrocyte adhesion, growth and gene expression. *Biomaterials, 26*(16), 3141-3151. doi:http://dx.doi.org/10.1016/j.biomaterials.2004.08.014

85. Wolny, P. M., Spatz, J. P., & Richter, R. P. (2010). On the Adsorption Behavior of Biotin-Binding Proteins on Gold and Silica. *Langmuir, 26*(2), 1029-1034. doi:10.1021/la902226b

86. Huang, S.-C., Stump, M. D., Weiss, R., & Caldwell, K. D. (1996). Binding of Biotinylated DNA to Streptavidin-Coated Polystyrene Latex: Effects of Chain Length and Particle Size. *Analytical Biochemistry, 237*(1), 115-122. doi:http://dx.doi.org/10.1006/abio.1996.0208

87. Dou, X.-Q., Zhang, J., & Feng, C. (2015). Biotin–Avidin Based Universal Cell–Matrix Interaction for Promoting Three-Dimensional Cell Adhesion. *ACS Applied Materials & Interfaces, 7*(37), 20786-20792. doi:10.1021/acsami.5b05828

88. Zhao, W., Teo, G. S. L., Kumar, N., & Karp, J. M. (2010). Chemistry and material science at the cell surface. *Materials Today, 13*(4), 14-21. doi:http://dx.doi.org/10.1016/S1369-7021(10)70056-0

89. Wang, T.-y., Leventis, R., & Silvius, J. R. (2005). Artificially Lipid-anchored Proteins Can Elicit Clustering-induced Intracellular Signaling Events in Jurkat T-Lymphocytes Independent of Lipid Raft Association. *Journal of Biological Chemistry, 280*(24), 22839-22846. doi:10.1074/jbc.M502920200

90. Hart, T., Zhao, A., Garg, A., Bolusani, S., & Marcotte, E. M. (2009). Human Cell Chips: Adapting DNA Microarray Spotting Technology to Cell-Based Imaging Assays. *PLoS ONE, 4*(10), e7088. doi:10.1371/journal.pone.0007088

91. Barr, K. (2013). *Bio-modification of non-biological surfaces with function-spacer-lipid constructs by methods including bioprinting* (Doctoral Thesis). Auckland University of Technology, Auckland. Retrieved from http://hdl.handle.net/10292/6938. Available from cat05020a database.

92. Hadac, E. M., Federspiel, M. J., Chernyy, E., Tuzikov, A., Korchagina, E., Bovin, N. V., . . . Henry, S. M. (2011). Fluorescein and radiolabeled Function-Spacer-Lipid constructs allow for simple in vitro and in vivo bioimaging of enveloped virions. *Journal of Virological Methods, 176*(1–2), 78-84. doi:http://dx.doi.org/10.1016/j.jviromet.2011.06.005

93. Frame, T., Carroll, T., Korchagina, E., Bovin, N., & Henry, S. (2007). Synthetic glycolipid modification of red blood cell membranes. *Transfusion, 47*(5), 876-882. doi:10.1111/j.1537-2995.2007.01204.x

94. Korchagina, E. Y., & Henry, S. M. (2015). Synthetic glycolipid-like constructs as tools for glycobiology research, diagnostics, and as potential therapeutics [journal article]. *Biochemistry (Moscow), 80*(7), 857-871. doi:10.1134/s0006297915070068

95. Blake, D. A., Bovin, N. V., Bess, D., & Henry, S. M. (2011). FSL Constructs: A Simple Method for Modifying Cell/Virion Surfaces with a Range of Biological Markers Without Affecting their Viability. *Journal of Visualized Experiments : JoVE*(54), 3289. doi:10.3791/3289

96. Harrison, A. L., Olsson, M. L., Jones, R. B., Ramkumar, S., Sakac, D., Binnington, B., . . . Branch, D. R. (2010). A synthetic globotriaosylceramide analogue inhibits HIV-1 infection in vitro by two mechanisms [journal article]. *Glycoconjugate Journal, 27*(5), 515-524. doi:10.1007/s10719-010-9297-y

97. Williams, E., Barr, K., Korchagina, E., Tuzikov, A., Henry, S., & Bovin, N. (2016). Ultra-Fast Glyco-Coating of Non-Biological Surfaces. *International Journal of Molecular Sciences, 17*(1), 118. doi:10.3390/ijms17010118

98. McIntosh, S. M., Henry, S., & Blake, D. (2009). *A novel technology for In Vitro and In Utero modification of Endometrial cells* [M. PhilThesis]: Auckland University of Technology. Retrieved from http://hdl.handle.net/10292/1040. Retrieved from cat05020a database.

99. Oliver, C. (2012). *Insights into the manipulation of the immune response to carbohydrate antigens with blood group functional-spacer-lipid constructs* (Doctoral Thesis). Auckland University of Technology. Retrieved from http://hdl.handle.net/10292/5520. Available from cat05020a database.

100. Henry, S. (2014). *Rapid biofunctionalization of magnetic beads with function-spacer-lipid constructs* Sepmag. Retrieved from http://www.sepmag.eu/blog/bid/401297/Rapid-biofunctionalization-of-magnetic-beads-with-function-spacer-lipid-constructs

101. Korchagina, E., Tuzikov, A., Formanovsky, A., Popova, I., Henry, S., & Bovin, N. (2012). Toward creating cell membrane glyco-landscapes with glycan lipid constructs. *Carbohydrate Research, 356*, 238-246. doi:http://dx.doi.org/10.1016/j.carres.2012.03.044

102. Abraham, R. T., & Weiss, A. (2004). Jurkat T cells and development of the T-cell receptor signalling paradigm [10.1038/nri1330]. *Nat Rev Immunol, 4*(4), 301-308.

103. Teare, D. O. H., Emmison, N., Ton-That, C., & Bradley, R. H. (2001). Effects of Serum on the Kinetics of CHO Attachment to Ultraviolet–Ozone Modified Polystyrene Surfaces. *Journal of Colloid and Interface Science, 234*(1), 84-89. doi:http://dx.doi.org/10.1006/jcis.2000.7282

104. Leitinger, B., & Hogg, N. (2002). The involvement of lipid rafts in the regulation of integrin function. *Journal of Cell Science, 115*(5), 963-972.

105. Goldmann, W. H. (2012). Mechanotransduction in cells1. *Cell Biology International, 36*(6), 567-570. doi:10.1042/CBI20120071

106. Alves, P., Pinto, S., Ferreira, P., Kaiser, J.-P., Bruinink, A., de Sousa, H. C., & Gil, M. H. (2014). Improving cell adhesion: development of a biosensor for cell behaviour monitoring by surface grafting of sulfonic groups onto a thermoplastic polyurethane [journal article]. *Journal of Materials Science: Materials in Medicine, 25*(8), 2017-2026. doi:10.1007/s10856-014-5233-1

107. Wang, Q., Cheng, H., Peng, H., Zhou, H., Li, P. Y., & Langer, R. (2015). Non-genetic engineering of cells for drug delivery and cell-based therapy. *Advanced Drug Delivery Reviews, 91*, 125-140. doi:http://dx.doi.org/10.1016/j.addr.2014.12.003

108. Curtis, A., Forrester, J., McInnes, C., & Lawrie, F. (1983). Adhesion of cells to polystyrene surfaces. *The Journal of Cell Biology, 97*(5), 1500-1506.

109. Hickman, G. J., Boocock, D. J., Pockley, A. G., & Perry, C. C. (2016). The Importance and Clinical Relevance of Surfaces in Tissue Culture. *ACS Biomaterials Science & Engineering, 2*(2), 152-164. doi:10.1021/acsbiomaterials.5b00403

110. Gusnard, D., & Kirschner, R. H. (1977). Cell and organelle shrinkage during preparation for scanning electron microscopy: effects of fixation, dehydration and critical point drying. *Journal of Microscopy, 110*(1), 51-57. doi:10.1111/j.1365-2818.1977.tb00012.x

111. Patra, M., Salonen, E., Terama, E., Vattulainen, I., Faller, R., Lee, B. W., . . . Karttunen, M. (2006). Under the Influence of Alcohol: The Effect of Ethanol and Methanol on Lipid Bilayers. *Biophysical Journal, 90*(4), 1121-1135. doi:10.1529/biophysj.105.062364

112. Osahor, A., Deekonda, K., Lee, C.-W., Sim, E. U.-H., Radu, A., & Narayanan, K. (2017). Rapid preparation of adherent mammalian cells for basic scanning electron microscopy (SEM) analysis. *Analytical Biochemistry, 534*, 46-48. doi:http://dx.doi.org/10.1016/j.ab.2017.07.008

113. Gigout, A., Levasseur, S., Girard-Lauriault, P.-L., Buschmann, M. D., Wertheimer, M. R., & Jolicoeur, M. (2009). CHO Cells Adhering to Nitrogen-Rich Plasma-Polymerised Ethylene Exhibit High Production of a Specific Recombinant Protein. *Macromolecular Bioscience, 9*(10), 979-988. doi:10.1002/mabi.200900079

114. Strober, W. (2001). Trypan Blue Exclusion Test of Cell Viability. In *Current Protocols in Immunology*: John Wiley & Sons, Inc. Retrieved from http://dx.doi.org/10.1002/0471142735.ima03bs21. doi:10.1002/0471142735.ima03bs21

115. Röder, A., García-Gareta, E., Theodoropoulos, C., Ristovski, N., Blackwood, K. A., & Woodruff, M. A. (2015). An Assessment of Cell Culture Plate Surface Chemistry for in Vitro Studies of Tissue Engineering Scaffolds. *Journal of Functional Biomaterials, 6*(4), 1054-1063. doi:10.3390/jfb6041054

116. Audiffred, J. F., Leo, S. E. D., Brown, P. K., Hale-Donze, H., & Monroe, W. T. (2010). Characterization and applications of serum-free induced adhesion in jurkat suspension cells. *Biotechnology and Bioengineering, 106*(5), 784-793. doi:10.1002/bit.22728

117. Henry, S. M. (2009). Modification of red blood cells for laboratory quality control use. *Current Opinion in Hematology, 16*(6), 467-472. doi:10.1097/MOH.0b013e328331257e

118. Kim, H., Doh, J., Irvine, D. J., Cohen, R. E., & Hammond, P. T. (2004). Large Area Two-Dimensional B Cell Arrays for Sensing and Cell-Sorting Applications. *Biomacromolecules, 5*(3), 822-827. doi:10.1021/bm034341r

119. Dutta, D., Pulsipher, A., Luo, W., & Yousaf, M. N. (2011). Synthetic Chemoselective Rewiring of Cell Surfaces: Generation of Three-Dimensional Tissue Structures. *Journal of the American Chemical Society, 133*(22), 8704-8713. doi:10.1021/ja2022569

120. Wang, B., Song, J., Yuan, H., Nie, C., Lv, F., Liu, L., & Wang, S. (2014). Multicellular Assembly and Light-Regulation of Cell–Cell Communication by Conjugated Polymer Materials. *Advanced Materials, 26*(15), 2371-2375. doi:10.1002/adma.201304593

121. Bhat, V. D., Truskey, G. A., & Reichert, W. M. (1998). Using avidin-mediated binding to enhance initial endothelial cell attachment and spreading. *Journal of Biomedical Materials Research, 40*(1), 57-65. doi:10.1002/(SICI)1097-4636(199804)40:1<57::AID-JBM7>3.0.CO;2-Q

122. Sarkar, D., Vemula, P. K., Teo, G. S. L., Spelke, D., Karnik, R., Wee, L. Y., & Karp, J. M. (2008). Chemical Engineering of Mesenchymal Stem Cells to Induce a Cell Rolling Response. *Bioconjugate Chemistry, 19*(11), 2105-2109. doi:10.1021/bc800345q

123. Anamelechi, C. C., Clermont, E. E., Brown, M. A., Truskey, G. A., & Reichert, W. M. (2007). Streptavidin Binding and Endothelial Cell Adhesion to Biotinylated Fibronectin. *Langmuir : the ACS journal of surfaces and colloids, 23*(25), 12583-12588. doi:10.1021/la702322n

124. Bogdanov, A. A., Gordeeva, L. V., Baibakov, B. A., Margolis, L. B., & Torchilin, V. P. (1991). Restoration of adhesive potentials of Ehrlich ascites carcinoma cells by modification of plasma membrane. *Journal of Cellular Physiology, 147*(1), 182-190. doi:10.1002/jcp.1041470123

125. Chung, H. A., Kato, K., Itoh, C., Ohhashi, S., & Nagamune, T. (2004). Casual cell surface remodeling using biocompatible lipid-poly(ethylene glycol)(n): Development of stealth cells and monitoring of cell membrane behavior in serum-supplemented conditions. *Journal of Biomedical Materials Research Part A, 70A*(2), 179-185. doi:10.1002/jbm.a.20117

126. Kato, K., Itoh, C., Yasukouchi, T., & Nagamune, T. (2004). Rapid Protein Anchoring into the Membranes of Mammalian Cells Using Oleyl Chain and Poly(ethylene glycol) Derivatives. *Biotechnology Progress, 20*(3), 897-904. doi:10.1021/bp0342093

127. Henry, S. M., Barr, K. L., & Oliver, C. A. (2012). Modeling transfusion reactions with kodecytes and enabling ABO-incompatible transfusion with function-spacer-lipid constructs. *ISBT Science Series, 7*(1), 106-111. doi:10.1111/j.1751-2824.2012.01563.x

128. Oliver, C., Blake, D., & Henry, S. (2011). Modeling transfusion reactions and predicting in vivo cell survival with kodecytes. *Transfusion, 51*(8), 1723-1730. doi:10.1111/j.1537-2995.2010.03034.x

129. Oliver, C., Blake, D., & Henry, S. (2011). In vivo neutralization of anti-A and successful transfusion of A antigen–incompatible red blood cells in an animal model. *Transfusion, 51*(12), 2664-2675. doi:10.1111/j.1537-2995.2011.03184.x

130. Stephan, M. T., & Irvine, D. J. (2011). Enhancing cell therapies from the outside in: Cell surface engineering using synthetic nanomaterials. *Nano Today, 6*(3), 309-325. doi:http://dx.doi.org/10.1016/j.nantod.2011.04.001

131. Chen, W., Fu, L., & Chen, X. (2015). Improving cell-based therapies by nanomodification [Article]. *Journal of Controlled Release, 219*, 560-575. doi:10.1016/j.jconrel.2015.09.054

132. Hobro, A. J., & Smith, N. I. (2017). An evaluation of fixation methods: Spatial and compositional cellular changes observed by Raman imaging. *Vibrational Spectroscopy, 91*, 31-45. doi:http://dx.doi.org/10.1016/j.vibspec.2016.10.012

133. Rysavy, N. M., Shimoda, L. M. N., Dixon, A. M., Speck, M., Stokes, A. J., Turner, H., & Umemoto, E. Y. (2014). Beyond apoptosis: The mechanism and function of phosphatidylserine asymmetry in the membrane of activating mast cells. *Bioarchitecture, 4*(4-5), 127-137. doi:10.1080/19490992.2014.995516

134. Swiston, A. J., Cheng, C., Um, S. H., Irvine, D. J., Cohen, R. E., & Rubner, M. F. (2008). Surface Functionalization of Living Cells with Multilayer Patches. *Nano Letters, 8*(12), 4446-4453. doi:10.1021/nl802404h

135. Mrksich, M. (2000). A surface chemistry approach to studying cell adhesion [10.1039/A705397E]. *Chemical Society Reviews, 29*(4), 267-273. doi:10.1039/A705397E

136. Lu, T., Chen, X., Shi, Q., Wang, Y., Zhang, P., & Jing, X. (2008). The immobilization of proteins on biodegradable fibers via biotin–streptavidin bridges. *Acta Biomaterialia, 4*(6), 1770-1777. doi:http://dx.doi.org/10.1016/j.actbio.2008.05.006

137. Reimhult, E., & Höök, F. (2015). Design of Surface Modifications for Nanoscale Sensor Applications. *Sensors, 15*(1), 1635.

138. Tsai, W.-B., & Wang, M.-C. (2005). Effects of an Avidin-Biotin Binding System on Chondrocyte Adhesion and Growth on Biodegradable Polymers. *Macromolecular Bioscience, 5*(3), 214-221. doi:10.1002/mabi.200400144

139. Curtis, A. S. G., Forrester, J. V., Mclnnes, C., & Lawrie, F. (1983). Adhesion of cells to polystyrene surfaces. *The Journal of Cell Biology, 97*(5), 1500-1506.

140. Dowling, D. P., Miller, I. S., Ardhaoui, M., & Gallagher, W. M. (2011). Effect of Surface Wettability and Topography on the Adhesion of Osteosarcoma Cells on Plasma-modified Polystyrene. *Journal of Biomaterials Applications, 26*(3), 327-347. doi:10.1177/0885328210372148

141. Schakenraad, J. M., & Busscher, H. J. (1989). Cell—polymer interactions: The influence of protein adsorption. *Colloids and Surfaces, 42*(3), 331-343. doi:http://dx.doi.org/10.1016/0166-6622(89)80349-X

142. Dewez, J. L., Lhoest, J. B., Detrait, E., Berger, V., Dupont-Gillain, C. C., Vincent, L. M., Rouxhet, P. G. (1998). Adhesion of mammalian cells to polymer surfaces: from physical chemistry of surfaces to selective adhesion on defined patterns. *Biomaterials, 19*(16), 1441-1445. doi:http://dx.doi.org/10.1016/S0142-9612(98)00055-6

143. Meng, G., Liu, S., & Rancourt, D. E. (2011). Synergistic Effect of Medium, Matrix, and Exogenous Factors on the Adhesion and Growth of Human Pluripotent Stem Cells Under Defined, Xeno-Free Conditions. *Stem Cells and Development, 21*(11), 2036-2048. doi:10.1089/scd.2011.0489

144. Lindroos, B., Boucher, S., Chase, L., Kuokkanen, H., Huhtala, H., Haataja, R., . . . Miettinen, S. Serum-free, xeno-free culture media maintain the proliferation rate and multipotentiality of adipose stem cells in vitro. *Cytotherapy, 11*(7), 958-972. doi:10.3109/14653240903233081

145. Tan, K. Y., Teo, K. L., Lim, J. F. Y., Chen, A. K. L., Reuveny, S., & Oh, S. K. W. (2015). Serum-free media formulations are cell line–specific and require optimization for microcarrier culture. *Cytotherapy, 17*(8), 1152-1165. doi:http://dx.doi.org/10.1016/j.jcyt.2015.05.001

146. Fang, R. H., Jiang, Y., Fang, J. C., & Zhang, L. (2017). Cell membrane-derived nanomaterials for biomedical applications. *Biomaterials, 128*, 69-83. doi:https://doi.org/10.1016/j.biomaterials.2017.02.041

147. Oelke, M., Maus, M. V., Didiano, D., June, C. H., Mackensen, A., & Schneck, J. P. (2003). Ex vivo induction and expansion of antigen-specific cytotoxic T cells by HLA-Ig-coated artificial antigen-presenting cells [10.1038/nm869]. *Nat Med, 9*(5), 619-625. doi:http://www.nature.com/nm/journal/v9/n5/suppinfo/nm869_S1.html

148. Li, W., Lee, S., Ma, M., Kim, S. M., Guye, P., Pancoast, J. R., . . . Hammond, P. T. (2013). Microbead-based biomimetic synthetic neighbors enhance survival and function of rat pancreatic β-cells [Article]. *3*, 2863. doi:10.1038/srep02863 https://www.nature.com/articles/srep02863#supplementary-information

149. Wan, C., He, Q., McCaigue, M., Marsh, D., & Li, G. (2006). Nonadherent cell population of human marrow culture is a complementary source of mesenchymal stem cells (MSCs). *Journal of Orthopaedic Research, 24*(1), 21-28. doi:10.1002/jor.20023

150. Kato, K., Umezawa, K., Funeriu, D. P., Miyake, M., Miyake, J., & Nagamune, T. (2003). Immobilized culture of nonadherent cells on an oleyl poly(ethylene glycol) ether-modified surface. *BioTechniques, 35*(5), 1014-1018, 1020-1011.

151. Kato, K., Umezawa, K., Miyake, M., Miyake, J., & Nagamune, T. (2004). Transfection microarray of nonadherent cells on an oleyl poly(ethylene glycol)ether-modified glass slide. *BioTechniques, 37*, 444-452.